EVALUATING THE ELECTRICAL RESPONSE OF POLYANILINE TO MECHANICAL STRAIN

A Thesis
Presented to the Faculty of
California Polytechnic State University,
San Luis Obispo

In Partial Fulfillment
of the Requirements for the Degree
Master of Science in Engineering,
with Specialization in Materials Engineering

by
Matthew L. Goebel
June 2009

COMMITTEE MEMBERSHIP

TITLE:	Evaluating the Electrical Response of Polyaniline to Mechanical Strain
AUTHOR:	Matthew L. Goebel
DATE SUBMITTED:	June 2009
COMMITTEE CHAIR:	Dr. Richard Savage Materials Engineering *California Polytechnic State University, San Luis Obispo*
COMMITTEE MEMBER:	Nikhil Bhat
COMMITTEE MEMBER:	Dr. William Hughes Materials Science & Engineering *Boise State University*

ABSTRACT

Evaluating the Electrical Response of polyaniline to Mechanical Strain

Matthew L. Goebel

This thesis focuses on the electrical output of polyaniline films subjected to uniaxial strain in hydrochloric acid solutions. Polyaniline belongs to novel class of materials known as conducting polymers. Alternating single and double bonds in the backbone of conducting polymers allow them to transmit electric charge when they are doped with negatively charged ions. Modifying the degree of doping and other electrical/chemical treatments allow conducting polymers to exhibit conducting, semi-conducting, or insulating electrical properties. Resilient mechanical properties, good processability, and low cost make conducting polymers good candidates for applications traditionally held by metals and semi-conductors.

When tensile strain is applied to polyaniline in an electrolyte solution, the material selectively absorbs negatively charged ions. This charge imbalance produces a measurable electrical output. Theoretical models based on Fick's second law of diffusion were compared against experimental results to determine fundamental material properties such as diffusivity and ion solubility in polyaniline. These properties were used to quantify polyaniline as a sensor material based on characteristics including sensitivity, accuracy, precision, range, linearity, and error. Films were cast from solutions of polyaniline powder (M_n = 65,000) in N-methyl-2-pyrrolidinone solvent, with thicknesses ranging from 2.72 to 158 µm.

Keywords: polyaniline, conducting polymer, mechanical sensors

ACKNOWLEDGEMENTS

Foremost I would like to appreciate the members of my thesis committee, Nikhil Bhat, without whom the conception and execution of this project would not have been possible, Dr. Will Hughes for being a friend and mentor during and after his time at Cal Poly, and Dr. Richard Savage for his wisdom and acceptance of an unconventional project.

I received some of my most invaluable guidance from within the student body. I would like to thank all of my colleagues who entertained my many distractions; namely Aaron Guerrero, Brian Stahl, Darin Grandfield, Greg Boban, Matt Lewis, Michelle Alexander, and Sean Kaylor. Special thanks to Dr. Philip Costanzo for offering knowledge and recourses beyond his academic obligations.

To my family. Thank you for the investment that you've made thus far; I will continue to live with all of the care and consideration you've taught me.

TABLE OF CONTENTS

LIST OF TABLES

LIST OF FIGURES

CHAPTER 1

INTRODUCTION

Polyaniline belongs to a novel class of materials known as conducting polymers. Alternating single and double bonds in the backbone of conducting polymers allow them to transmit electric charge when they are doped with ions. Changing the degree of doping and other electrical/chemical treatments allow conducting polymers to exhibit conducting, semi-conducting, or insulating electrical properties. Resilient mechanical properties, good processability, and low cost make conducting polymers good candidates for applications traditionally held by metals and semi-conductor materials which include LEDs, photovoltaics, biological/chemical sensors, and actuators. The biocompatibility of most conjugated polymers make them excellent candidates for development as "artificial muscles", for which they have been the subject of study for the past two decades.

In addition to linear expansion and contraction, skeletal muscle is proprioceptive, meaning it is able to *sense* externally applied forces. To date, the study of conducting polymer materials as artificial muscles has mostly neglected this function. Coupling strain sensing and actuation functions would allow the development of artificial muscles to more closely mimic mammalian skeletal muscle. A realistic short term goal is to develop devices to benefit people with impaired function to critical muscles in the body such as those which control valves in the digestive, circulatory, or repertory systems by detecting when the muscles are not operating properly, then taking corrective action. In the long term, muscular functions for individuals suffering from degenerative muscle disorders could be restored.

The electrical energy produced by polyaniline sensors may be used as a metric for displacement as well as a means of powering electrical devices. Organs in the body which undergo constant and repetitive motion, such as the heart, could be outfitted with a bending sensor/generator, and a simple rectifier circuit to convert cyclic output into DC power. Although the electrical energy generated would be small, it may be enough to power devices such as pacemakers or wireless communication devices.

This thesis will focus on assessing the electrical response of polyaniline to mechanical strain at its most fundamental level in order to provide a framework for future research or development of functional mechanical sensors. Polyaniline films were prepared by casting solutions of chemically polymerized polyaniline to obtain various thicknesses. The current and potential outputs of polyaniline films under tensile strain were used to establish a set of characteristic sensor properties including sensitivity, signal input and output ranges, resolution, linearity, and acceptable operating environments. Material characteristics which are relevant to sensor applications such as yield strength, Young's modulus, conductivity, and ion diffusivities were also evaluated.

CHAPTER 2

BACKGROUND

This chapter provides a synopsis of work which has been performed in the field of conducting polymers and is relevant to this thesis. It is intended to provide adequate background and set the stage for experimental techniques, analyses, and outcomes.

2.1 Conducting Polymers

The first study which described conductivity in a linear chain polymer was published by D. E. Weiss *et al.* in 1963, [1] in which conductivity of polypyrrole was observed when the polymer was *doped* by introducing iodide ions. The authors demonstrated that the conductivity of the polymer could be tuned with doping level, molecular weights, and other processing parameters. A mechanism for charge transport was proposed which involved shifting double bonds in the polymer backbone. After the initial discovery, the field was quiet until 1977, when Alan Heeger, Alan MacDiarmid, and Hideki Shirakawa reported observing metallic-like conductivity in iodine doped polyacetylene [2]. For this discovery, and subsequent work identifying charge transport mechanisms in a variety of conducting polymers, the three were jointly awarded the Nobel Prize in Chemistry in 2000.

Conducting polymers typically contain alternating, or “conjugated”, single and double bonds in their backbones as shown in the structures of common conducting polymers in Figure 2.1. When used in reference to these materials, the terms *conducting polymer* and *conjugated polymer* are synonymous, and may be used interchangeably.

Conducting polymers have exhibited conductivities as great as 10^5 S cm^{-1}, however more typical conductivities fall within the range of 0.01 to 200 S cm^{-1} [3-4]. These conductivities are lower than those of most metals (>10^4 S cm^{-1}), but far greater than those of insulating polymers (<10^{-9} S cm^{-1}).

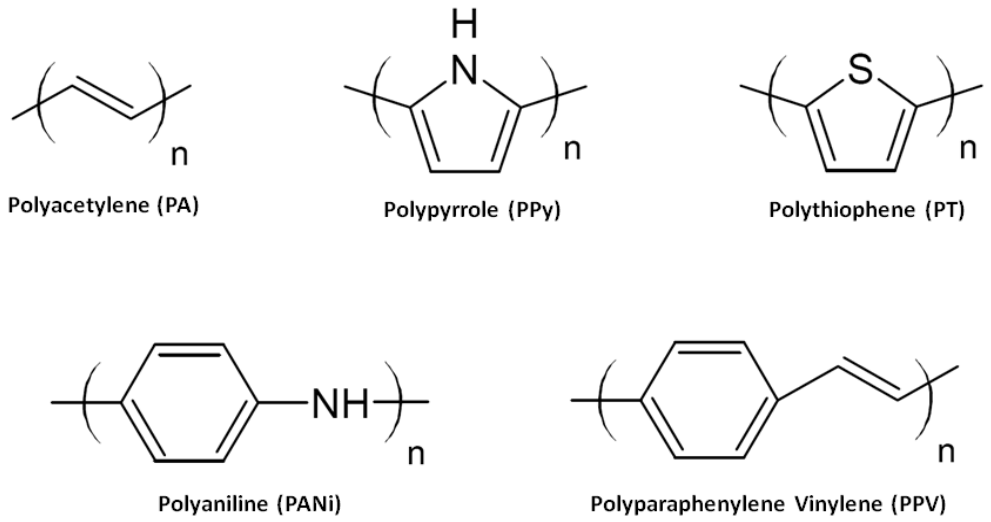

Figure 2.1. Structures of five common conducting polymers.

Most conducting polymers may exhibit conducting, semi-conducting, or insulating electrical properties depending on oxidation state and doping level. For this reason, conjugated polymers are being explored to fill roles in the electronics industry typically held by metals and semiconductors. Most promising are applications in optical systems. Sony has recently released an 11" organic LED TV boasting better efficiency, color, resolution, and contrast in a slimmer package than comparable inorganic LED systems [5]. Organic photovoltaics have achieved efficiencies as high as 6.7 % in single junction cells, [6] with higher efficiencies foreseeable in the near future. Companies such as Konarka and Plextronics have successfully demonstrated reel to reel printing of organic solar cells on industrial scales.

Most conducting polymers are chemically and biologically inert relative to metals, which makes them appealing for biocompatible electronic devices such as chemical sensors, actuators, and electrodes. Conducting polymers can be covalently bonded with other polymers or biological molecules, and will exhibit slight changes in electrical properties depending on the state of the secondary compound. In this manner, a host of chemical and biological sensors have been developed to detect inputs such as pH or glucose concentration [7-10].

Conjugated polymer actuators exhibit characteristic which approach those of skeletal muscle. Most reported actuators exhibit strains of 1 to 5%, although strains as great as 30% have been demonstrated. Maximum applied stresses in these actuators range from 3 to 30 MPa depending on configuration [10]. Although mammalian muscle typically exhibits lower maximum stress (0.25 Mpa) and greater maximum strain (25 – 35 %), the differences can be compensated for by varying mechanical configuration. They can be continuously controlled and consume no energy when held at a constant strain. Most conjugated polymers are biocompatible, stable at body temperatures, and can operate using electrolytes found in the body, making them suitable for implantable devices. Polyaniline and polypyrrole are the two most common conjugated polymer actuator materials due to their performance as well as good strength and toughness properties.

2.2. Polyaniline Overview

Polyaniline is a popular conducting polymer because it is easily synthesized, high conductivities can be attained without special treatments, and it has excellent mechanical properties. Challenges of using polyaniline opposed to similar conductive polymers such as polypyrrole or polythiophene arise from its relatively complex oxidation chemistry, and that it must usually be doped through submersion in a strong acid solution to achieve a conductive state. When doping is performed, protons and anions diffuse into the material and alter the chemical structure as explained in the following section.

2.2.1. Oxidation Chemistry

Polyaniline may exist in any combination of three oxidation states, which depend on the level of protonation (number of hydrogen atoms) and relative amounts of imine and amine groups in the polymer backbone. Each oxidation state can exist in a neutral *base* or a positive *salt* state, depending on whether the polyaniline has been doped to protonate and positively charge the nitrogen atoms (Figure 2.2). The protonated states are called salts because their positively charged imine or amine groups typically form ionic complexes with free anions. In the fully oxidized state, *pernigraniline*, only amine links exist in the polymer backbone. In the fully reduced state, *leucoemeraldine*, only imine links exist in the polymer backbone. The numbers of imine and amine links are equal in the *emeraldine* state.

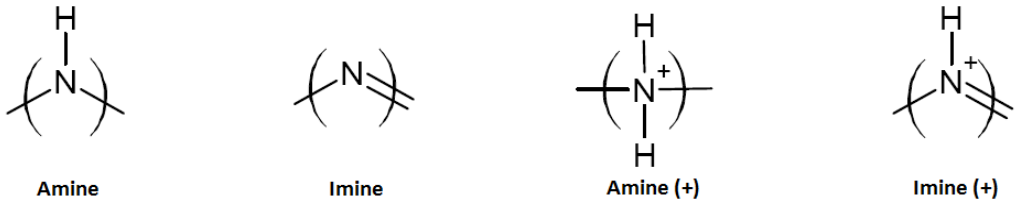

Figure 2.2. The four possible configurations of the nitrogen atoms in polyaniline depend on oxidation state and the level of doping.

Figure 2.3 shows the six fundamental states of polyaniline, of which only the emeraldine salt state is electrically conductive [12]. This conductive state cannot be sustained in aqueous solutions with a pH greater than 4, as insufficient hydrogen ion concentrations will cause the polymer to deprononate into the emeraldine base state [13]. To achieve high and uniform conductivity, polyaniline is usually doped in aqueous solutions of pH 0 to 2 [14]. The oxidation state can be controlled through the application of an electric charge while the polyaniline is in an acid solution, which acts as an anion and proton reservoir.

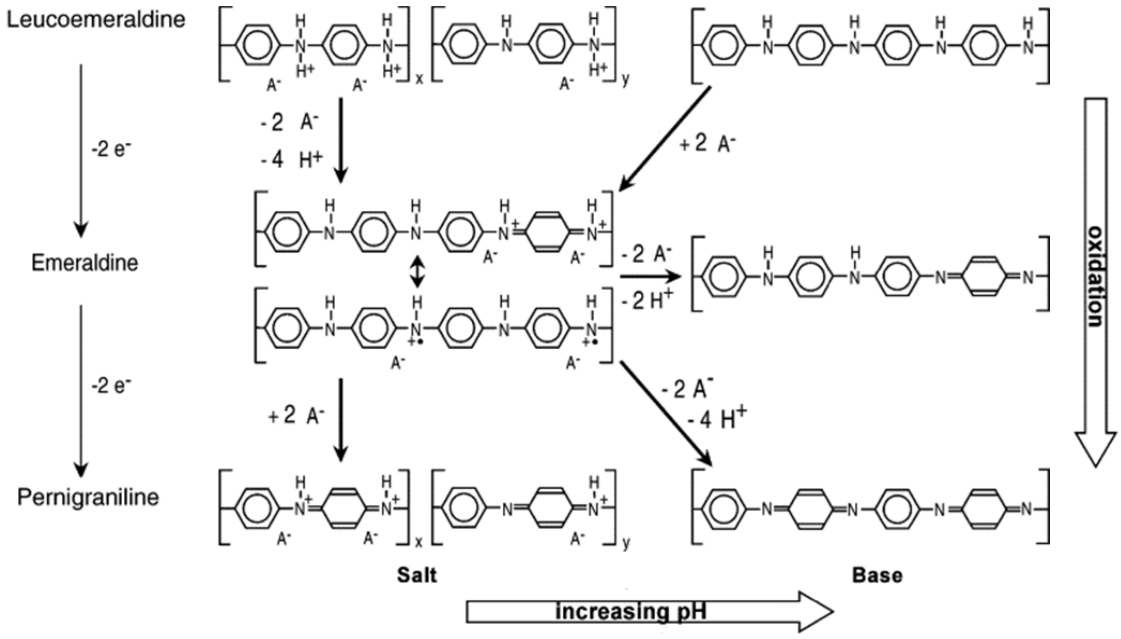

Figure 2.3. The primary oxidation states of polyaniline illustrating the transport of anions, protons, and electrons during a shift in oxidation state. Adapted from E. Smela [12].

In addition to electrical characteristics, each oxidation state of polyaniline has distinct mechanical properties. The pernigraniline state is more brittle than the reduced states, so leucoemeraldine and emeraldine are the preferred states in applications where the materials will be subjected to mechanical stress. This embrittlement is a product of the shift from amine to imine nitrogen containing groups in more oxididized state. Unlike the σ-bonds of the amine, which may rotate 360˚ about the bond axis, the π-bonds which are formed in the imine configuration are stiffer and may only be subject to limited rotation before breaking. The result of polyanilne with a high imine:amine ratio is a limited chain flexibility which cannot change its conformation to accomidate plastic deformation.

2.2.2. Synthesis

Polyaniline is an attractive conducting polymer for commercial applications because it is inexpensive and easily synthesized. The aniline monomer, shown in Figure 2.4, is a simple molecule which is already mass produced for industrial polyurethane synthesis. Aniline is typically derived from benzene and nitric acid. Depending on the desired properties and configurations, polyaniline powder can be synthesized via chemical oxidative polymerization and then processed into the desired form, or it can be directly deposited onto a conductive substrate via electrochemical polymerization.

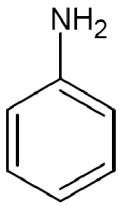

Figure 2.4. Aniline monomer used to synthesis of polyaniline.

2.2.2.1. Chemical Oxidative Polymerization

The most common method of preparing polyaniline is through chemical oxidative polymerization of aniline because it offers good control of the molecular weight distribution, and the products can be easily recovered and processed. Ammonium peroxydisulfate is most commonly used as the oxidizing agent, in a ratio of 1 mol aniline to 1.25 mol peroxydisulfate (Figure 2.5) [15]. Synthesis is typically carried out in water at temperatures near 0°C, which simplifies isolation of the products because all of the reagents are water soluble while polyaniline is not. Organic solvents may be used when lower temperatures are desired in order to achieve higher molecular weights [16-18]. Figure 2.6 shows the effect of polymerization temperature on the molecular weight of polyaniline and the polydispersity index (PDI), which is a measure of the variation of molecular weights within a sample. Lower temperatures reduce the probability of side-reactions during polymerization which could lead to chain-end termination.

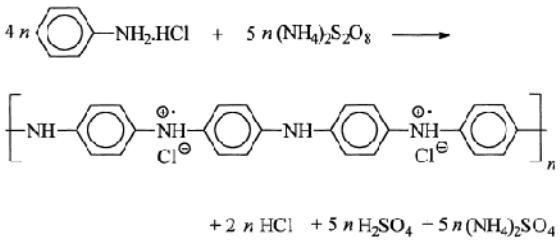

Figure 2.5. Chemical polymerization polyaniline with ammonium peroxydisulfate.

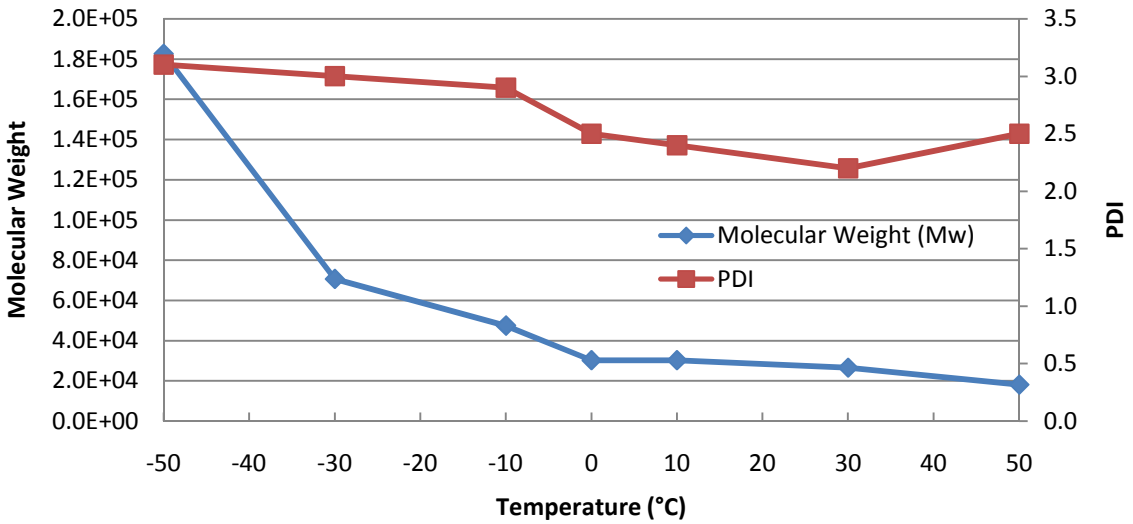

Figure 2.6. Effects of polymerization temperature on the molecular weights and polydispersities of polyaniline prepared via oxidative polymerization with an HCl concentration of 0.2 M [18].

2.2.2.2. Electrochemical Polymerization

Electrochemical polymerization of polyaniline involves the oxidation of aniline at the surface of a conductive electrode. The polymerization setup consists of an electrochemical cell containing an acidic solution with aniline monomer, an inert cathode, and an anode onto which the polyaniline is deposited. Galvanostatic, potentiostatic, or potentiodynamic polymerization methods may then be used. Unlike the products of chemical oxidative polymerization, the polyaniline produced by this method is difficult to process because a fine, easily dissolved powder cannot be produced, and it may be difficult to remove from the anode. As a result, the anode onto which the polyaniline is deposited is usually the final form of a device. Once polymerized, these polyaniline chains lack the mobility to achieve more stable conformations, so they tend to be highly amorphous. An amorphous microstructure with relatively low molecular weight chains result in weaker mechanical properties; however electrochemical polyerization is preferred when good adhesion with a conductive substrate is desired, as is the case in

many electrochemical actuator and chemical sensor applications. Electrochemical polymerization is often employed for micro-scale applications, because polyaniline is selectively deposited within conductive domains, which are easily created using conventional microfabrication techniques [19].

A scheme for the electrochemical polymerization of polyaniline (Figure 2.7), first proposed by Wantanabe *et al*, shows that the oxidation of aniline occurs when electrons are withdrawn at a positive electrode [20]. Polymerization initiates when two aniline monomers bond at the electrode surface. Propagation of the polyaniline continues because electrons can be conducted from the chain end to the electrode. The thickness of polyaniline films can be controlled in this method by regulating the total electric charge applied to a specified surface area. Electrochemical polymerization typically produces polyaniline with lower conductivity than oxidative polymerization methods because the microstructure tends to be more amorphous with greater porosity. High initiation rates observed with this method result in low average molecular weights. The initiation rate may be reduced relative to the propagation rate by reducing the polymerization potential, which is dictated by the rate of applied charge.

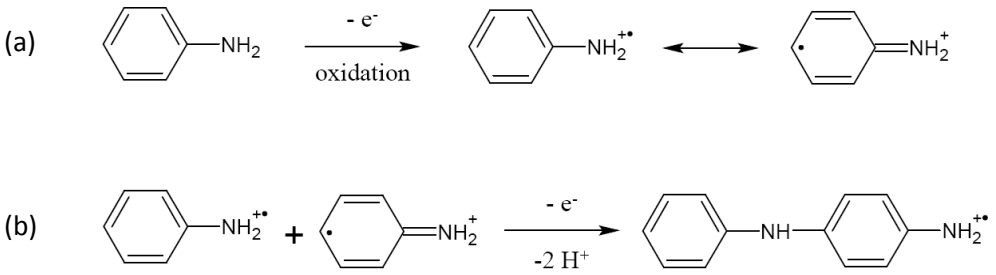

Figure 2.7. Electrochemical polymerization scheme of polyaniline showing the oxidation of aniline monomer (a) and the addition of oxidized aniline to the polyaniline chain end (b).

2.2.3. Conductivity

In order to exhibit bulk electrical conductivity, both intrachain and interchain charge transport must occur. The latter can be explained through examination of the molecular structure of the emeraldine salt state of polyaniline. Upon doping, the imine groups protonate and become positively charged, forming *bipolarons* (Figure 2.8). Anions stabilize these positively charged sites, which allow them to separate into radical cations known as a *polarons*. The conjugated π structure enables the mobility of polarons along the length of the molecule. This mobility accounts for the intrachain conductivity of polyaniline [21]. Polarons in polyaniline follow the traditional definition applying to polarons in a crystal lattice, in that the polaron exists as an electric field and a conformational distortion. In polyaniline, the conformational distortion results from differential bond lengths and geometries corresponding to amine and imine groups.

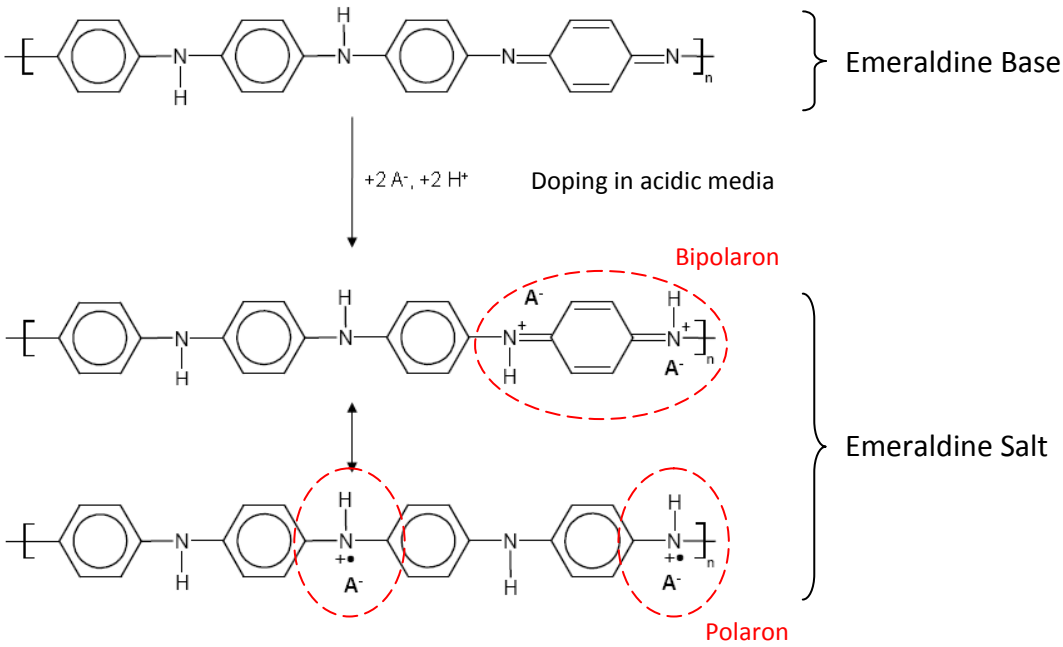

Figure 2.8. Doping of emeraldine base to form conductive emeraldine salt. (15)

Interchain charge transport occurs within crystalline regions where polyaniline molecules align and π-π stacking is prominent. Here, polarons are able to transfer among adjacent molecules through overlapping π orbitals (Figure 2.9) [22]. To support this theory, x-ray diffraction experiments demonstrated that a higher degree of crystallinity resulted in greater conductivity in polyaniline samples [23]. It is proposed that the conductivity of polyaniline is highly dependent on the rate in which charge carriers can percolate through a network of highly conductive crystalline regions surrounded by a more amorphous microstructure.

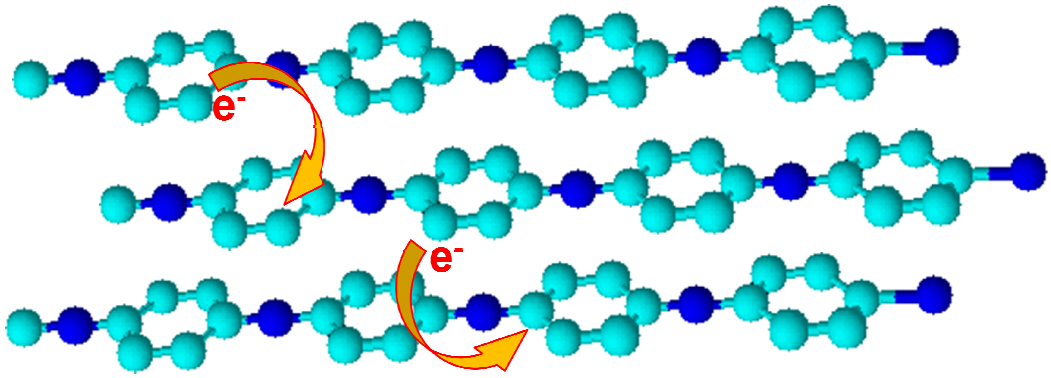

Figure 2.9. Schematic of crystalline polyaniline molecules exhibiting interchain electron mobility.

The molecular weight of polyaniline prepared via oxidative polymerization can be controlled with stoichiometry and reaction conditions, and has strong effects on the conductivity of polyaniline. Higher molecular weights produce a greater degree of crystallinity (Figure 2.10), which increases the number of sites at which interchain charge transport can take place. A linear increase in conductivity with increasing percent crystallinity is observed. Additionally, the bulk mobility of electrons via intrachain mechanisms increases because polarons can travel farther on a single chain.

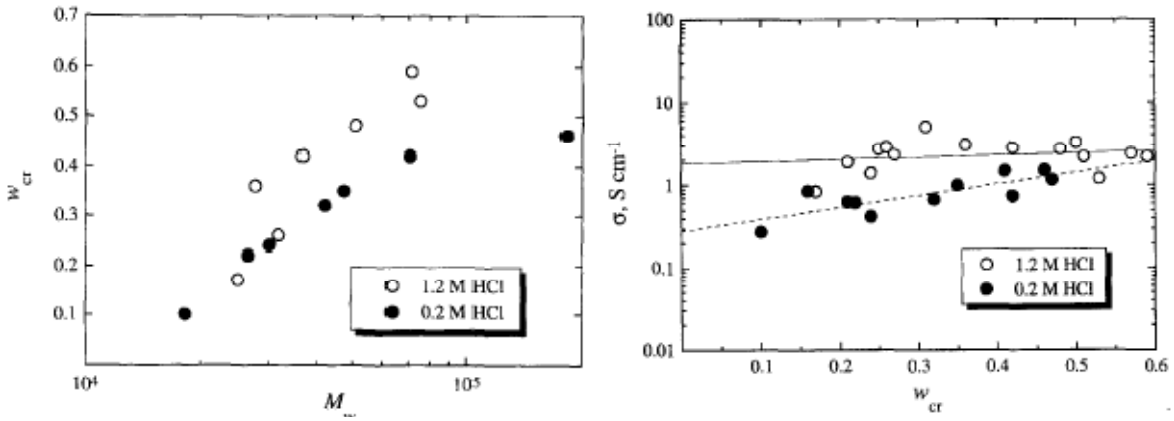

(a) (b)

Figure 2.10. Relationship between molecular weight (M_w) and degree of crystallinity (w_{cr}) (a), and the subsequent effects on the bulk conductivity (b) of polyaniline prepared via oxidative polymerization in supporting electrolyte concentrations of 0.2 M and 1.2 M. Crystallinity was determined using x-ray diffraction [18].

If the polymerization solution did not contain the desired dopant, the polymer can be de-doped to its base state in an alkaline solution, and then doped with the desired species. This process is only possible with smaller dopants such as HCl, HF, or H_2SO_4, which are able to diffuse through the polymer matrix [24]. This is common because some dopants, such as hydrochloric acid, are favorable for synthesizing high molecular weight polyaniline, while others, such as perchloric or sulfuric acids, produce higher conductivities [25].

After chemical oxidative polymerization of polyaniline, the polymer is typically dissolved into a solvent such as N-methyl-2-pyrrolidinone (NMP), and then cast or spun into coatings or films. Ryu *et al* observed a 30% increase in conductivity when the concentration of polyaniline in NMP solvent was increased from 3 wt% to 11 wt%, however this increase leads to processing difficulties associated with rapid gelling of the polymer [23]. The increase in conductivity is attributed to increased crystallinity achieved in the more concentrated solutions, evident by the XRD analysis of the polymers (Figure

2.11). Increasing crystallinity and gelling appear to be a result of the same phenomenon; while in solution, the polymers have more freedom and are able to coordinate to one another as they would in a crystalline polymer. As the solvent evaporates, the polyaniline molecules remain in the in a crystalline orientation.

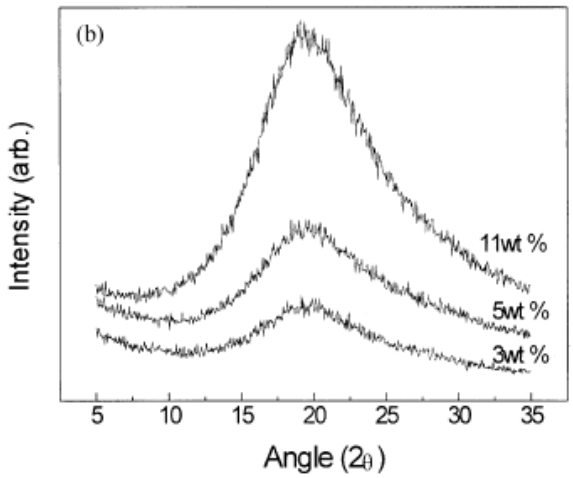

Figure 2.11. XRD spectra of polyaniline films cast from solutions of various polyaniline concentrations in NMP. Higher concentrations yielded greater crystallinity and conductivity [23].

Ryu *et al* also demonstrated that stretching of polyaniline leads to an increase in crystallinity and a corresponding increase in conductivity. When a high molecular weight polyaniline film was stretched to 400% its original length, the conductivity parallel to the stretching axis exhibited an eight fold increase, while the conductivity perpendicular to the stretching remained constant (Figure 2.12). When the molecular weight of the polyaniline was relatively low (M_w < 30,000), neither stretching nor concentration in solution had substantial impacts on the conductivity. Crystallinity is increased as the polymer chains align in the axis of stretching and can more easily coordinate to one another, which is evident from the increased definition of peaks in the XRD spectrum in Figure 2.12 as a polyaniline sample was elongated (increasing L/L_0).

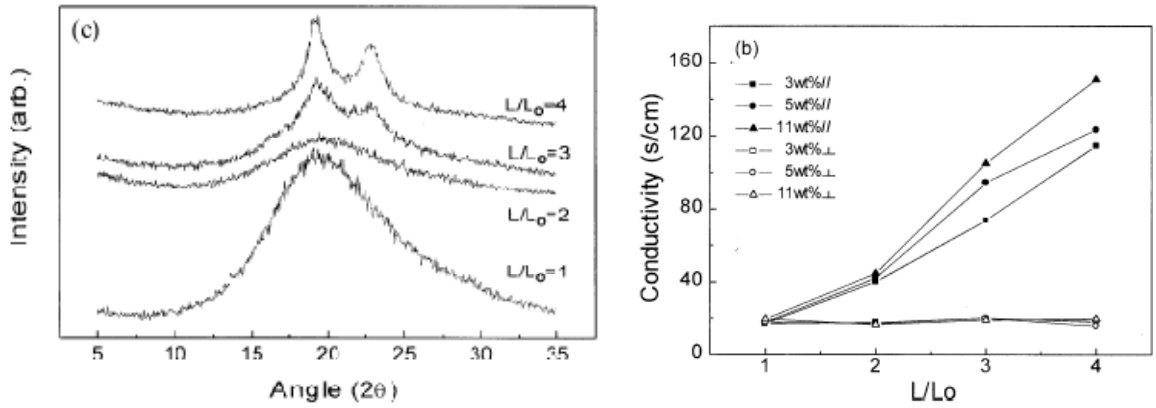

(a) (b)

Figure 2.12. XRD spectra showing increase in crystallinity with stretching (a) and corresponding increase in conductivity (b) parallel to the stretching axis of a polyaniline film doped in 1.0 M HCl. (23)

Annealing polyaniline films at temperatures below 140°C produces an increase in conductivity of polyaniline (Figure 2.13). Thermal energy allows the polyaniline chains to re-orient into the lower more stable π-stacked conformation, increasing interchain charge transport [26]. Although polyaniline is thermally stable until ~370°C, [27] annealing temperatures of 140°C and above resulted in a loss of conductivity in HCl doped polyaniline due to the diffusion of the dopant species out of the polymer [28].

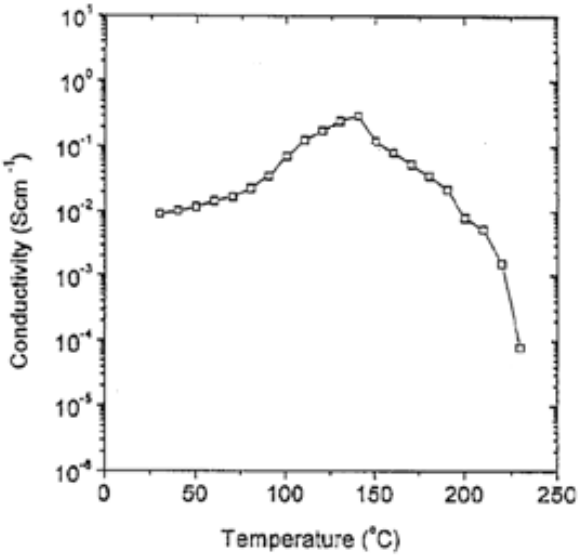

Figure 2.13. Conductivity vs. annealing temperature for an HCl doped polyaniline film, exhibiting increased conductivity with annealing temperature until ~140°C, when dopant ions begin to diffuse out of the material [28].

2.3. Polyaniline Transducers

A transducer is any device or material which converts one type of energy into another. Mechanical transducers include actuators, which typically convert electrical energy into a physical deflection or stress, and sensors, which convert strain into a measureable output. The characteristics of polyaniline actuators will be examined in detail because their behavior is inversely related to that of polyaniline sensors, and they have been the subject of intensive study.

2.3.1. Actuators

Physical displacement in polyaniline actuators is achieved through volume change resulting from ion and solvent exchange with an electrolyte. An electric or chemical potential between the polyaniline and the surrounding electrolyte is the driving force for ion exchange. Because the polymer accepts or donates electrons to remain in a charge

neutral state, actuation is always associated with the oxidation or reduction of a polyaniline.

A major pitfall of conducting polymer actuators is that they must have a medium with which to exchange ions, which usually requires that they operate in a solution. These are most often aqueous solutions, however the use of ionic electrolytes such as tetrafluoroborate in 1-butyl-3-methyl imidazolium have been shown to reduce the chemical degradation of polyaniline actuators [29]. Polyethylene oxide gel swollen with an electrolyte can be operated outside of solution, but these devices tend to dry out unless a sealant is applied, which has not yet been effectively demonstrated. Solid polymer electrolytes are more stable in air, but they reduce the rate of electrolyte exchange with the conjugated polymer, slowing actuation rates [30].

When polyaniline is oxidized or reduced, the material must absorb or expel charged ions in order to maintain a neutral net charge. The manner in which this effect occurs depends on the dopants used during synthesis. If the polymer is doped with small anions such as chlorine, then they will be expelled into solution when electrons are added to the material, resulting in a negative volume change of the polyaniline. If anions which are large and immobile within the polymer matrix, such as dodecylbenzene sulfonate (Figure 2.14), are introduced into the polymer during synthesis, anion expulsion is not possible and positive ions must be absorbed to balance charge resulting in a positive volume change of the polyaniline. Neutral solutions containing positive mobile ions such as sodium or potassium can support actuation when large dopant ions are used, although lower conductivities of the polymer reduce actuation rates. Large and small dopant ion mechanisms are shown in Figure 2.15 [31].

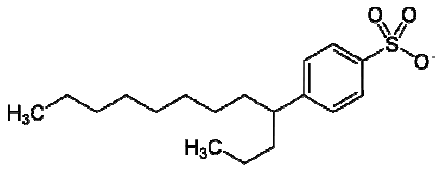

Figure 2.14. Dodecylbenzene sulfonate (DBS^-) anion, which is not mobile in polyaniline, and will be retained by polyaniline when it is reduced.

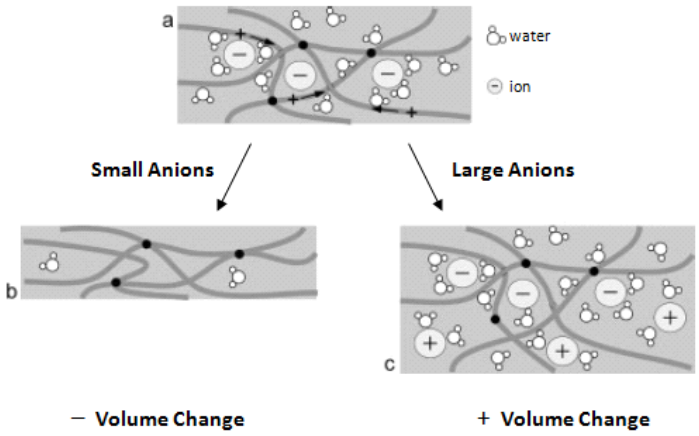

Figure 2.15. Mechanisms for volume change with the addition of electrons in a doped conjugated polymer (a) using small (b), and large (c) anions [12].

The osmotic potential produced by the adsorption of ions drives the subsequent adsorption of solvent molecules into the material, as indicated in Figure 2.15. The transport of solvent in addition to ions greatly increases the volume change during red/ox cycling. Additionally, some volume change has been attributed to the differential lengths of the C-C and C=C bonds, changes in bond directionality, and inter-chain interactions; all of which vary with oxidation state [32-34].

Conjugated polymer actuators have been developed in a variety of scales and configurations. The simplest are linear actuators which utilize volume change to generate displacement in one direction. The deflection along a single axis can be enhanced by restricting the deflection in other axes, achieved by adding higher modulus components in directions perpendicular to the primary axis of deflection (Figure 2.16) [35]. A more

common format for amplifying deflection is the use of multi-layer bending structures. Asymmetrical expansion of a polyaniline layer relative to an inactive layer or an opposing polyaniline layer can produce dramatic bending angles from relatively small strains (Figure 2.17). Bending actuators can easily be scaled to produce micro-scale actuators. Elizabeth Smela and colleagues have successfully fabricated “cell clinics” which enclose single cells in boxes which are opened and closed with polypyrrole based bilayer actuators [12].

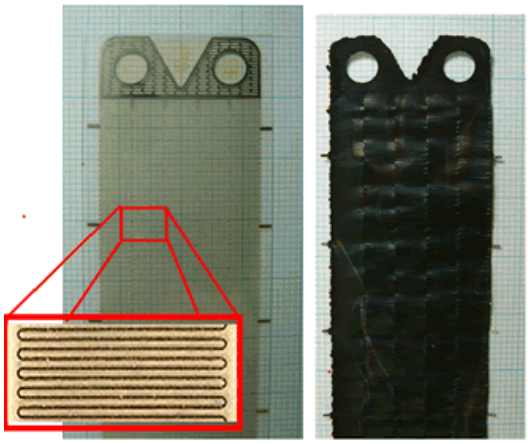

Figure 2.16. The zigzag wire in this polypyrrole linear actuator restricts the expansion and contraction of the material in the horizontal direction, amplifying its vertical displacement [35].

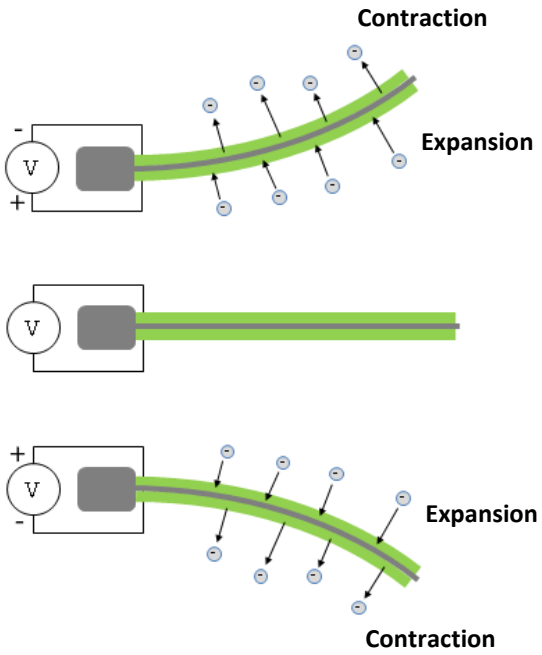

Figure 2.17. Anion transport and subsequent deflection caused by application of oxidation and reduction potentials to a polyaniline bilayer actuator.

2.3.2. Sensors

Just as the transport of ions can induce a volume change in polyaniline, a mechanically induced volume change should drive ion transport. When this occurs, a charge imbalance in the material will result in the generation or consumption of electric charge. The magnitude of an applied strain should correlate with the amount of electric charge generated or consumed, which can be measured as an electric current.

2.3.2.1. Sensor Characteristics

Before assessing the strain sensing properties of polyaniline, it is important to understand the characteristics which are used to quantify all sensors. The following are descriptions of important sensor characteristics, and how they relate to the evaluation of polyaniline as a strain sensing material [36].

Accuracy

The accuracy of a sensor relates to its ability to measure the absolute value of a specified metric. Very accurate sensors typically require calibration to a known standard to account for drift and changes in environmental conditions. For example, a user will typically *tare* a microbalance before making a precise weight measurement. This characteristic is particularly relevant to polyaniline sensors because the electrochemical properties of polyaniline may vary widely with environmental characteristics such as electrolyte species/concentration and temperature, as well as material characteristics such as oxidation state, microstructure, and molecular weight.

Precision

Precision is a measure of a sensor's ability to produce the same output with identical inputs. Precision incorporates repeatability, when multiple measurements are taken over a short period of time, as well as reproducibility, when multiple measurements are taken over long periods of time, by different users, with different instruments, or at different locations. The key to high reproducibility in polyaniline sensors is to ensure that the pretreatment of the polymer is consistent, as the equilibrium chemical state of polyaniline depends on its oxidation history.

Resolution

The resolution, also known as discrimination, of a strain sensor is defined as the smallest deflection which produces a detectable output. While this is important characteristic in any strain sensing device, it is generally a result of noise within all the

components of a strain measuring instrument, and not the sensing element alone. For this reason, examining resolution is not particularly relevant to the fundamental electrochemical properties of polyaniline.

Range

The input range will dictate the operational conditions of a sensor, and the output range will dictate the system required to interpret the signal. The input range of a polyaniline sensor is limited by the greatest strain which can be applied to the material before inducing permanent damage or deformation. The output range will influence the type of circuitry required to interpret the signal, primarily whether amplification is necessary.

Sensitivity

Sensitivity is a measure of the slope of the output with increasing input. The magnitude of the electrical output of polyaniline will depend on how efficiently work done applied by stretching a polyaniline film can be converted into electrical energy. This characteristic will dictate the viability of polyaniline based energy harvesting devices.

Linearity

Like sensitivity, linearity takes into account the slope of the output with increasing input; however it focuses on variation in the slope over the functional range of

the sensor. Non-linear sensors require more complex systems to interpret the output signal, but non-linearity can be corrected with a calibration curve.

Hysteresis

Hysteresis is the dependency of the output signal on the trajectory of the input. In a polyaniline sensor, hysteresis may depend on input factors such as strain rate or whether applied strain is positive or negative.

Random Error

Also called noise, random error is sensor output which does not result from the input. This type of error typically affects the resolution of a sensor; as the output signal to noise ratio (S/N) approaches 1, it becomes difficult to distinguish the two. The time dependency of ion diffusion into polyaniline will reduce high frequency noise produced by ambient vibrations.

Systemic Error

Systemic error is introduced through inputs which are unintentional or out of the control of the user. These inputs can be introduced via operational/observational variation (user error), drift, attenuation or distortion of the signal in the transmission system, or environmental changes such as temperature variation. Systemic errors typically affect the accuracy of a sensor, and can be corrected using compensation methods such as internal calibration standards, filtering, and feedback. Ensuring that test fixturing is well

constructed and methodologies are consistent will help to reduce systemic variation in polyaniline sensor output. Testing polyaniline in steady state conditions will reduce drift.

2.3.2.2. Prior Work

The earliest study which evaluated the electrical response of polyaniline to a mechanical stimulus was published in 1997 by Takashima *et al* [37]. When 1.3 MPa loads were applied using 10 g weights to the polyaniline films in a 1 molar HBF_4 solution, currents were induced as shown in Figure 2.18. The authors called this phenomenon the mechanochemoelectrical (MCE) effect, which they attributed to a redox current induced by a change in the density of states of the polymer. The induced charge, which was found by integrating the current, was observed to be linear with increasing loads from 0.5 to 3.5 MPa, which was the full range of published data. Observations of the induced charge at various relative potentials indicated that polyaniline only exhibited the MCE effect when in its emeraldine oxidation state, which is consistent with observed variation in polyaniline conductivity at different oxidation potentials.

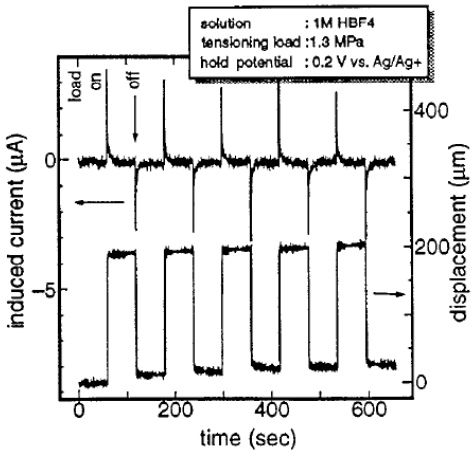

Figure 2.18. Displacements and induced currents produced by tensile loads on a 30 μm x 2 mm x 10 mm polyaniline specimen in an HBF_4 solution [37].

Apart from Takashima *et* al, there has been no published work examining the electrical response of polyaniline to mechanical strain; however the investigation of these affects in polypyrrole, a similar conducting polymer, can offer additional insight. Polypyrrole was likely chosen by more authors due to its simple oxidation chemistry, with only two stable oxidation states. A similar experiment to that in Figure 2.18 was conducted using DBS^- doped polypyrrole (Figure 2.19) [38]. This study provided a more detailed examination of the factors affecting output current. A linear increase in current amplitude with increasing applied stress (Figure 2.20a) was observed, however the peak amplitude does not necessarily correlate directly with the power output of the sensor, so many of the sensing characteristics of this material remain unknown. The application of 0.8 MPa stresses at various potentials relative to an Ag/AgCl reference electrode indicated a strong dependence of the electrical output on the oxidation state of the polymer (Figure 2.20b).

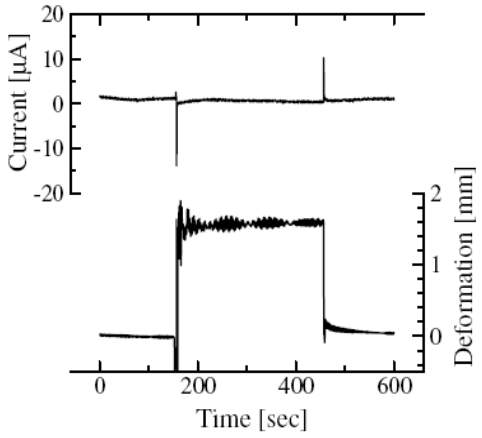

Figure 2.19. Current and deformation profiles of a 23 µm x 4.0 mm x 10.0 mm DBS doped polypyrrole film during the application of a 10.0 g load [38].

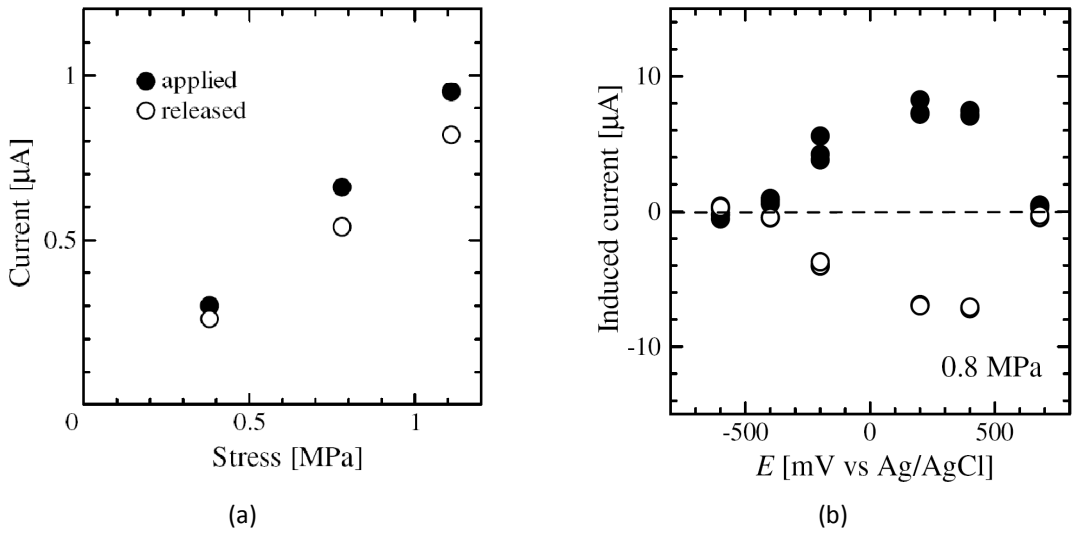

Figure 2.20. Linearly increasing current observed when increasing loads were applied to a polypyrrole film (a) and dependence of induced current in a polypyrrole film on the applied oxidation potential (b) [38].

A recent study at the University of Wollongong, Australia, examined the dynamic properties of polypyrrole bilayer sensors. By observing the current and potentials produced at a range of sinusoidal displacement frequencies, they were able to derive a set of transfer functions to predict the current and potential response at any frequency. Figure 2.21 shows the current and voltage responses when a 170 μm thick bilayer was flicked with a ruler, illustrating the frequency response attainable in these devices. In a parallel study, authors were able to control the polarity of the output current by varying the size of the dopant ions used during synthesis (Figure 2.22), which correlates to the actuation characteristics presented in section 3.2.1. Figure 2.22 also shows the dependence of electrical output on oxidation state [40].

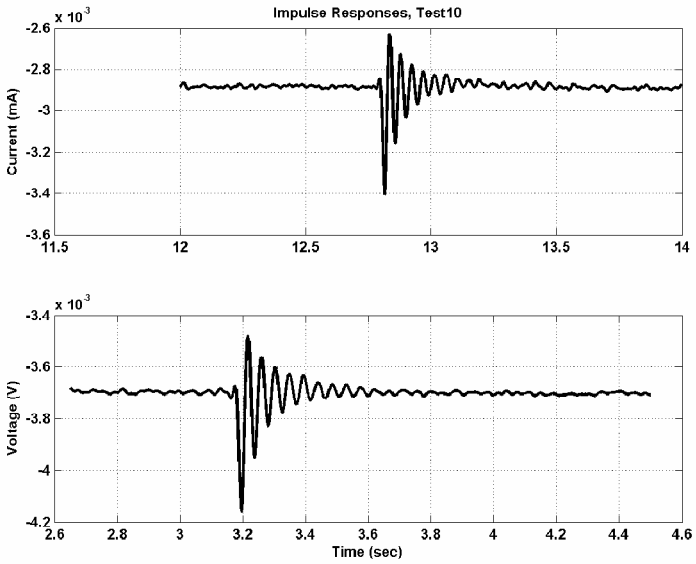

Figure 2.21. Current and voltage profiles produced when a polypyrrole bending bilayer sensor was flicked with a ruler [40].

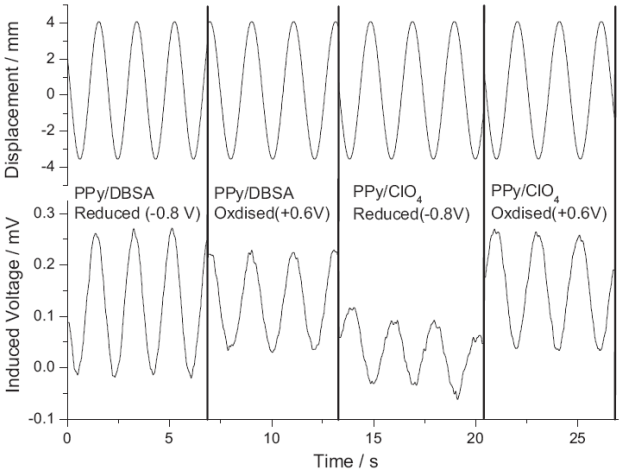

Figure 2.22. Output voltage resulting from sinusoidal input deflections to the end of polypyrrole bilayer sensors with large (DBSA) and small (ClO_4) dopants in oxidized and reduce states [40].

2.4. References

[1] B. Bolto, R. Mcneill, D. Weiss. "Electronic Conduction in Polymers." *Australian Journal of Chemistry*, vol. 16, pp. 1076 – 1089, 1963.

[2] C. K. Chiang, C. R. Fincher, Y. W. Park, A. J. Heeger, H. Shirakawa, E. J. Louis, S. C. Gau, and A. G. McDiarmid. "Electrical Conductivity in Doped Polyacetylene." *Physical Review Letters*, vol. 39, pp. 1098 – 1101, 1977.

[3] T. Vernitskaya, O. Efimov. "Polypyrrole: a Conducting Polymer; it's Synthesis, Properties, and Applications." *Russian chemical reviews*, vol. 66, 1997.

[4] S. Masubwhi, S. Kazama, R. Matsushitaz, T. Matsuyama. "The Influence of Dopant Species on Transport Properties in As-Grown Polypyrrole Films Prepared by Electrochemical Method." *Synthetic Metals*, vol. 69, pp. 345-346, 1995.

[5] Sony Electronics, Inc. Sony. 2008. <http://www.sonystyle.com> (accessed February 16, 2009).

[6] C. Brabec, J. Durrant. "Solution Process Organic Solar Cells." *MRS Bulletin*, vol. 33, pp. 670-675, 2008.

[7] D. Wei, A. Ivaska. "Electrochemical Biosensors Based on Polyaniline." *Chem Anal*, vol. 51, pp. 893, 2006.

[8] Z. Tahira, E. Alociljaa, D.Groomsb. "Polyaniline synthesis and its biosensor application." *Biosensors and Bioelectronics*, vol. 20, pp. 1690–1695, 2005.

[9] D. DeBerry. "Corrosion protective polyaniline epoxy blend coatings on mild steel." *Journal of The Electrochemical Society*, vol. 132, pp. 1022, 1985.

[10] W. Lu, R. Elsenbaumer, B. Wessling. "Corrosion protection of mild steel by coatings containing polyaniline." *Synthetic Metals*, vol. 71, pp. 2163-2166, 1995.

[11] T. Otero. Conductive Polymers: Transport, Photophysics, and Applications. New York: John Wiley & Sons, 1997.

[12] E Smela, W Lu, BR Mattes. "Polyaniline actuators Part 1. PANI(AMPS) in HCl." *Synthetic Metals*, vol. 151, pp. 25-42, 2005.

[13] D. Orata, D. Buttry. "Determination of Ion Populations and Solvent Content as Functions of Redox State and pH in Polyaniline." *Journal of the American Chemical Society*, vol. 109, pp. 3574–3581, 1987.

[14] G. Wallace, P. Dastoor, D. Officer, C. Too. "Conjugated polymers: New materials for photovoltaics." *Chemical Innovation*, vol. 30, pp. 14-22, 2000.

[15] J. Stejskal. "Polyaniline. Preparation of a Conducting Polymer." *International Union of Pure and Applied Chemistry*, vol. 74, pp. 857–867,2002.

[16] S. Palaniappan, A. Chellachamy. Process for the preparation of polyaniline salt . Patent 6630567, 2003.

[17] P. Adams, P. Laughlin, A. Monkman. "Synthesis of high molecular weight polyaniline at low temperatures." *Synthetic Metals*, vol. 76, pp. 157-160, 1996.

[18] J. Stejskal, A. Riede, D. Hlavat, J. Proke, M. Helmstedt, P. Holler. "Effect of polymerization temperature on molecular weight, crystallinity, and electrical conductivity of polyaniline." *Synthetic Metals*, vol. 96, pp. 55-61, 1998.

[19] E. Smela. "Microfabrication of PPy microactuators and other conjugated polymer devices." *Journal of Micromechanics and Microengineering*, vol. 9, pp. 1–18, 1999.

[20] A. Watana, K. Mori, Y. Asa, S. Urakami, Y. Akamura. "Polyanilines Prepared by Eletrochemical Polymerization: Molecular Weight of Polyaniline Films." *Journal of Polymer Science: Part A: Polymer* Chemistry, vol. 27, 1989.

[21] J. Kim, S. Park, N. Scherer. "Ultrafast Dynamics of Polarons in Conductive Polyaniline: Comparison of Primary and Secondary Doped Forms." *Journal of Physical Chemistry*, vol. 122, pp. 15576-15587, 2008.

[22] K. Lee, S. Cho, S. Park, A. Heeger, C. Lee, S. Lee. "Metallic transport in polyaniline." *Nature*, vol. 441, pp. 65-68, 2006.

[23] K. Ryu, S. Chang, S. Kang, E. Oh, C. Yo. "Physicochemical and Electrical Characterization of Polyaniline Induced by Crosslinking, Stretching, and Doping." *Bulletin of the Korean Chemical Society*, vol. 20, pp. 333-335, 1999.

[24] T. Skotheim, J. Reynolds. Handbook of Conjugated Polymers. CRC Press, 2007.

[25] M. Catedral, A.Tapia, R. V. Sarmago, J. Tamayo, E. Rosario. “Effect of Dopant Ions on the Electrical Conductivity and Microstructure of Polyaniline (Emeraldine Salt)”. Quezon City: University of the Philippines, 2004.

[26] R. Ansari, W. E. Price, G. G. Wallace. "Effect of thermal treatment on the electroactivity of polyaniline." *Polymer*, vol. 37, pp. 917-923, 1996.

[27] H. Wang, R. Romero, B. Mattes, Y. Zhu, M. Winokur. "Effect of Processing Conditions on the Properties of High Effect of Processing Conditions on the Properties of High." *Journal of Polymer Science*, vol. 38, pp. 194–204, 2000.

[28] S. Kim, I. Chung. "Annealing effect on the electrochemical property of polyaniline complexed with various acids." *Synthetic Metals*, vol. 97, pp. 127-133, 1998.

[29] W. Lu, A. Fadeev, B. Qi, E. Smela, B. Mattes, J. Ding, G. Spinks, J. Mazurkiewicz, D. Zhou, G. Wallace, D. MacFarlane, S. Forsyth, M. Forsyth.

"Use of Ionic Liquids for pi-Conjugated Polymer Electrochemical Devices." *Science*, vol. 297, pp. 983 – 987, 2002

[30] E. Smela. "Conjugated Polymer Actuators for Biomedical Applications." *Advanced Materials*, vol. 15, pp. 481-494, 2003.

[31] W. Takashima, B. Dufour, S. Pandey, K. Kaneto, A. Pron. "Electrochemically generated deformations of polyaniline film plasticized with di-2-butoxy-2-ethoxy-ethyl ester of sulfosuccinic acid." *Sensors and Actuators B*, vol. 99, pp. 601–607 , 2004.

[32] E. Kupila, J. Lukkari, and J. Kankare. "Redox Processes in Thick Films of Polypyrrole/Dodecylsulfate in the Presence of Alkali Chlorides." *Synthetic Metals*, vol. 74, pp. 207-215, 1995.

[33] R. Baughman. "Conducting Polymer Artificial Muscles." *Synthetic Metals*, vol. 78, pp. 339-354, 1996.

[34] M. Winokur, P. Walmsley, J. Moulton, P. Smith, A Heeger. "Structural Evolution of Iodine Doped Poly(3-alkylthiophenes)." *Macromolecules*, vol. 24, pp. 3812–3815, 1991.

[35] S. Hara, T. Zama, A. Ametani, W. Takashima, K. Kaneto. "Enhancement in electrochemical strain of a polypyrrole–metal composite film actuator." Journal of Materials Chemistry vol. 14, pp. 2724 – 2725, 2004.

[36] R. Gutierrez-Osuna. Lecture 2: Sensor characteristics. Wright State University. Intelligent Sensor Systems.

[37] W. Takashima, T. Uesugi, M. Fukui, M. Kaneko, K. Kaneto. "Mechanochemoelectrical Effect of Polyaniline Film." *Synthetic Metals*, vol. 85, pp. 1395-1396, 1997.

[38] W. Takashima, K. Hayasi, K. Kaneto. "Force detection with Donnan equilibrium in polypyrrole film." *Electrochemistry Communications*, vol. 9, pp. 2056–2061, 2007.

[39] Y. Wu, G. Alici, J. Madden, G. Spinks, G. Wallace. "Soft Mechanical Sensors Through Reverse Actuation of Polypyrrole." *Advanced Functional Materials*, vol. 17, pp. 3216–3222, 2007.

[40] G. Alici, G. Spinks, J.Madden, Y. Wu, G. Wallace. "An Investigation into Behaviour of Electroactive Polymers as Mechanical Sensors." IEEE/ASME International Conference on Advanced Intelligent Mechatronics. 2007.

CHAPTER 3

THEORETICAL MODELING

Mathematical models which predict the electrical response of polyaniline films subjected to uniaxial tensile strain will be developed in this chapter. Later, these models will be contrasted against experimental results to determine properties such as diffusivity and ion solubility in polyaniline, and to reveal any deviations from a diffusion based model of ion transport.

3.1. Charge Displacement

When strains are applied to a material, a volume change will result.

$$\Delta V = V_f - V_i \tag{3.1}$$

$$V_i = X \cdot Y \cdot Z \tag{3.2}$$

$$V_f = (X + X\varepsilon_X)(Y + Y\varepsilon_Y)(Z + Z\varepsilon_Z) \tag{3.3}$$

When strains are applied along one axis (Z), Poisson's ratio (ν) will dictate the subsequent strains in perpendicular axes (X and Y):

$$\varepsilon_X = \varepsilon_Y = -\nu\varepsilon_Z \tag{3.4}$$

When applied to Equation 3.3, this yields:

$$V_f = (X - X\nu\varepsilon_Z)(Y - Y\nu\varepsilon_Z)(Z + Z\varepsilon_Z) \tag{3.5}$$

or,

$$V_f = (X \cdot Y \cdot Z)(1 - \nu\varepsilon_Z)^2(1 + \varepsilon_Z) \tag{3.6}$$

When immersed in an appropriate electrolyte solution, polyaniline will absorb anions until they reach a steady state anion concentration. The steady state anion concentration in the polyaniline is not necessarily equal to the concentration in the solution, but may be a function of both solution concentration (C_s) and anion solubility in polyaniline (C_∞) [1]. A change in volume between the strained and unstrained conditions will result in a change in anion concentration within the film (Equation 3.7).

$$\Delta C = C_s - C_\infty \tag{3.7}$$

Where,

$$C_s = C_\infty \frac{V_i}{V_f} \tag{3.8}$$

Equations 3.6 and 3.8 are substituted into Equation 3.7 to yield Equation 3.9, which describes change in anion concentration in terms of steady-state concentration and uniaxial strain on the polymer film.

$$\Delta C = C_\infty \left(\frac{1}{(1 - \nu\varepsilon_Z)^2(1 + \varepsilon_Z)} - 1 \right) \tag{3.9}$$

The total number of anions absorbed or desorbed (N_A-) is the product of the change in anion concentration and the initial volume (Equation 3.10). Subsequently, the total electric charge displaced is a product of the number of anions absorbed or displaced and the valency (n) of the ions, which will be 1 for most ions (Equation 3.11). This assumes that no positive ions are absorbed by the polymer. It should be noted that an additional factor of 96,493 ($C/mol \cdot e^-$) is needed to convert moles of ions to Coulombs of charge displaced.

$$N_{A^-} = \Delta C(XYZ) \tag{3.10}$$

$$Q = nN_{A^-} \tag{3.11}$$

This yields the total electrical charge displaced by uniaxial strain (Equation 3.12). Figure 3.1 shows is a plot of Equation 3.12 which has been normalized with respect to concentration and sample dimension and assumes a Poisson's ratio of 0.35, which is typical of polymeric materials and is in the range of published values for polyaniline [2-3]. Based on this plot, the charge displaced when small strains on the order of 0 – 3 % are applied may be approximated as linear with increasing strain amplitude.

$$\boldsymbol{Q = C_{\infty}(XYZ)\left(\frac{1}{(1-\nu\varepsilon_Z)^2(1+\varepsilon_Z)} - 1\right)} \tag{3.12}$$

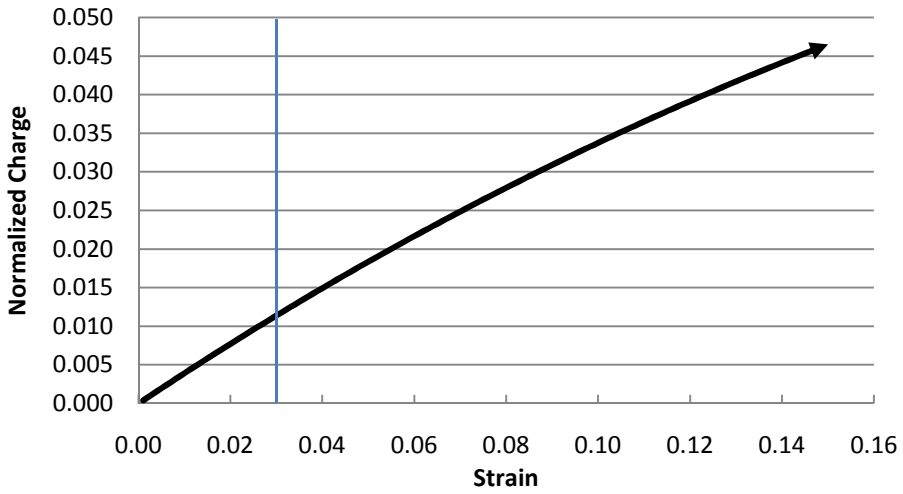

Figure 3.1. The total charge displaced by uniaxial strain on a polyaniline film with ν = 0.35 through the absorption of anions.

3.2. Diffusion

The previous section describes the total number of anions which are expected to be transported between initial application of strain and steady state conditions. As with any process involving mass transport, the absorption of ions is not instantaneous. With

the assumption that ion transport is solely an effect of imbalance in ion concentration, the rate of ion absorption in these conditions is dictated by the process of diffusion.

3.2.1. Diffusion Rate

This model assumes that the rate of anion transport through the polymer is much slower than that in the surrounding electrolyte solution, and therefore the effects of the depletion region in the electrolyte/film interface are negligible. This assumption is supported by empirical which has shown that the diffusivity of chlorine ions in water is typically 10^3 greater than in polyaniline [4].

The diffusion of anions within polyaniline follows Fick's second law (Equation 3.13), which describes the diffusion of a species in non-steady-state conditions. Fick's second law assumes that diffusivity is independent of the diffusing species concentration, which should be valid in this application because the operational concentration gradients are small.

$$\frac{dC}{dt} = D\frac{d^2C}{dx^2} \tag{3.13}$$

Fick's second law as it is expressed in Equation 3.13 assumes an infinite diffusion path length, therefore it must be modified for a system of finite volume (Figure 3.2). Crank and Park developed such a model in 1968 to describe the absorption of solvent into polymer samples. A numerical model must be used to express concentration at point (x) and time (t) (Equation 3.14), or as the amount of diffusing species (N_t) which has entered the polymer at time (t) (Equation 3.15) [5].

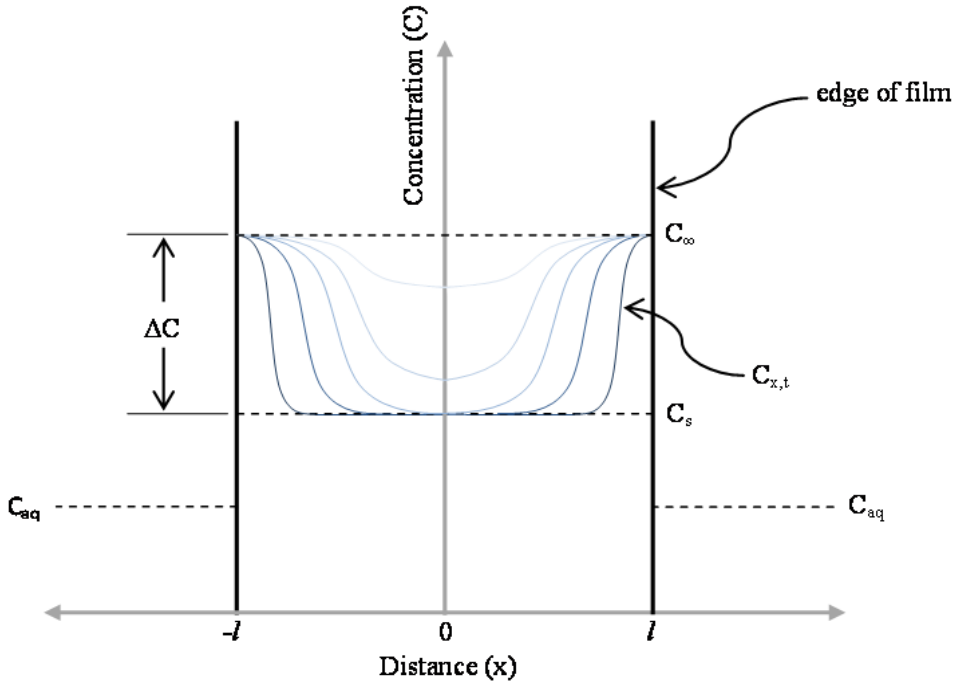

Figure 3.2. Schematic cross section of a conducting polymer film after a positive strain has been applied. The aqueous anion concentration (C_{aq}), the steady state anion concentration in the conducting polymer (C_∞), the anion concentration in the conducting polymer immediately after straining (C_s), and the anion concentration at point (x) and time (t) within the polymer ($C_{x,t}$) are shown.

$$\frac{C_{x,t} - C_\infty}{C_s - C_\infty} = \frac{4}{\pi}\sum_{n=0}^{\infty}\frac{1}{2n+1}sin\left(\frac{(2n+1)\pi x}{l}\right)\exp\left(-\frac{(2n+1)^2\pi^2}{l^2}\right)Dt \tag{3.14}$$

$$\frac{N_\infty - N_t}{N_\infty} = \frac{8}{\pi^2}\sum_{n=0}^{\infty}\frac{1}{(2n+1)^2}exp\left(-\frac{D(2n+1)^2\pi^2 t}{l^2}\right) \tag{3.15}$$

N_∞ is the total number of ions which enter the polymer between the initial application of strain (t = 0) and steady-state (t = ∞) conditions. For shorter times, when $\frac{N_t}{N_\infty} \leq 0.50$, Equation 3.15 may be simplified to Equation 3.16 with less than 0.1 % error. For longer times, when $\frac{N_t}{N_\infty} \geq 0.55$, Equation 3.15 may be simplified to Equation 3.17 with less than 0.1% error [6]. Both of these equations may be used in conjunction to predict ion absorption from the initial application of strain until steady-state conditions are reached.

$\frac{N_t}{N_\infty} \leq 0.50$; $$N_t = N_\infty \frac{8}{l}\left(\frac{Dt}{\pi}\right)^{1/2} \quad (3.16)$$

$\frac{N_t}{N_\infty} \geq 0.55$; $$N_t = N_\infty - N_\infty \frac{8}{\pi^2} exp\left(-\frac{\pi^2 Dt}{l^2}\right) \quad (3.17)$$

3.2.2. Output Current

Electric current is defined as the rate of electric charge transfer. For this application, electric current can be expressed as the number of ions which enter the polymer within a specified time interval. Therefore, electric current is equal to the derivative of the number of ions which have entered the polymer with respect to time after converting the amount of diffusing species into coulombs of charge (Equations 3.18 & 3.19). This method assumes a zero resistance electrical pathway out of the polymer, so that capacitive charge build up does not affect the absorption kinetics of the diffusing species.

$\frac{N_t}{N_\infty} \leq 0.50$; $$\boldsymbol{i = Q\frac{4}{l}\left(\frac{D}{\pi t}\right)^{1/2}} \quad (3.18)$$

$\frac{N_t}{N_\infty} \geq 0.55$; $$\boldsymbol{i = Q\frac{8D}{l^2} exp\left(-\frac{\pi^2 Dt}{l^2}\right)} \quad (3.19)$$

3.2.3. Output Potential

When the circuit to the polyaniline sample is held open, accumulation of charge in the material will result in a potential between the film and its surroundings. As anions are absorbed and the potential difference increases, electrostatic forces will begin to repel anions from the film, and fewer anions will be absorbed than would be in a closed circuit technique. Steady-state conditions will be achieved when the osmotic potential driving

the adsorption of ions is in equilibrium with the electrostatic potential repelling anions. This effect of both osmotic and electrostatic potentials affecting absorption across a membrane or interface is known as the Gibbs-Donnan effect [7].

The potential of a film resulting from a tensile strain will be equal to the total charge displacement predicted in Equation 3.12 less a factor (cV) resulting from the Gibbs-Donnan effect, and divided by its capacitance (Equation 3.20). Predicting the potential in a single film in tensile strain is difficult because many variables and assumptions must be used to calculate the capacitance of the system. If a bending bilayer format is used (Figure 2.17), opposing polyaniline films can be modeled as a parallel plate capacitor (Equation 3.21), where d is the distance between films, ε_r is the permittivity of the material between the films, ε_0 is the permittivity of free space (ε_0 = 8.854x10^{-12} F/m), and A is the area of overlap between the two films.

$$V = \frac{Q(1 - cV)}{C} \tag{3.20}$$

$$V = \frac{Q(1 - cV)d}{\varepsilon_r \varepsilon_0 A} \tag{3.21}$$

3.2.4. Cutoff Frequency

If a series of opposing strains are applied at low frequencies, when $\frac{N_t}{N_\infty}$ is able to approach 1, each strain will produce an independent current peak per Equations 3.18 & 3.19. If a series of opposing strains are applied at higher frequencies, when $\frac{N_t}{N_\infty} < 1$, the diffusing species will not have time to reach steady state concentration (C_∞), and the conversion efficiency of mechanical work into electrical energy will be reduced. This

decrease in efficiency with increasing frequency will follow the profile of Figure 3.3, and is analogous to the cutoff frequency in an RC lowpass filter, and is expressed as:

$$\frac{N_t}{N_\infty} = 1 - \frac{8}{\pi^2} exp\left(-\frac{\pi^2 D}{l^2 f}\right) \tag{3.22}$$

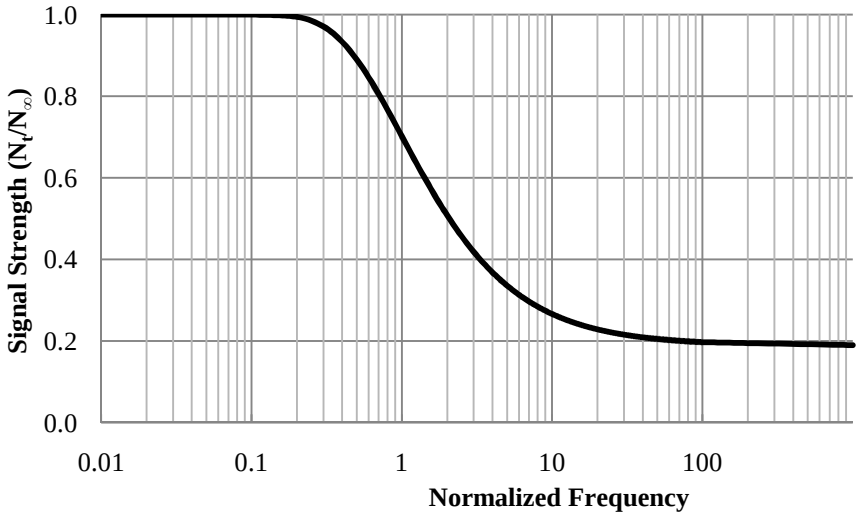

Figure 3.3. Fraction of maximum charge displacement as a function of oscillation frequency, which has been normalized with respect to diffusion path length and diffusivity.

3.3. References

[1] A. Makradi, S. Ahzi, R. Gregory. "Modeling of the Mechanical Response and Evolution of Optical Anisotropy in Deformed Polyaniline." *Polymer Engineering and Science*, vol. 40, pp. 1716-1723 ,2000.

[2] A. Tang, O. Sanda. "Diffusion coefficient of chlorine in water at 25-60 C." *Journal of Chemical & Engineering Data*, vol. 30, pp. 189-191, 1985.

[3] E. Erdem, M. Karakısla, M. Sacak. "The chemical synthesis of conductive polyaniline doped with dicarboxylic acids." *European Polymer Journal*, vol. 40, pp. 785–791, 2004.

[4] E. Glueckauf, R. Watts. "The Donnan Law and Its Application to Ion Exchanger Polymers." Proceedings of the Royal Society of London. Series A, Mathematical and Physical. The Royal Society, 1962. 339-349.

[5] G. Park, J. Crank. Diffusion in Polymers. London and New York: Academic Press, 1968.

[6] S. Choa, D. Kima, S. Park. "Effects of self-assembled monolayers of aminothiophenols on polyaniline films." *Electrochemistry of Electroactive Materials*, vol. 53, pp. 3820-3827, 2008.

[7] J. Vergnaud. Liquid transport processes in polymeric materials. Prentice Hall, 1991.

CHAPTER 4

SAMPLE FABRICATION

Polyaniline films were fabricated with electrochemical polymerization and solution casting techniques. Polyaniline films cast from solutions containing commercially prepared polyaniline powder with NMP and HPMI co-solvents were chosen for further analysis because they exhibited superior mechanical properties to electrochemically prepared films. This chapter details the processes and difficulties associated with the development of each method.

4.1. Electrochemical Polymerization

Electrochemical polymerization of aniline monomer (Sigma-Aldrich, CAS #: 62-53-3) onto conductive substrates in acidic media was conducted using constant potential and constant current methods. Aqueous solutions of 0.1 M aniline, 1.0 M H_2SO_4 (prepared from 30 wt% H_2SO_4 in H_2O, Sigma-Aldrich, CAS#: 7664-93-9) in DI water were used. Conductive substrates were prepared by attaching 5 cm strips of copper tape to the top of 2 cm x 4 cm sheets of low-density polyethylene cut from sections of a Ziploc bag, and then sputtering gold over the LDPE and copper tape for 280 seconds in a Pelco Model 3 with ~15 mA ion current. The copper tape served as an electrical contact, and was not exposed to fluids throughout the polymerization or testing processes, as it is not inert in acidic solutions. Electrochemical polymerization samples are show in Figures 4.2 & 4.4.

4.1.1. Constant Potential Polymerization

Constant potential polymerization was performed using a common three electrode cell (Figure 4.1). In this configuration, the working electrode (substrate) is held at a constant positive potential relative to the reference electrode by regulating the current between the counter and working electrodes.

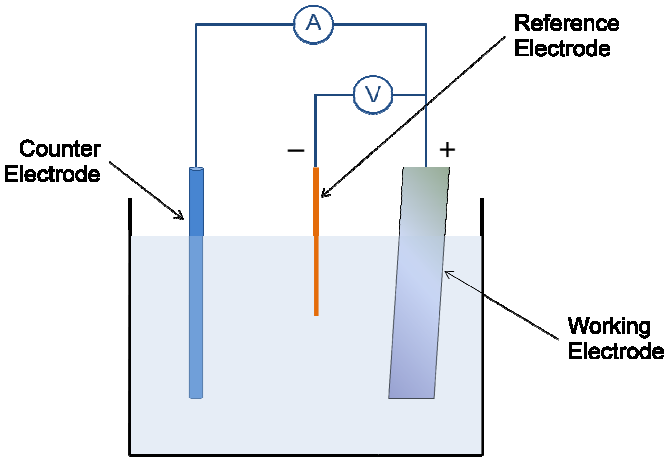

Figure 4.1. Schematic of a 3-electrode cell used for constant potential polymerization of polyaniline. A positive potential caused aniline to polymerize out of the supporting electrolyte solution at the working electrode.

Figure 4.2 shows the polymerization setup and the deposition of polyaniline onto the working electrode with a silver wire reference electrode and a carbon counter electrode. When a polymerization potential of 700 mV was applied, roughly 0.5 mA/cm^2 of current was consumed after 5 minutes, with initial polymerization currents in excess of 1.0 mA/ cm^2. At these rates, the polyaniline layer became completely opaque with total coverage of the working electrode after approximately 15 seconds. The polyaniline formed a gel layer with poor cohesion, resulting in some polyaniline drifting into solution. Scanning electron microscopy of the sample revealed its porous structure as seen in Figure 4.3. Poor cohesion of these films resulted in poor mechanical properties.

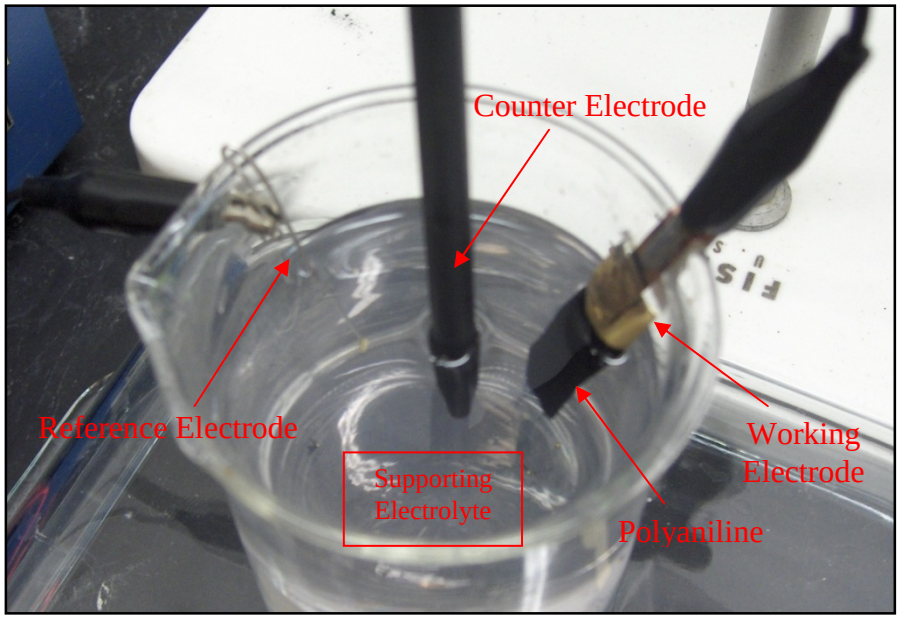

Figure 4.2. Experimental setup for constant potential polymerization of polyaniline from a 0.1 M aniline, 1.0 M H_2SO_4 solution. Polyaniline has been deposited onto the gold working electrode.

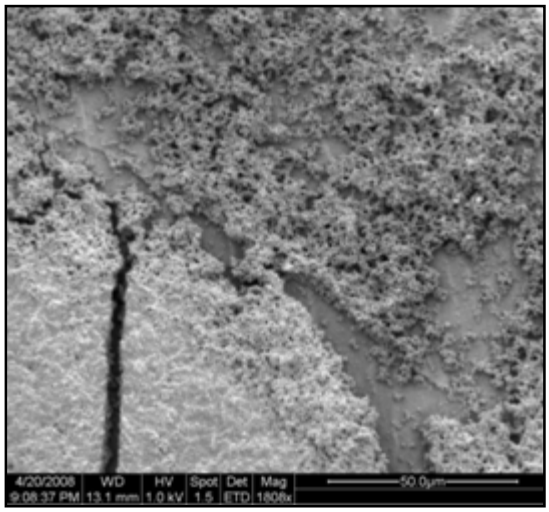

Figure 4.3. A scanning electron micrograph of a porous polyaniline layer polymerized from a 0.1 M aniline, 1.0 M H_2SO_4 solution onto a gold substrate under constant potential. Most of the polyaniline in the upper right half of the image has been removed to show the cross-section and the underlying gold substrate.

When actuation of the polyaniline/LDPE bilayers was attempted in order to demonstrate their electrochemical activity, little or no deflection was observed. This is likely because local expansion and contraction of the polyaniline did not translate into net expansion and contraction of the layer due to its porous structure. Electrochemical

activity was observed as color changes of the polymer. The polyaniline was initially blue when it was removed from the polymerization solution, but upon reduction with -600 mV relative to a carbon counter electrode in 1.0 M H_2SO_4, the polyaniline changed color to green. Oxidation with +600 mV had the reverse effect, followed by a color change to red. Color changes, shown in Figure 4.4, result from the shifting band gap energies as the polyaniline undergoes molecular changes between its three primary oxidation states [1].

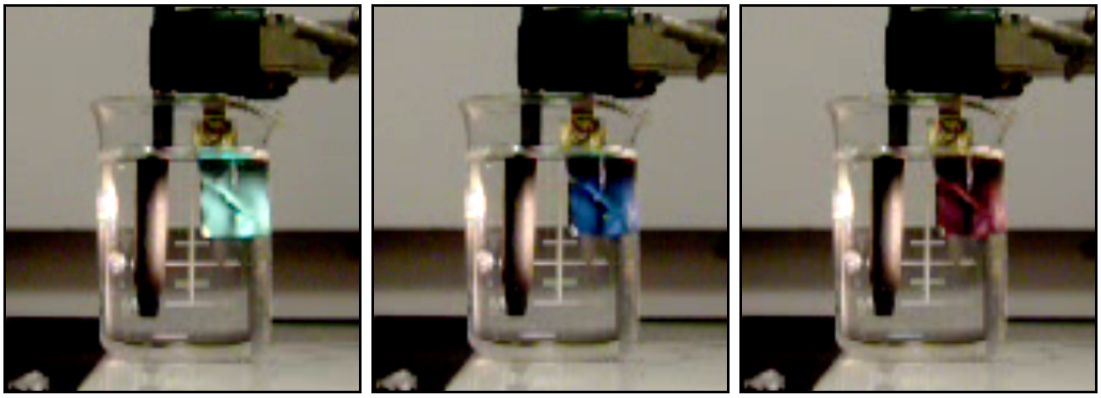

Figure 4.4. Color change in electrochemically polymerized polyaniline films during oxidation and reduction.

4.1.2. Constant Current Polymerization

Polyaniline was polymerized at the working electrode when a constant current was applied between the counter and working electrodes in a two electrode cell (Figure 4.5). This method provided much better control of polymerization rates and film properties. Sub-micron thickness polyaniline films prepared with this method exhibited 100% density at 10,000x magnification (Figure 4.6). Reducing the polymerization rates by lowering polymerization currents or using lower aniline concentrations improved the density, uniformity, and adhesion of films. Polyaniline films prepared in constant current conditions continued to display poor cohesion when subjected to tensile stresses.

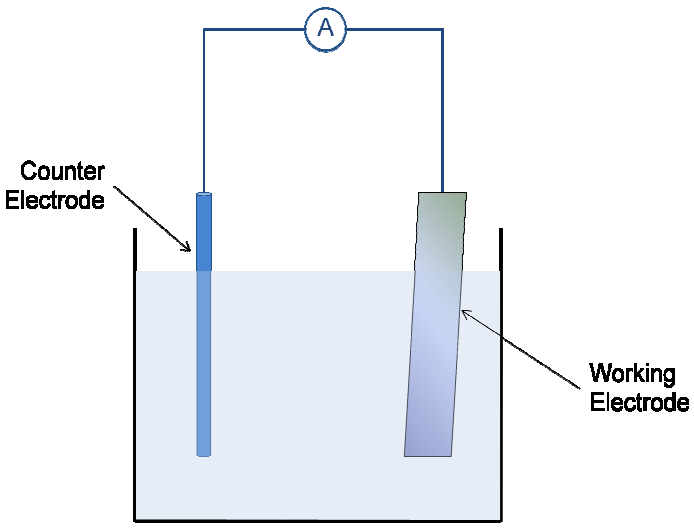

Figure 4.5. Schematic of a 2-electrode cell used to in constant current polymerization of polyaniline. Constant current is applied between the counter electrode (cathode) and working electrode (anode).

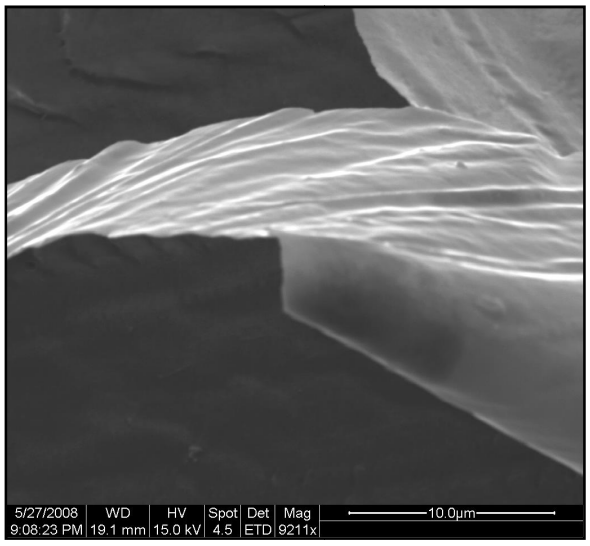

Figure 4.6. A flap of polyaniline peeled from the edge of a silicon/gold substrate polymerized with 150 µA/cm^2 constant current for 30 minutes in 0.1 M aniline and 1.0 M sulfuric acid. The visible edges of the film indicate that the film has low porosity and sub-micron thickness.

When polymerization current densities greater than 300 µA/cm^2 were used, the polyaniline films developed the nodule-like surface defects shown in Figure 4.7. These observations indicated that the polymerization current was too great to sustain consistent growth across the polyaniline surface, and non-uniform growths developed to increase

the effective surface area, decreasing current density. Below 50 µA/cm^2, no polymerization was observed, indicating that this was the approximate leakage current of the cell.

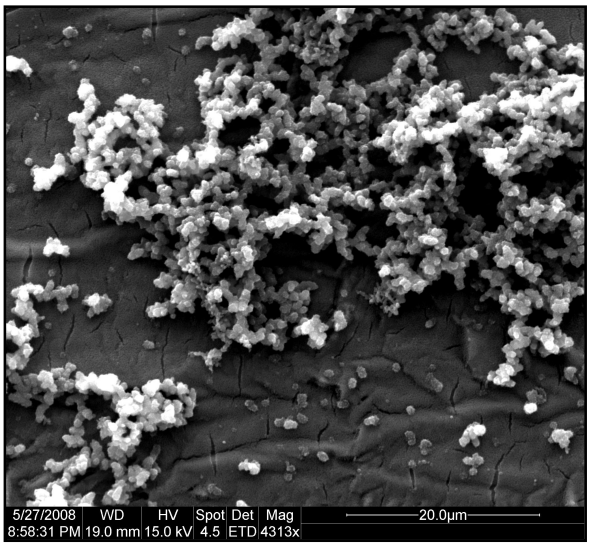

Figure 4.7. Nodule like growths of polyaniline on the surface of a polyaniline film polymerized with 400 µA/cm^2 constant current for 10 minutes in 0.1 M aniline, 1.0 M sulfuric acid.

Ultimately, the mechanical properties required to evaluate the electrical response of polyaniline films to mechanical strain could not be achieved using electrochemical polymerization methods. Electrochemically polymerized films exhibited lower strength, toughness, and ductility than chemically prepared polyaniline. Additionally, film thicknesses greater than 10 µm could not be achieved with this method, which were necessary in order to test the effects of diffusion path length. Electrochemical polymerization should not be discredited as a method of synthesizing polyaniline for strain sensing devices, as its methodology is compatible with the fabrication of micro-scale devices.

4.2. Solution Casting

Polyaniline films were solution cast by dissolving polyaniline emeraldine base powder (M_n=65,000, Sigma-Aldrich, CAS#: 25233-30-1) in an organic solvent, depositing the solution onto glass slides, and finally evaporating the solvent. The target thicknesses of the polyaniline films were calculated based on the weight percent of polyaniline in solution, the volume of solution deposited per area, and a polyaniline density of 1.3 g/cm^3 [2]. The volume of solution that could be applied to a slide was limited based on surface tension, which prevented the solution from running off the edges.

4.2.1. Process Development

Initial attempts to cast polyaniline films from 5 wt% polyaniline solutions in organic solvents such as N,N-dimethylacetamide, tetrahydrofuran, and acetone produced films with poor cohesion (Figure 4.8). Although the polyaniline appeared to partially dissolve in these solvents, the granular quality of films indicates that homogeneous solutions were not achieved at a molecular level.

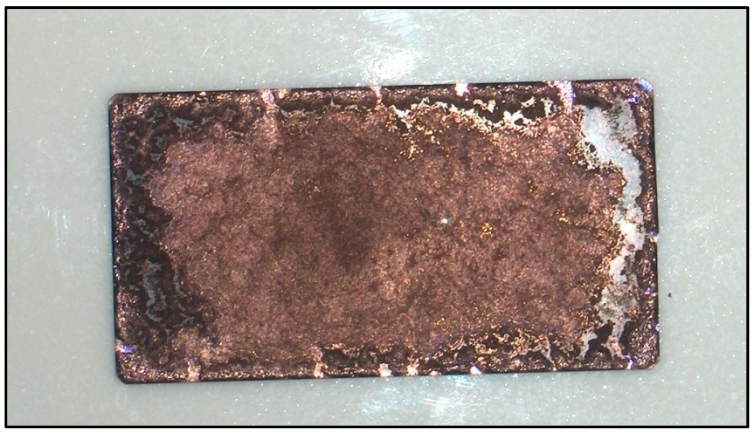

Figure 4.8. Polyaniline film cast from a 5 wt% solution polyaniline in N,N-Dimethylacetamide solvent exhibiting poor cohesion.

To achieve more homogeneous solutions, the solvent N-methyle-2-pyrrolidinone (NMP), which is employed industrially as a paint stripper and had been demonstrated to dissolve polyaniline, was used [3]. Films cast from 5 wt% solutions of polyaniline in NMP demonstrated high cohesion, indicating that solution homogeneity at a molecular level was achieved, however the films contained a large number of particle defects (Figure 4.9). It was determined that the particulates formed when the polyaniline was not sufficiently dispersed as it was added to the solvent. Adding the polyaniline slowly while rapidly stirring the solution at an elevated temperature (~60°C) reduced the number of particles, but did not eliminate them completely. Additionally, these solutions would turn into a gel within seconds to several minutes of adding the polyaniline, and the semi-solid material could not be cast into a film. The gelation time decreased with increasing polyaniline concentrations, and casting films from solutions with greater than 5 wt% polyaniline was not feasible because the solutions could not be deposited before gelation occurred.

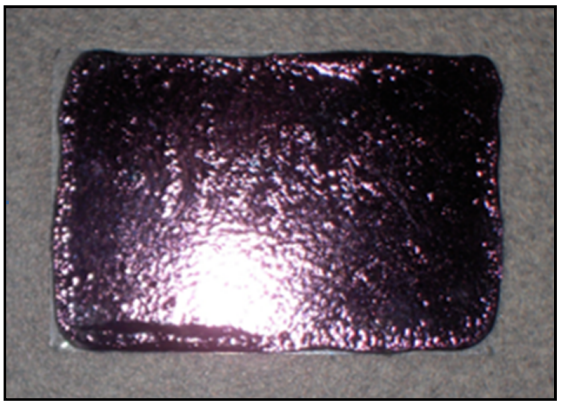

Figure 4.9. Polyaniline film cast from a 5 wt% solution of polyaniline in N-methyl-2-pyrrolidinone solvent exhibiting good cohesion but poor uniformity.

The gelation phenomenon is discussed in a number of technical proceedings, and is most likely the result of polyaniline chains coordinating to one another in a semi-crystalline manner, much like they do in the crystalline regions of bulk polyaniline. Secondary bonds between π-stacked polyaniline chains are slightly more stable than interactions between polyaniline and NMP molecules, so the material behaves like a gel. To overcome this difficulty, Wang *et al*. developed a method employing an NMP solvent as well as amine compounds such as Heptamethylemeimine (HPMI) (Figure 4.10) as "gel inhibitors". The amine group of the HPMI interacts preferentially with the amines in the polyaniline chain, and the bulky ring structure sterically inhibits interactions between adjacent polyaniline chains. HMPI has a boiling point of 52°C, much lower than the 203°C of NMP, so it readily evaporated upon heating, allowing the polymer to crystallize once it has been cast into the desired shape.

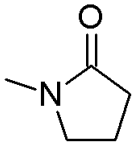

N-methyl-2-pyrrolidinone

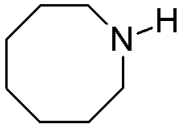

Heptamethyleneimine

Figure 4.10. Solvent N-methyl-2-pyrrolidinone and gel inhibitor heptamethyleneimine were used to produce homogeneous polyaniline solutions.

To obtain 100 % homogeneous solutions, a Thinky ARE-100 planetary centrifugal mixer, which spins the solution at high RPM's along two different axes, was used (Figure 4.11). This motion produced large sheer stresses within the solution, which was effective in breaking up particles formed during initial mixing.

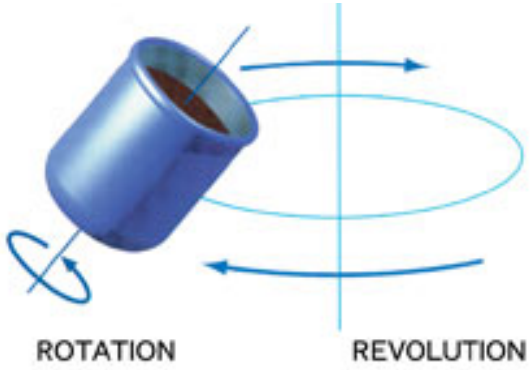

Figure 4.11. Schematic of the Thinky ARE-100 mixer used to prepare homogeneous polyaniline solutions.

4.2.2. Final Sample Preparation

Cast polyaniline films with 150, 50, and 25 µm target thicknesses were fabricated for electrical testing. Glass slides were carefully leveled in a vented oven prior to casting. Solutions were mixed in a Thinky ARE-100 and then deposited onto slides in proportions shown in Table 4.1. The film with a target thickness of 150 µm could not be cast from a 5 wt% solution because it required a greater volume of solution than what would stay on the slide with surface tension effects alone, so a 10 wt% solution was used. A slight molar excess of gel inhibitor, 1.1 HPMI (Aldrich, CAS#: 1121-92-2) per 1.0 aniline repeat unit, was used to ensure that amines in adjacent polyaniline molecules did not interact. The samples were heated in at 120°C for 2 hours to evaporate the solvent and anneal the films.

Table 4.1. Properties of Solutions Used to Cast Polyaniline Films

Target Thickness (µm)	Solution Concentration (wt%)	NMP per cm^2 (µL)	HPMI per cm^2 (µL)	Polyaniline per cm^2 (mg)	Solution per cm^2 (µL)
150	10	149	21.5	19.5	185.7
50	5	113	7.18	6.5	125.18
25	5	56.5	3.59	3.25	62.6

The films were removed from the glass slides by submersing in 1.0 M HCl, which doped the Polyaniline, causing them to contract and change color (Figure 4.12). Compressive stresses caused the films to delaminate from the glass slides. To expose the cross sections for thickness measurements, a section from each film was dried in its doped state, submerged in liquid nitrogen, and then fractured. Thickness measurements were made using Adobe Photoshop software to analyze scanning electron micrographs (Figure 4.13) of the films obtained using a FEI Quanta 200 scanning electron microscope. Measured thicknesses of films are shown in Table 4.2.

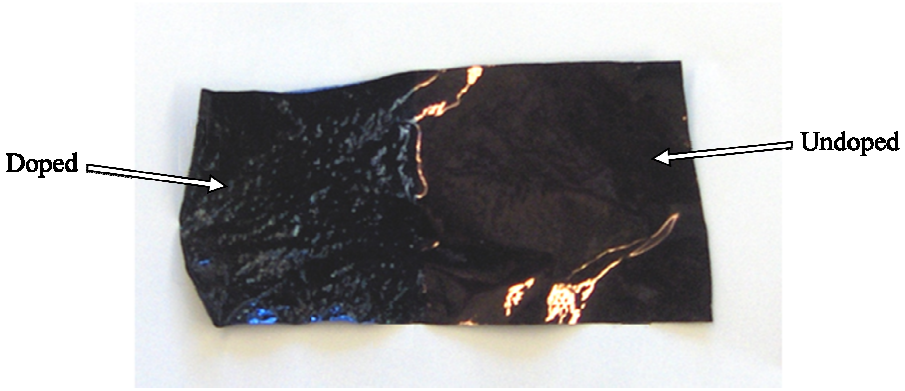

Figure 4.12. A cast polyaniline film, half of which has been doped with 1.0 M HCl.

Table 4.2. Polyaniline Film Thickness Measurements

Batch	Solution Concentration (wt%)	Target Thickness (µm)	Measured Thickness (µm)
1	10	150	158
2	5	50	54.8
3	5	25	11.4
4	5	25	2.72

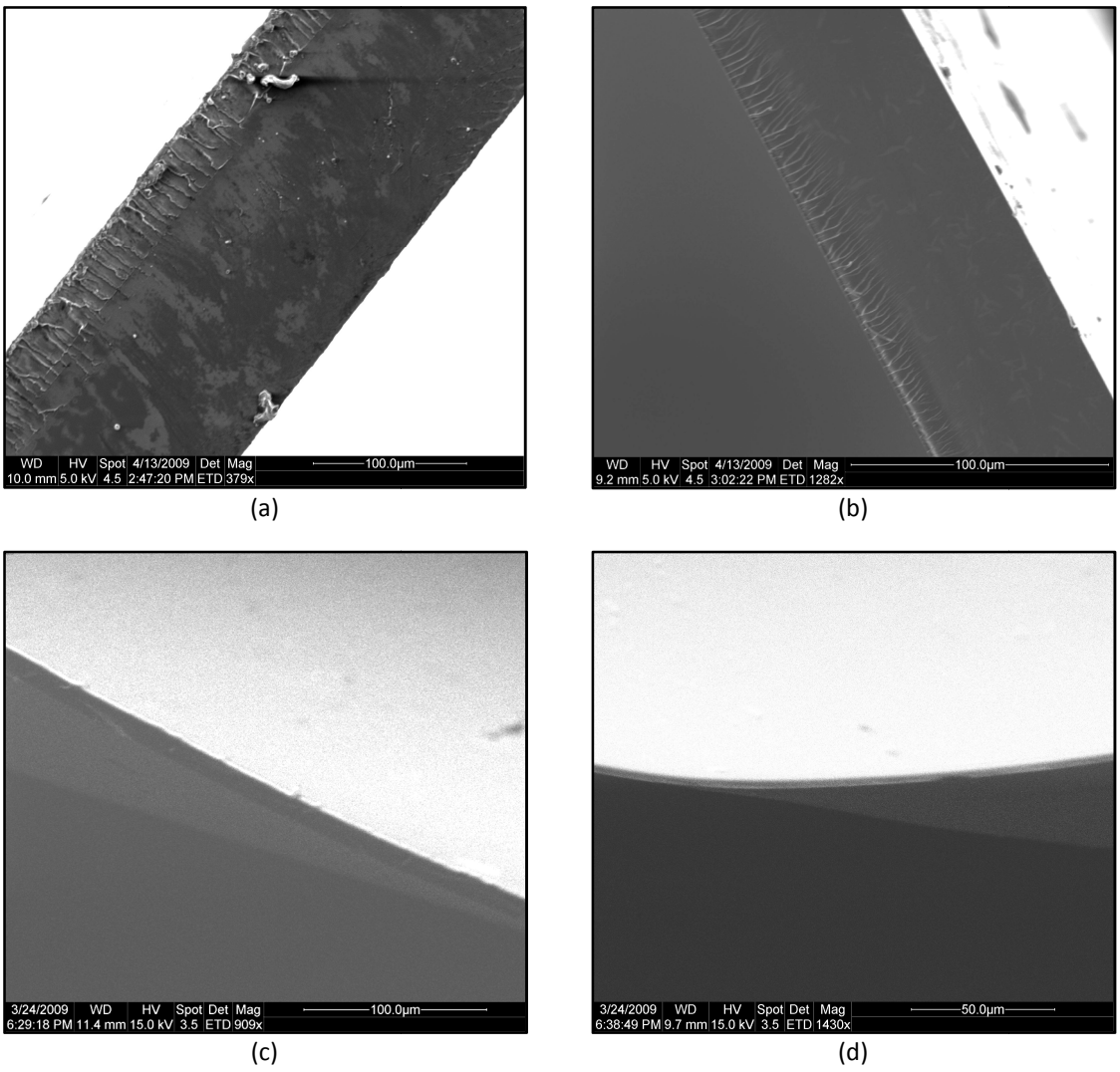

Figure 4.13. SEM images of the exposed cross sections of polyaniline films used to measure their 158, 54.8, 11.4, and 2.72 µm thicknesses (a-d, respectively).

The measured thicknesses of films with 25 µm target thicknesses were thinner than expected. After verifying that the densities of these films were consistent with those used to calculate the target thicknesses, it was determined that the thinning of the films was due to the buildup of material around the perimeter of the film, as shown in Figure 4.14. Buildup of material at the edges of the 50 and 150 µm films did not occur because greater amounts of material likely marginalized the surface tension effects. Although the

films did not match their target thicknesses, they were fit for testing once the outer 10 mm of each film was removed because the thicknesses were consistent throughout the interior of the films and the range in film thicknesses was a great enough to assess their effects on electrical properties. All films were stored in 1.0 M HCl for at least 48 hours before testing to ensure complete and uniform doping

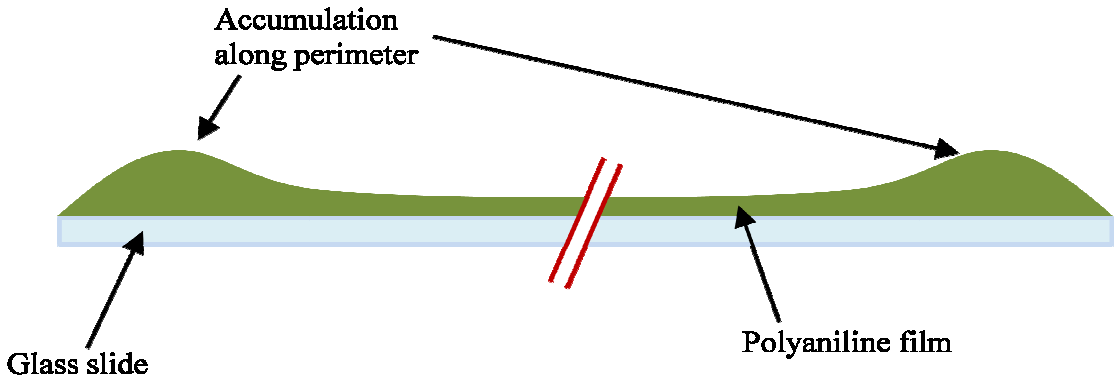

Figure 4.14. A schematic cross-section view of a cast polyaniline film showing the accumulation of polyaniline around the edges of the slide which resulted in lower than expected film thicknesses.

Doped polyaniline films were cut into rectangular 30 mm long strips in the desired widths with a sharp razor blade and a straight edge. Conductive carbon tape was applied to the upper and lower 10 mm on both sides of the film, leaving a 10 mm gauge length as shown in Figure 4.15. The carbon tape prevented the film from slipping in the gold/polyethylene grips, and decreased contact resistance between the sample and gold electrodes.

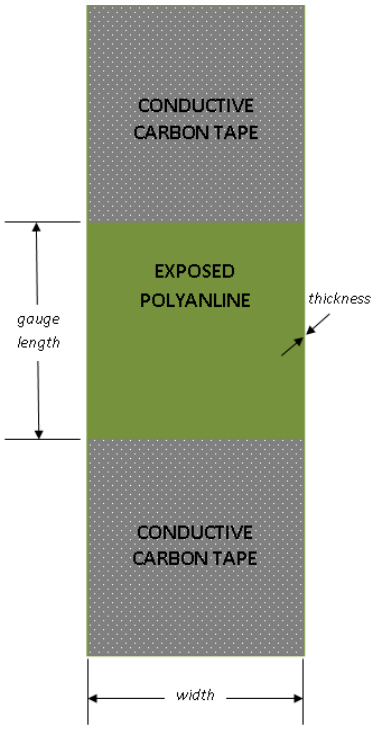

Figure 4.15. Schematic of a polyaniline sample for testing the electrical response to tensile strain. Sample dimensions varied depending on specific test methods.

4.3. References

[1] M. Bernard, A. Goff, V. Bich, W. Zeng. "Study by optical multichannel analysis of the electrochromic phenomena in polyaniline doped with camphorsulfonic acid." *Synthetic Metals*, Vol. 81, pp. 215-219, 1996.

[2] H. Wang, J. Gao, J.Sansinena, P. McCarthy. "Fabrication and Characterization of Polyaniline Monolithic Actuators Based on a Novel Configuration: Integrally Skinned Asymmetric Membrane." *Chemistry of Materials*, vol. 14, pp. 2546-2552, 2002.

[3] M. Angelopoulos, G. Asturias, S. Ermer, A. Ray, E. Scherr, A. Macdiarmid, M. Akhtar, Z. Kiss, A. Epstein. "Polyaniline: Solutions, Films and Oxidation State." *Molecular Crystals & Liquid Crystals*, vol. 160, pp. 151-163, 1988.

CHAPTER 5

EXPERIMENTAL METHODS

This chapter presents the equipment and procedures which were used to measure the electrical response of polyaniline to mechanical strain. Some experimental results which were critical in determining experimental methods are presented.

5.1. Closed Circuit Current

The closed circuit current during and after mechanical strain was measured in order to observe the total amount of charge displaced between polyaniline samples and the electrolyte solution. Ideally, this setup consists of a zero resistance electrical pathway between sample and counter electrode.

5.1.1. Test Fixture

A partial schematic of the experimental setup used to strain polyaniline films while measuring electrical output is shown in Figure 5.1. A solution bath fixture with gold electrical contacts was fabricated from a HDPE body and clear polycarbonate faceplate. Push-clamps were used in upper and lower sample grips, which applied positive pressure on the grips when they were in the closed position. The lower grip and push-clamp were connected via concentric cylinders containing O-rings to seal the interface and prevent leakage of the solution. The bath surrounding the lower grips of the fixture held enough solution to completely submerge a 10 mm sample and the lower portion of the upper sample grips. A 1.0 cm^2 gold electrode was attached to each face of

the sample grips which would be in contact with the polyaniline films, and they were connected to electrical leads with 0.25 mm diameter gold wire. A 2.0 cm^2 gold counter electrode was positioned so that it faced parallel to the sample at a distance of 1.0 cm, and was connected to an electrical lead with 0.25 mm gold wire. Dimensioned drawings of the solution bath fixture are in Appendix A.

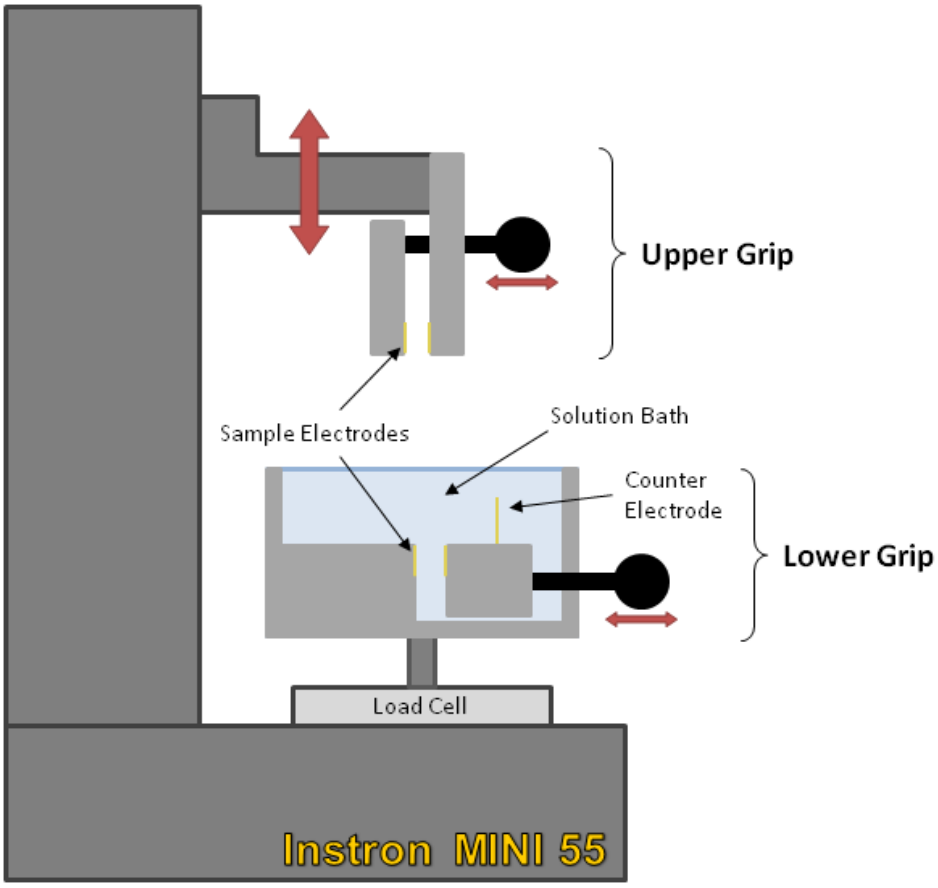

Figure 5.1. Schematic sectioned side-view of the experimental setup to strain polyaniline films in solution. The top and bottom have mobile grips which lock to secure the film. Gold foil on the clamping surfaces of the grips provides electrical contact with the sample.

5.1.2. Preliminary testing

A tensile test of a 54.8 µm thick polyaniline film in 1.0 M HCl with a 5 mm/minute strain rate shows a yield strain of 8.5 % (Figure 5.2). Strains below 8.5 %

exhibited nonlinear stress-strain characteristics due to viscoelastic relaxation of the polymer. Electrical properties were assessed below 8.5 % strain to ensure that the films would not undergo plastic deformation during testing.

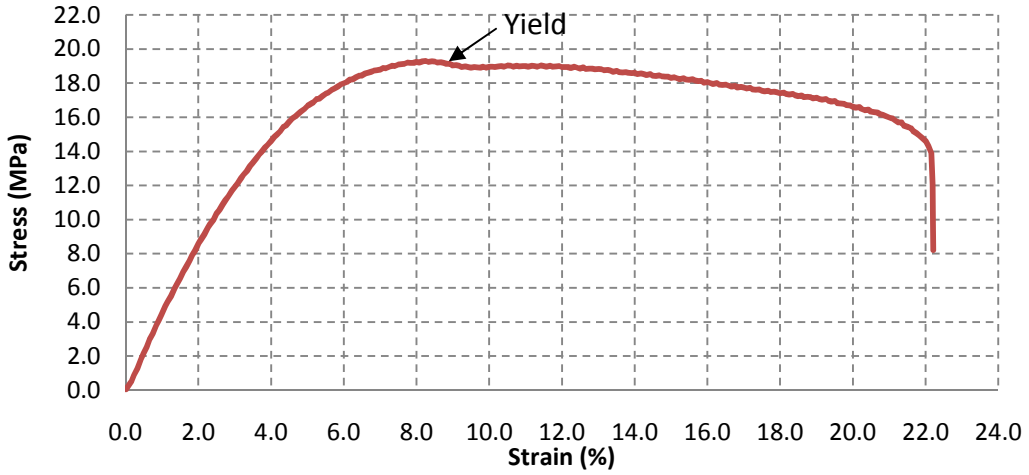

Figure 5.2. Tensile stress-strain profile of a 54.8 x 5 mm x 10 mm polyaniline film showing elastic/viscoelastic properties below 8.5 % strain.

Preliminary testing showed that the optimal strain amplitude was 3.0 %, which minimized the effects of relaxation in the polymer while still insuring that an adequate signal to noise ratio would be achieved. A 15 second hold between strain steps was used to allow complete diffusion of ions into the polyaniline, and to allow viscoelastic relaxation recovery to occur at 0.0 % strain. A maximum strain rate of 1.0 mm/s was used to minimize the strain time while assuring that the target strain was not overshot. The samples were pre-stressed to 2.0 MPa in each method to ensure that the sample was fully elongated and starting strains were similar.

5.1.3. Standard Test Method

The following method was used for all tests which measured the current outputs of polyaniline films in uniaxial strain. Figure 5.3 shows a schematic of the test cell used

for the standard test method. Deviations from this method are stated in individual test descriptions.

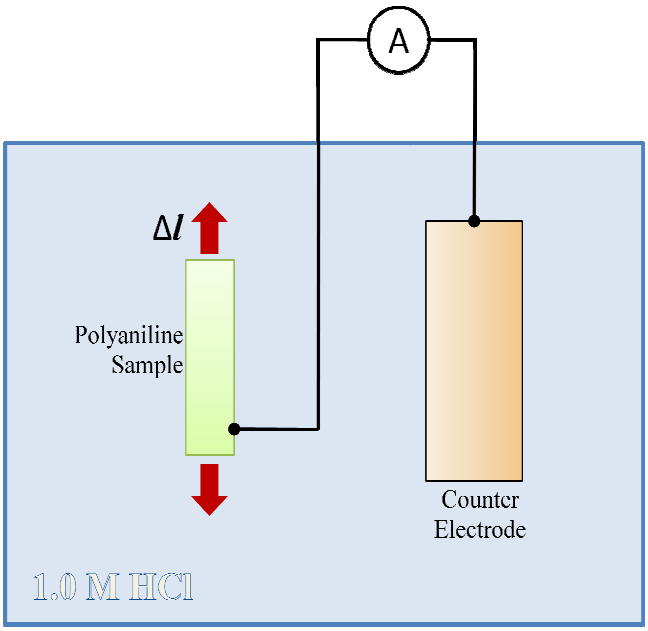

Figure 5.3. Schematic of the electrochemical test cell used in the standard method to test the current output from films under uniaxial strain.

Polyaniline films were elongated longitudinally using an Instron model MINI 55 equipped with the solution bath test fixture. C-clamps were used to fix the upper and lower grips of the fixture to the Instron MINI 55. Instron Bluehill software was used to control the Instron MINI 55 and collect load and extension data. The Instron was outfitted with a 500 N load cell, which was calibrated and balanced prior to testing each sample.

All data examining current and charge displacement was acquired with a PARSTAT 2273 potentiostat/galvanostat interfaced with a PC operating with PowerSuite software. Individual tests were performed in 200 second potentiostatic tests with a data sampling rate of 50 Hz. Prior to the start of each test, the sample was held at the testing potential (0.0 V unless otherwise stated) for 120 seconds. Working (green) and sensing

(grey) electrodes were connected to the sample. Counter (red) and reference (white) electrodes were connected to the counter electrode. The ground (black) lead was not used. The electrode setup is shown in Figure 5.4.

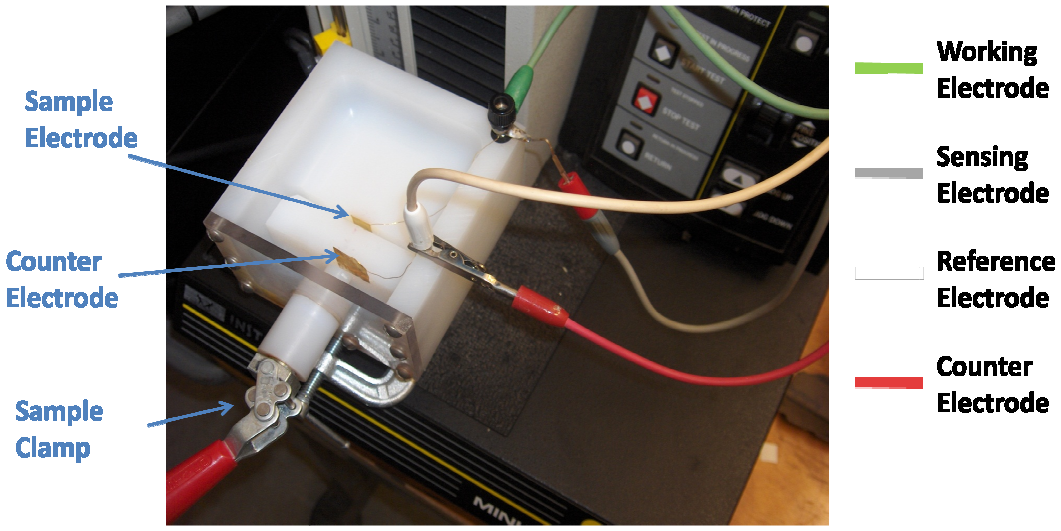

Figure 5.4. Test fixture electrode setup used to apply uniaxial strain to polyaniline films while measuring electrical output.

Hydrochloric acid solutions were prepared from analytical grade 37 wt% hydrochloric acid (Sigma-Aldrich, CAS#: 7647-01-0) and DI water. Before loading each sample, the solution bath was filled with approximately 200 mL of 1.0 M HCl until the solution was 5 mm below the top of the bath. The sample was then loaded into the upper grip above the test bath. Special care was taken to ensure that the sample was vertical in the grip, and that only the gauge length was left unclamped. With the lower grip open, the sample was lowered to a preset gauge length of 10 mm, and lower grip was then clamped onto the sample.

The standard 3.0 % strain test profile in Figure 5.5 was made by inputting values from Table 5.1 into the Instron Bluehill test profiler. The profile was set to cycle continuously until stopped by the user. The “pre-stress” function was programmed to

ramp the strain at 1.0 mm/min until the tensile stress reached 2.0 MPa before initiating the strain profile.

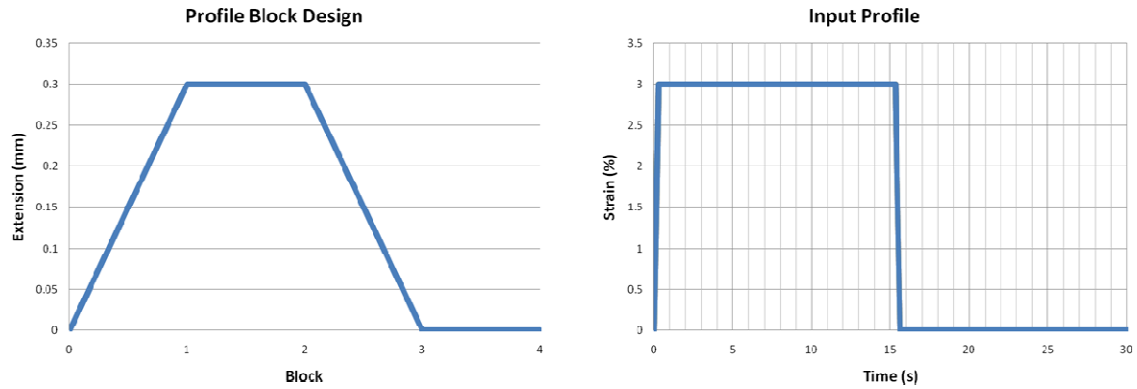

(a) (b)

Figure 5.5. Profile block design (a) which yields the input profile (b) from Instron Bluehill tensile test method profiler used for the standard 3.0 % strain tests.

Table 5.1. Instron Profiler Commands for the Standard Test Method

Block	Type	Duration	Extension	Rate
1	Relative Ramp	-	0.3 mm	1.0 mm/s
2	Hold	15.0 s	-	-
3	Relative Ramp	-	0.3 mm	-1.0 mm/s
4	Hold	15.0 s	-	-

5.1.4. Specific Test Methods

The following tests utilize the standard test method with some modifications and additions in order to evaluate specific characteristics of polyaniline films.

5.1.4.1. Surface Area

The effects of sample surface area on output current were assessed using the standard test method with a 54.8 µm thick polyaniline sample. A sample with a width of 10 mm was first tested, then removed and trimmed to a width of 5 mm, reducing its surface area by a factor of 2. The 5 mm wide sample was then tested.

5.1.4.2. Thickness

Polyaniline films with 158, 54.8, 11.4, and 2.72 µm thickness films in 10 mm widths were each tested in order to observe the effects of diffusion path length on the output current.

5.1.4.3. Concentration

A polyaniline film with a 158 µm thickness and 5 mm width was tested in the solution concentrations listed in Table 5.2. To eliminate variability associated with loading and changing samples, a single sample was used without removing it from the sample grips. Between tests, the solution was replaced with a syringe while the Instron continued to apply oscillating strains. The sample was tested in the 1.0 M HCl solution first, and then the lower concentration solutions were prepared by diluting the solution used in the previous test with DI water.

Table 5.2. Solutions Used in Concentration Testing

Run	HCl Concentration (mol/L)	Dilution by Volume (DI H_2O : solution)
1	1.0	-
2	0.5	1 : 1
3	0.1	4 : 1
4	0.01	9 : 1
5	0.001	9 : 1
6	0.00001	99 : 1

5.1.4.4. Linearity

Instantaneous and stepwise strain profiles were applied to examine the linearity of charged displaced with strain, and to observe the affects of relative and absolute strains. To minimize relaxation, a maximum strain of 2.0 % was used in both methods.

An instantaneous strain method was used to measure the charge displaced when a film was strained from the baseline 2.0 MPa to designated amplitudes. Instron Bluehill tensile test method profiler was programmed using commands in Table 5.3 to obtain test profiles in Figure 5.6. The polyaniline film was held for 5.0 seconds after each strain to allow complete diffusion of ions into or from the polymer.

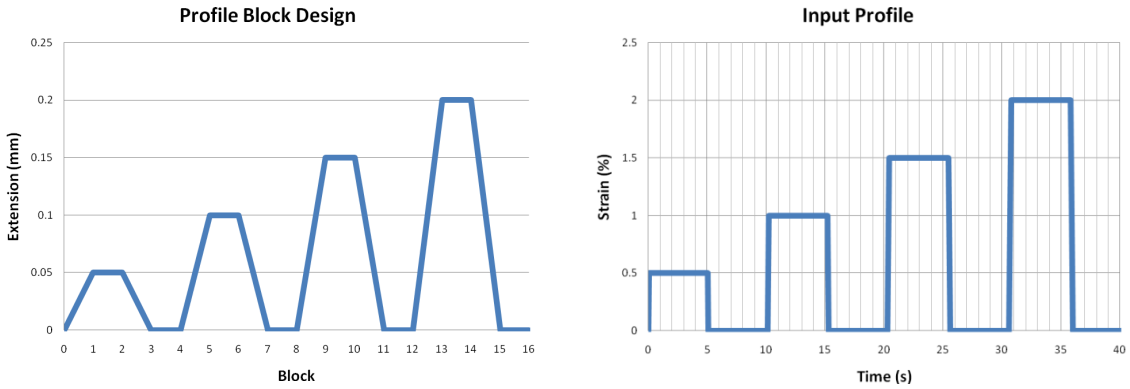

(a) (b)

Figure 5.6. Profile block design (a) which yields the input profile (b) from Instron Bluehill tensile test method profiler for instantaneous strain linearity measurements.

Table 5.3. Instron Profiler Commands for Instantaneous Strain

Block	Type	Duration	Extension	Rate
1	Relative Ramp	-	0.05 mm	1.0 mm/s
2	Hold	5.0 s	-	-
3	Relative Ramp	-	0.05 mm	-1.0 mm/s
4	Hold	5.0 s	-	-
5	Relative Ramp	-	0.10 mm	1.0 mm/s
6	Hold	5.0 s	-	-
7	Relative Ramp	-	0.10mm	-1.0 mm/s
8	Hold	5.0 s	-	-
9	Relative Ramp	-	0.15 mm	1.0 mm/s
10	Hold	5.0 s	-	-
11	Relative Ramp	-	0.15 mm	-1.0 mm/s
12	Hold	5.0 s	-	-
13	Relative Ramp	-	0.20 mm	1.0 mm/s
14	Hold	5.0 s	-	-
15	Relative Ramp	-	0.20 mm	-1.0 mm/s
16	Hold	10.0 s	-	-

A stepwise strain method was used to determine the charge displaced when a strain was applied to a film already in an initial strained state. Instron Bluehill Software's tensile test method profiler was programmed using commands in Table 5.4 to obtain test profiles in Figure 5.7. The polyaniline film was held for 5.0 seconds after each strain to allow complete diffusion of ions into or from the polymer.

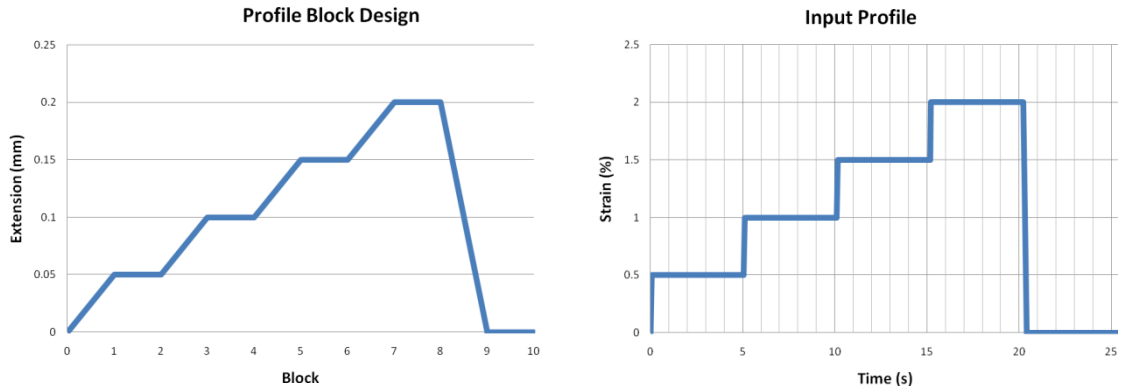

(a) (b)

Figure 5.7. Profile block design (a) which yields the input profile (b) in Instron's Bluehill tensile test method profiler which was used for stepwise strain linearity measurements.

Table 5.4. Instron Profiler Commands for Stepwise Strain

Block	Type	Duration	Extension	Rate
1	Relative Ramp	-	0.05 mm	1.0 mm/s
2	Hold	5.0 s	-	-
3	Relative Ramp	-	0.05 mm	1.0 mm/s
4	Hold	5.0 s	-	-
5	Relative Ramp	-	0.05 mm	1.0 mm/s
6	Hold	5.0 s	-	-
7	Relative Ramp	-	0.05 mm	1.0 mm/s
8	Hold	5.0 s	-	-
9	Relative Ramp	-	0.20 mm	-1.0 mm/s
10	Hold	5.0 s	-	-

5.1.4.5. Oxidation State

Cyclic voltammetry (CV), which measures current as a sample is cycled through a potential range, was used to determine the oxidation and reduction potentials of polyaniline samples in conditions identical to those used to measure the electrical response to tensile strain. Polyaniline undergoes chemical changes at various potentials, consuming or producing free electrons which are measured as an electrical current. A current peak will therefore indicate a rapid chemical change over a specific potential range corresponding to the oxidation or reduction potential of the sample. CV was conducted using a 54.8 µm x 10 mm x 10 mm polyaniline film between -0.6 V to +0.9 V relative to a 2.0 cm^2 gold counter electrode at a rate of 40 mV/s. Two initial cycles were performed for equilibration of the polyaniline to ensure that the initial oxidation state of the polymer did not affect the measurements, and data from the third cycle was used to determine oxidation and reduction potentials.

The current output was measured using the standard test method while the polyaniline sample was held at potentials between -0.5 V and +0.5 V relative to the counter electrode at 0.1 V increments. A 54.8 µm x 10 mm x 10 mm sample was used.

5.2. Open Circuit Potential

When the circuit between the working and counter electrodes was held open, charge buildup resulted in a potential across the circuit. The open circuit potential was measured using an oscilloscope with polyaniline films in the standard test method setup, and a bilayer sensor device.

5.2.1. Bilayer Sensor

A proof of concept device was fabricatied to demonstrate that polyaniline films could be used in a sensor with position sensitivity (Figure 5.8). The device was fabricated from 11.4 μm x 5 mm x 20 mm polyaniline films adhered to either side of a 1.0 mm thick PET substrate with double sided tape. Silver epoxy was used for electrical contacts between each film and insulated copper wires. The contacts were encapsulated in epoxy to insulate them. The schematic in Figure 5.9 represents a cross section view of the device, and shows the potentials expected from positive and negative deflections at the tip of the sensor.

The positive and negative terminals of an oscilloscope were connected to the leads of the bilayer sensor, and the device was immersed in a 1.0 M HCl solution. The tip of the sensor was deflected ~45° in each direction using a human finger while recording the potential between opposing polyaniline films.

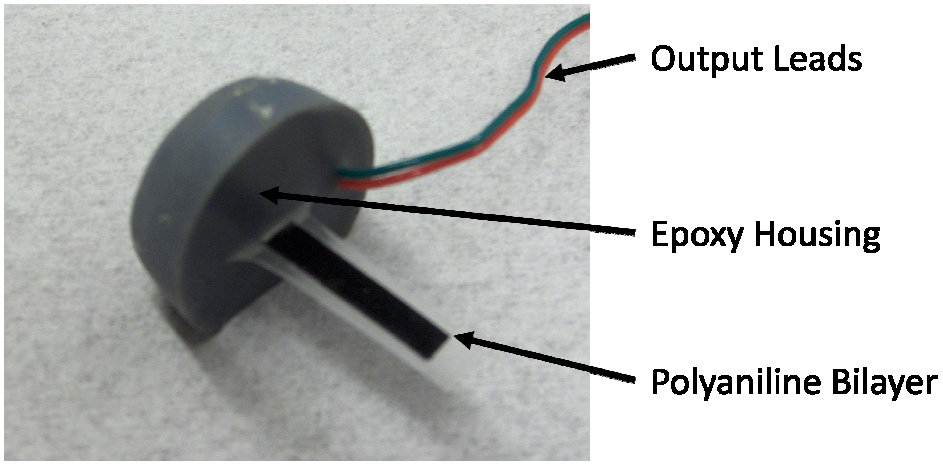

Figure 5.8. Polyaniline bilayer sensor.

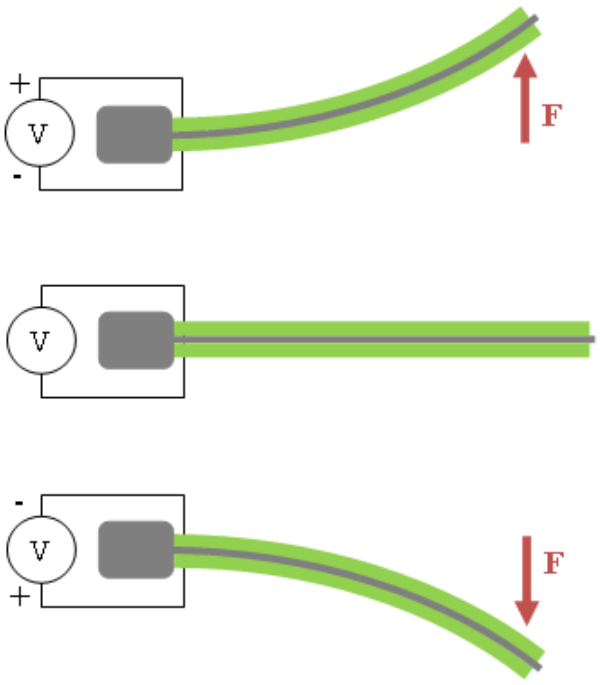

Figure 5.9. Schematic of a polyaniline bilayer sensor showing potentials produced by negative and positive deflections at the tip.

5.2.2. Tensile Strain

For a more precise analysis of the output potential, single polyaniline films were subjected to uniaxial strain in a experimental setup similar to that used in the standard test method for output current. An oscilloscope was used to measure the output potential of the polyaniline relative to a gold counter electrode (Figure 5.10). Using Instron Bluehill software, various strain profiles were programmed to test position sensitivity and frequency reponse of a 54.8 µm x 10 mm x 10 mm polyanline film in tensile strain. To minimize overshooting the target strain, 4 Hz and 1.0 mm/s were the highest cycling frequency and strain rate which could be applied. Before testing cycles were initiated, the film was prestrained to 2.0 MPa to ensure that the sample was fully elongated.

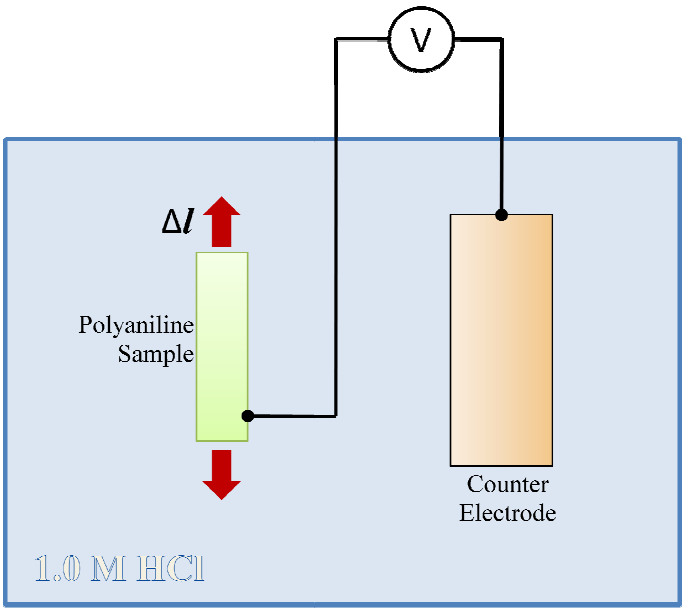

Figure 5.10. Schematic of the experimental setup to apply a tensile strain to a polyaniline film in 1.0 M HCl while measureing the potential relative to a gold counter electrode.

CHAPTER 6

RESULTS & DISCUSSION

This chapter will present and interpret the experimental results from the tests outlined in Chapter 5. A summary of the material and sensor characteristics determined in this chapter can be found in Chapter 7, Conclusions.

6.1. Closed Circuit Current

When positive tensile strains were applied to polyaniline films, positive anodic currents were produced. This indicated that electrons were flowing out of the polyaniline upon being displaced by negatively charged chlorine ions. When negative strains were applied, returning the samples to its original lengths, the opposite effect was observed as negative current peaks. Figure 6.1 shows typical experimental output. Exponential decay of anodic current is concurrent with diffusion based ion transport.

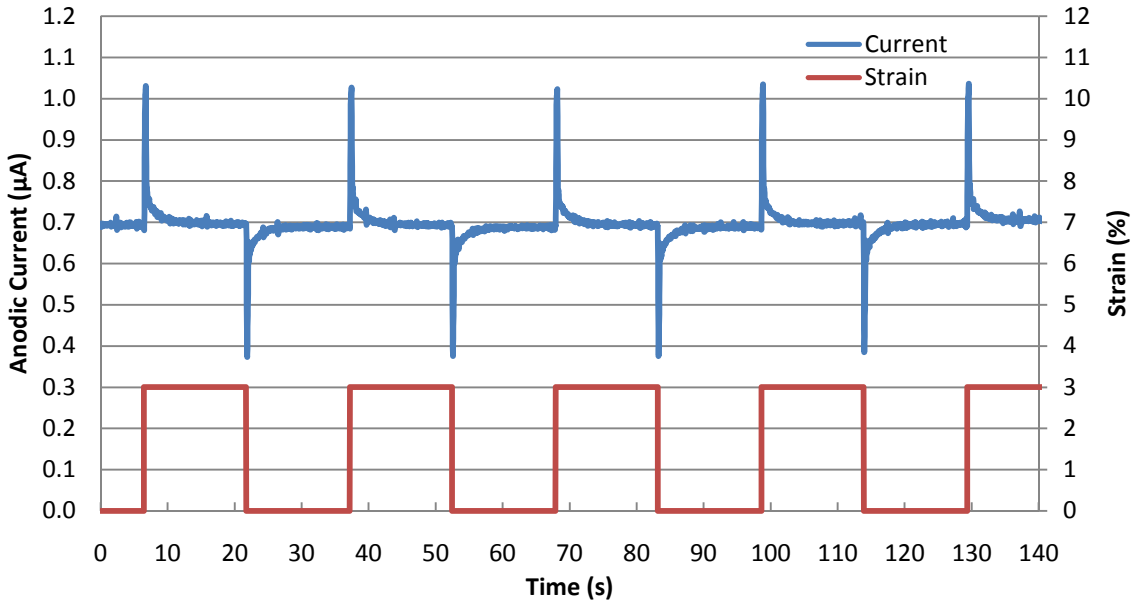

Figure 6.1. Current from a 158 µm x 10 mm x 10 mm polyaniline film when 3 % strains were applied.

Random variation in the output current (noise) occurred throughout the experimentation process with no observed dependence on sample dimensions. This variation was a result of factors including mechanical vibrations from the Instron fan and floor, oscillations of fluid in the test bath, and electromagnetic interference from nearby electrical devices. The electrostat used to measure output current had negligible contribution to the noise. The average noise level in the output signal was found by calculating the standard deviation of the current output during steady state conditions (Figure 6.2). The average noise in the output signal was 0.034 µA.

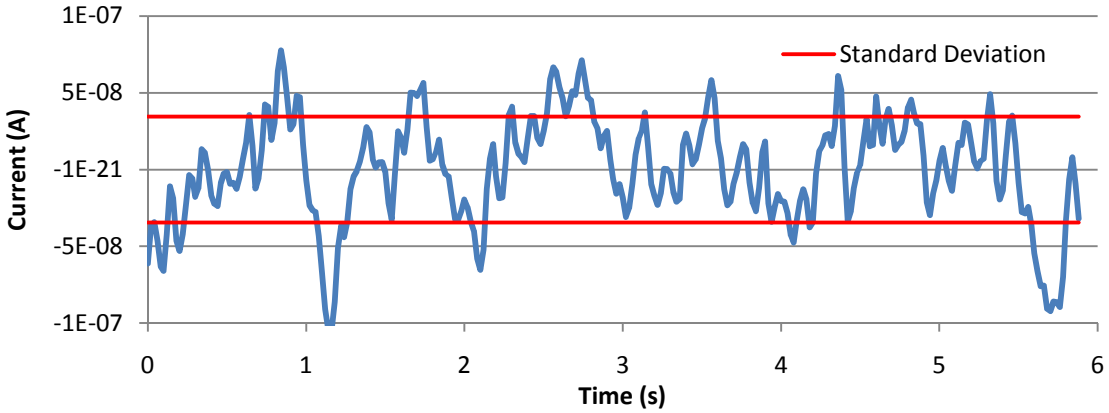

Figure 6.2. The standard deviation of the current output in steady-state conditions was used to define the average noise level.

When polyaniline samples were held at a constant positive strain, large amounts of relaxation were observed in the stress profile (Figure 6.3). The magnitude and rate of relaxation increased with increasing strain. Relaxation resulted in buckling of the samples when they were returned to their original positions corresponding to 0.0 % strain, because the samples had elongated beyond their original gauge lengths. Although most of the relaxation recovered while the film was held at zero strain, residual relaxation reduced the stress amplitude during subsequent cycles, as shown in Figure 6.4. Smaller volume changes occurred during repeated strains because the initial volume was not recovered,

which ultimately resulted in a reduction in charge displacement. After approximately 20 cycles, a steady-state condition was achieved in which there was negligible variation between cycles. Electrical measurements were taken during steady-state conditions, which resulted in a 10 – 20 % reduction in charge displacements.

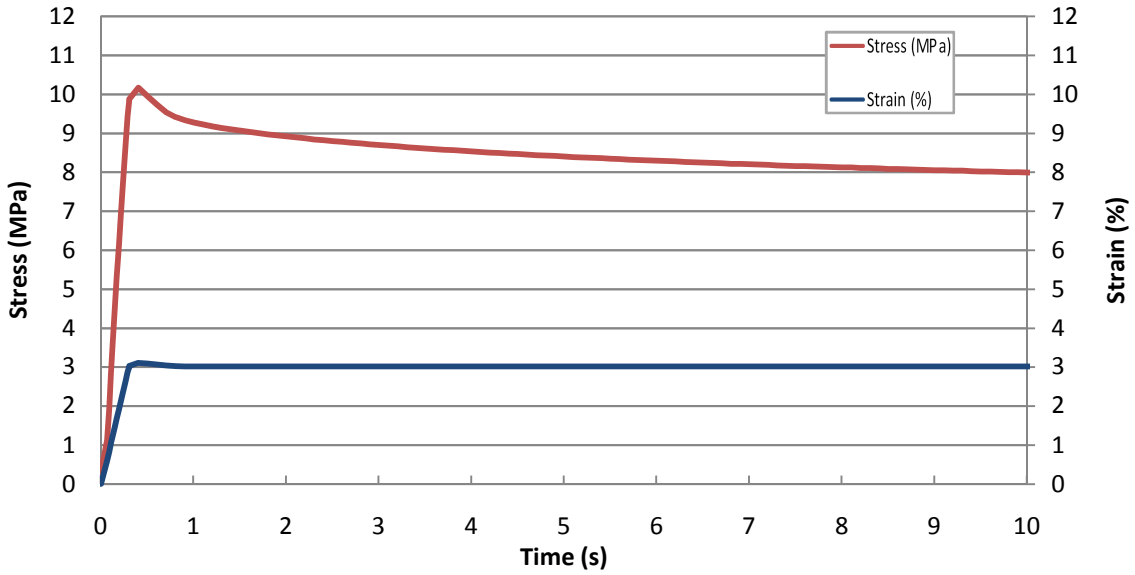

Figure 6.3. Stress resulting from a 3.0 % strain to a 158 µm x 10 mm x 10 mm polyaniline film, showing the effects of relaxation over time.

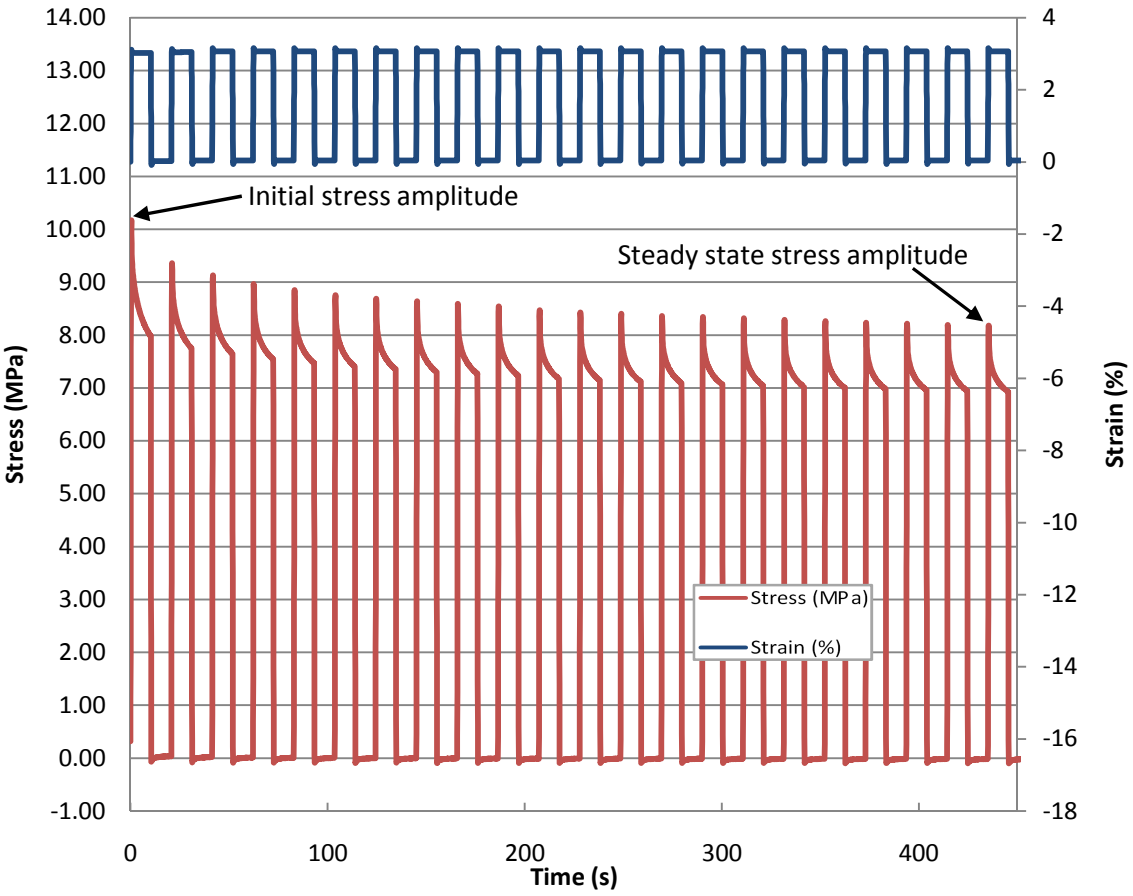

Figure 6.4. Cyclic applied strain and resulting stress profiles from a 158 µm x 10 mm x 10 mm film, showing the effects of relaxation.

6.1.1. Surface Area

The current output when 3 % strains were applied to 54.8 µm thick by 10 mm long films in widths of 5 mm and 10 mm is shown in Figure 6.5. The magnitude of the current output from the 10 mm wide film is greater because the total surface area and volume are both double that of the 5 mm wide film. The decay time of the current output is independent of sample width because the diffusion path length is constant. The total charge displaced when the 10 mm wide film was strained was approximately double that of the 5 mm wide sample (Table 6.1). This was expected because total charge

displacement should have a linear dependence on sample volume based on theoretical predictions presented in Chapter 3.

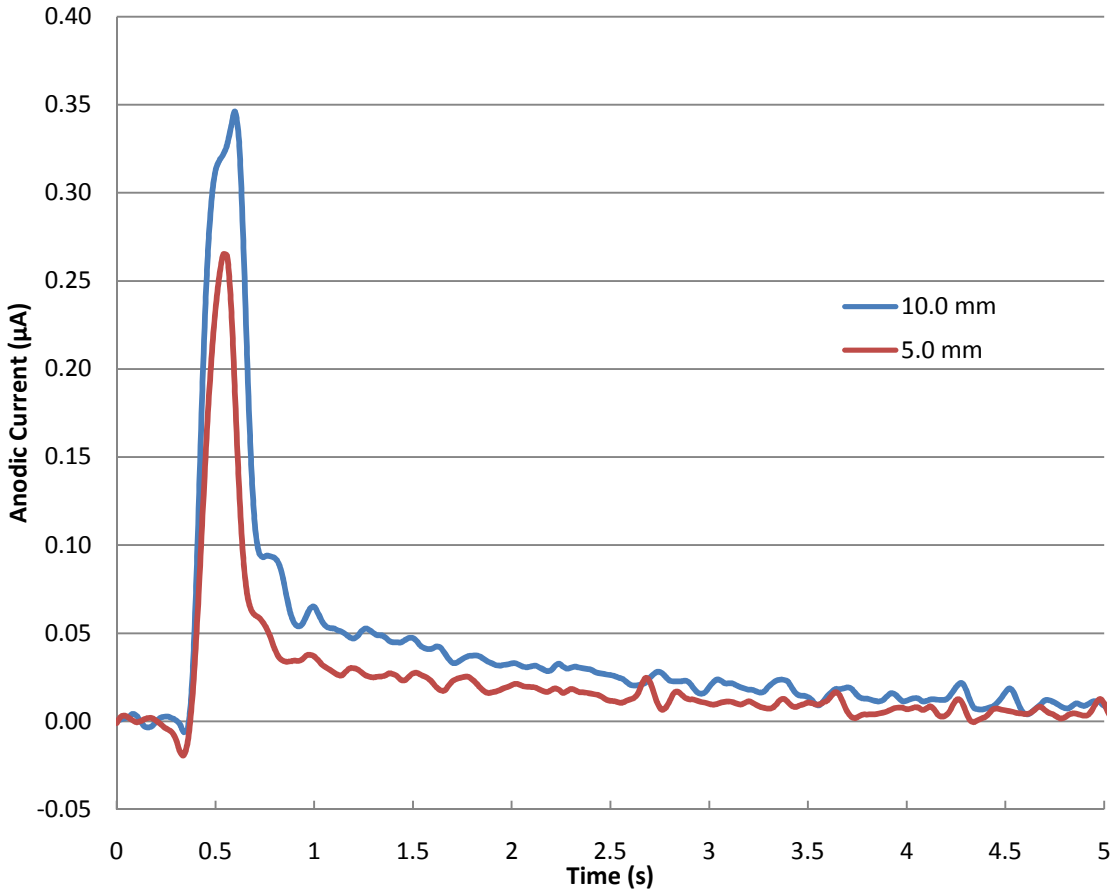

Figure 6.5. Anodic current peaks of identical 54.8 µm thick polyaniline films in 5 mm and 10 mm widths while a 3% tensile strain was applied.

Table 6.1. Effect of Film Width on Charge Displacement

Width (mm)	Mean Charge Displacement (µC)	Standard Deviation (µC)	n
10.0	0.230	0.0130	5
5.0	0.121	0.0124	6

6.1.2. Film Thickness

Polyaniline films with 158, 54.8, 11.4, and 2.7 µm thicknesses were subjected to tensile strains in order to observe the effects of diffusion path lengths on the decay time of the resulting current peaks. Films with 2.7 µm thicknesses could not be used for this analysis because output currents decayed too rapidly, falling below acceptable S/N levels. Equation 6.1, derived in Chapter 3 to model the current with respect to time when $\frac{N_t}{N_\infty} \geq 0.55$, was fit to experimental data to determine the diffusivity of chlorine ions in polyaniline. Data corresponding to currents produced after $\frac{N_t}{N_\infty} \geq 0.55$ for a series of peaks from each thickness were isolated as shown in Figure 6.6. Regression was performed with this data to find the coefficients in Equation 6.2 which correspond to constants in Equation 6.1.

$$i = Q\frac{8D}{l^2}exp\left(-\frac{\pi^2 Dt}{l^2}\right) \tag{6.1}$$

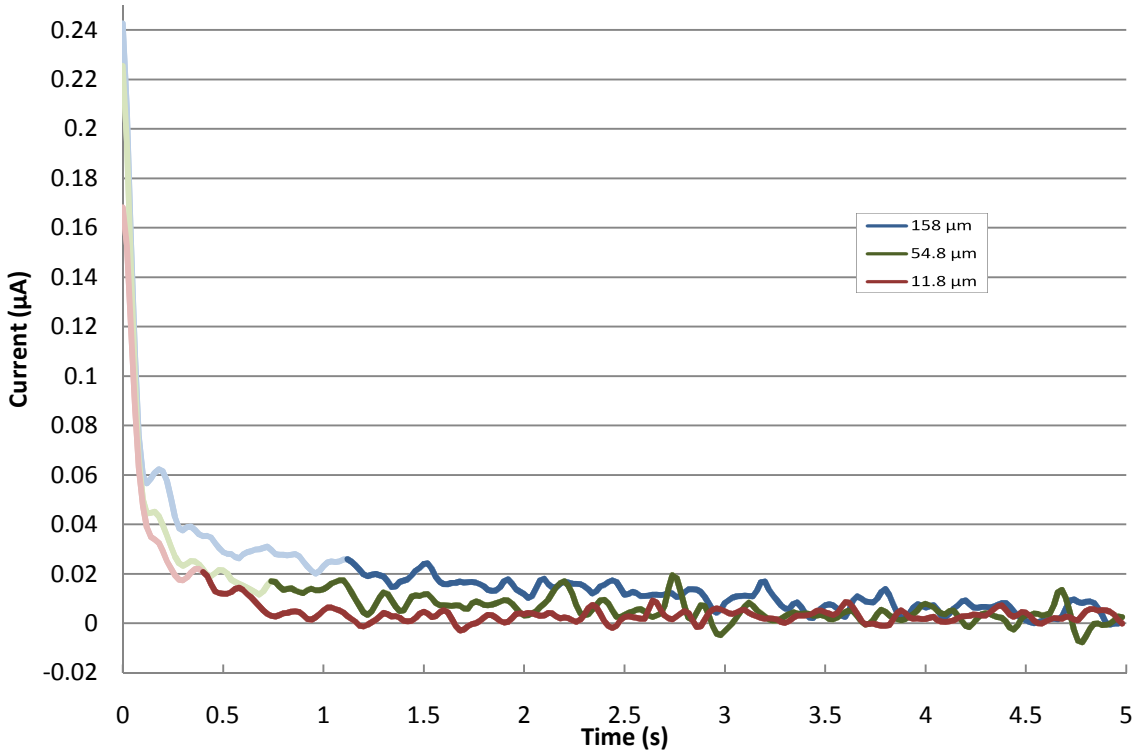

Figure 6.6. Current produced by 3 % strains in polyaniline films of 158 , 54.8, and 11.4 µm thicknesses. Regression was performed on data after 55 % of total charge had been displaced, as indicated in each curve.

$$y = m1 + m2 \cdot exp\left(-{}^{x}/_{m3}\right) \tag{6.2}$$

$m1 = \text{vertical offset}$

$$m2 = Q\frac{8D}{l^2}$$

$$m3 = \frac{l^2}{\pi^2 D}$$

The exponential current decay function (Equation 6.1) used to model the current relative to time must asymptotically approach zero, so the constant *m*1 was included in the regression to account for any non-zero vertical offset in experimental data. The constant *m*2 is dependent on the diffusivity (D) of anions in polyaniline, sample dimensions, and the total charge (Q) displaced. The constant *m*3 is similar to an

exponential decay time constant, and was used to determine the anion diffusivity because time (t) and diffusion path length (l) were defined for this experiment. Figures 6.7-9 show curves generated from mean regression coefficients overlaid onto examples of experimental data for each thickness.

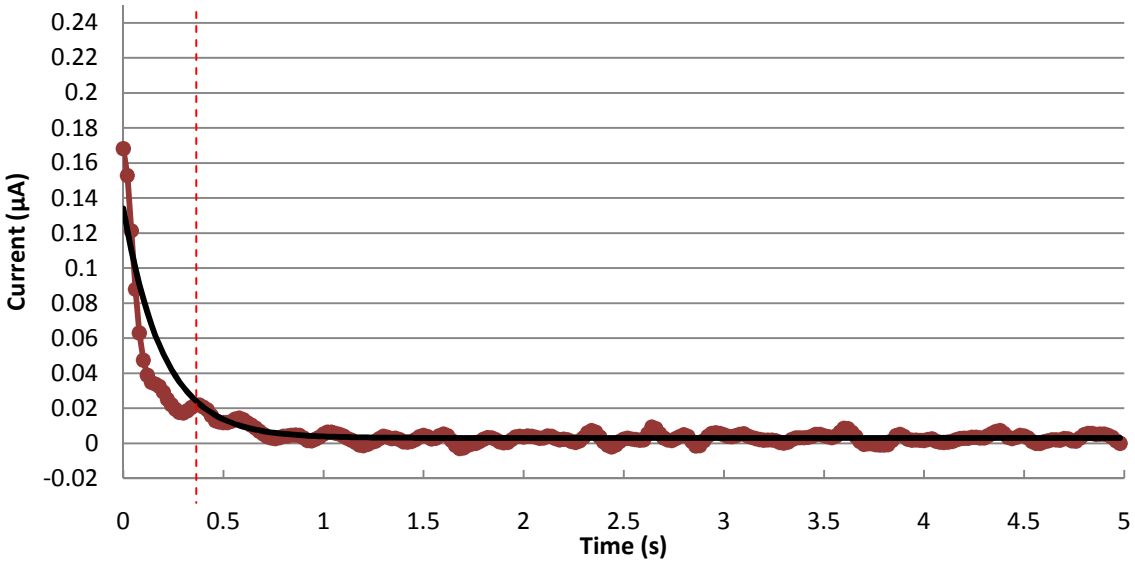

Figure 6.7. Anodic current from an 11.4 µm x 10 mm x 10 mm sample after a 3.0 % tensile strain was applied. The regression line was fitted to current data after the dashed line, which indicates 55 % of total charge displacement at 0.36 seconds.

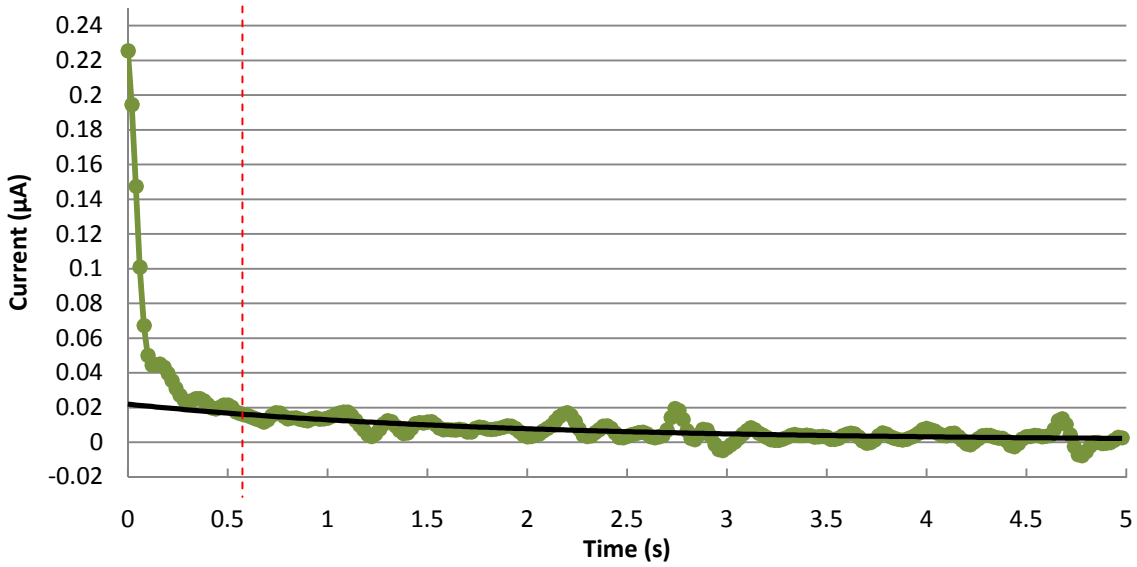

Figure 6.8. Anodic current from a 54.8 µm x 10 mm x 10 mm sample after a 3.0 % tensile strain was applied. The regression line was fitted to current data after the dashed line, which indicates 55 % of total charge displacement at 0.58 seconds.

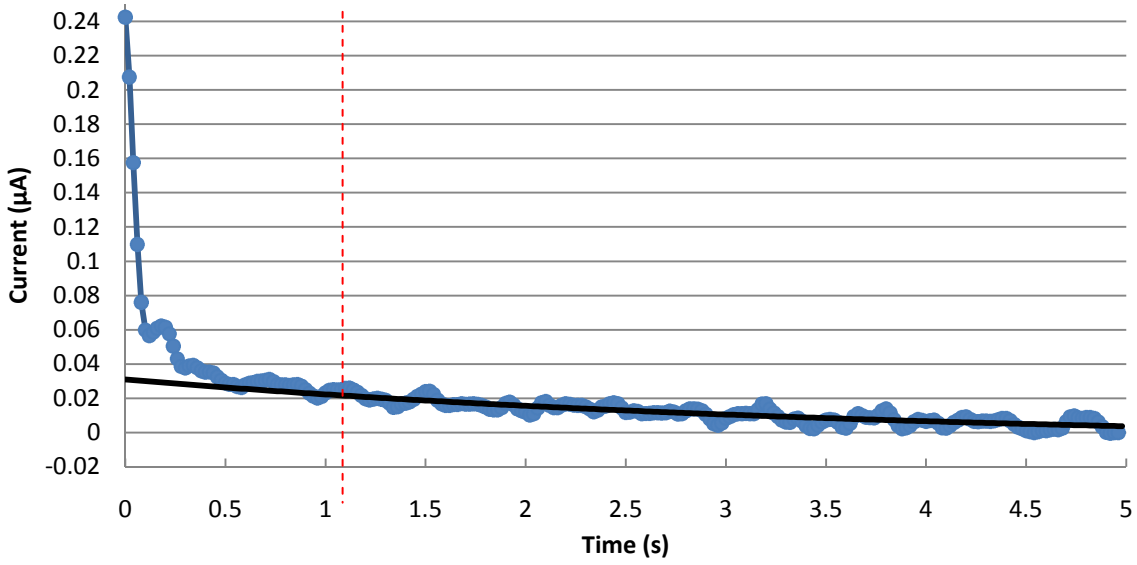

Figure 6.9. Anodic current from a 158 µm x 10 mm x 10 mm sample after a 3.0 % tensile strain was applied. The regression line was fitted to current data after the dashed line, which indicates 55 % of total charge displacement at 1.10 seconds.

The calculated diffusivities and regression constants from each of the film thickness are shown in Table 6.2. The constant $m1$ is not shown because it is a result of

galvanic current between the working and counter electrodes, and is not relevant to the electrical properties of polyaniline. The mean calculated diffusivities for 54.8 and 11.4 μm films fall within the range of published values (2.0×10^{-8} to 1.05×10^{-6} cm^2/s) for chlorine in polyaniline [1-4].

Table 6.2. Regression Calculated Diffusivity of Chlorine in Polyaniline

Thickness (μm)	**Mean Regression Data**		Mean Calculated Diffusivity (cm^2/s)	Standard Deviation (cm^2/s)
	m3	m2 (μA)		
158	3.717	0.037	1.70×10^{-6}	5.19×10^{-7}
54.8	1.786	0.023	4.15×10^{-7}	2.02×10^{-8}
11.4	0.199	0.131	1.65×10^{-7}	1.86×10^{-8}

The charge displaced by 3% strains in polyaniline films determined based on regression constants, integration of experimental data, and application of the theoretical modeling are shown in Table 6.3. The diffusivity calculated from *m*3 at each thickness was used to calculate the charge displaced based on the constant *m*2. This was an ineffective method of determining the total charge displacement because it compounded the error in constants *m*2 and *m*3, and it did not account for charge which was displaced in the first 0.3 seconds before the sample reached its final 3% strain. The integration method produced larger charge displacements and exhibited a more consistent trend in charge displacement with increasing thickness. The theoretical charge displacements based on assumptions of a 1.0 M concentration of chlorine ions in the polyaniline, a Poisson's ratio of 0.35, and selective absorption negative ions were 1-2 orders of magnitude larger than observed displacements.

Table 6.3. Determination of Charge Displaced by 3% Tensile Strain via Various Methods

Thickness (μm)	Charge Displacement (C)		
	Regression	Integration	Theoretical
158	1.70×10^{-7}	2.37×10^{-7}	1.74×10^{-5}
54.8	5.05×10^{-8}	1.45×10^{-7}	6.03×10^{-6}
11.4	3.22×10^{-8}	5.29×10^{-8}	1.54×10^{-6}
2.72	-	2.83×10^{-8}	2.99×10^{-7}

The assumption that polyaniline is completely selective to negative ions likely accounts for lower experimental charge displacements that the theoretical model suggests. It is known that H_3O^+ ions are absorbed and deprotonated when polyaniline undergoes a shift in oxidation state, so it is likely that these cations will be somewhat soluble in polyaniline. If a Cl^- anion is absorbed simultaneously with a H_3O^+ cation, the net charge displacement will be zero and there will be no electrical output. It is apparent from the sign of the current peak that polyaniline exhibits some anion selectivity; however cation absorption likely plays a role in attenuating the electrical output.

Losses in the electrical contacts and connections were negligible, as preliminary testing showed that the number and surface area of the gold contact electrodes had no effect on the electrical output. Large resistive effects would have caused a broadening and reduction in amplitude of the current peaks, resulting in a lower calculated diffusivity. This does not appear to be the case, as the calculated diffusivities are consistent with those found in literature.

The decreasing charge displacement per volume of polyaniline at increasing film thicknesses (Table 6.3 & Figure 6.10) was not consistent with the theoretical predictions. This trend may have resulted from the incomplete diffusion of chlorine ions into the core of thicker films. The diffusion path length (thickness/2) would therefore have been reduced, which justifies the unexpected increase in calculated diffusivity with increasing

thickness, shown in Table 6.2. When it is assumed the effective path lengths at increasing film thicknesses are reduced, the inconsistencies in both charge displaced and diffusivity with respect to film thickness are resolved.

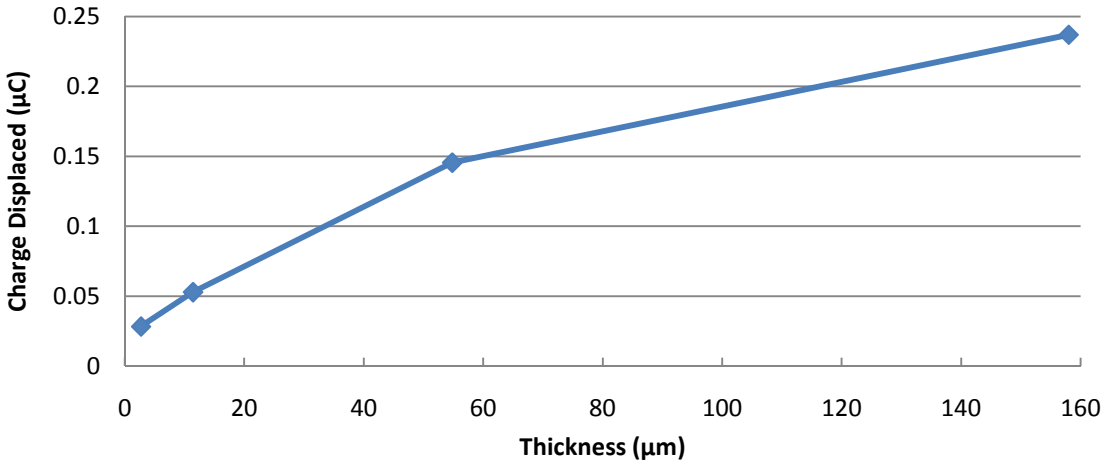

Figure 6.10. Non-linear increase in charge displacement with increasing film thickness based on integration of experimental data.

Relaxation of polyaniline during individual strains steps (Figure 6.3) may account for a reduced effective path length. Relaxation is a viscoelastic (time-dependent) phenomenon, and therefore the electrical outputs of thicker films will be more affected because the diffusion time is greater. It has been demonstrated theoretically and experimentally that the Poisson's ratio of polymers such as PE and PTFE, which have viscoelastic properties similar to polyaniline, will increase with time [5-7]. Relaxation occurs as the polymer chains align in the direction of stress. This alignment results in greater packing efficiency; increasing the density and decreasing the sample dimensions perpendicular to the axis of applied strain. Per Equation 3.9, a greater Poisson's ratio will result in smaller change in volume and reduced charge displacement. If this hypothesis is correct, the observed rate of decay in the current vs. time plot is a function of both anion diffusion and relaxation rates, with an increase in either factor resulting in a more rapid

current decay. The model to determine regression constants assumed that the current decay was only a function of anion diffusion, therefore any effects of relaxation would have increased the calculated diffusivity. Thicker films experienced greater relaxations before steady state currents were observed, which explains how the calculated anion diffusivities are greater than those observed in thinner films, although the true diffusivities remained constant.

Surface adsorption of anions may explain the initial large increase in charge displacement the lowest (2.72 µm) thickness. Positive strain increases the surface area of the polyaniline film by a factor of $\varepsilon(1 - \nu)$, exposing more positive amine sites to the solution and increasing the number of anions which will adsorb to the surface. Assuming that the area of the edges of the film is negligible, the change in surface area is independent of the thickness of the film.

To validate the model used for regression, the diffusivity and displaced charge which were determined via regression using the long model ($\frac{N_t}{N_\infty} \geq 0.55$) were used to plot the equation for the short model ($\frac{N_t}{N_\infty} \leq 0.50$). As illustrated using the experimental current output from a 158 µm thick film in Figure 6.11, this yields a reasonable fit to experimental data.

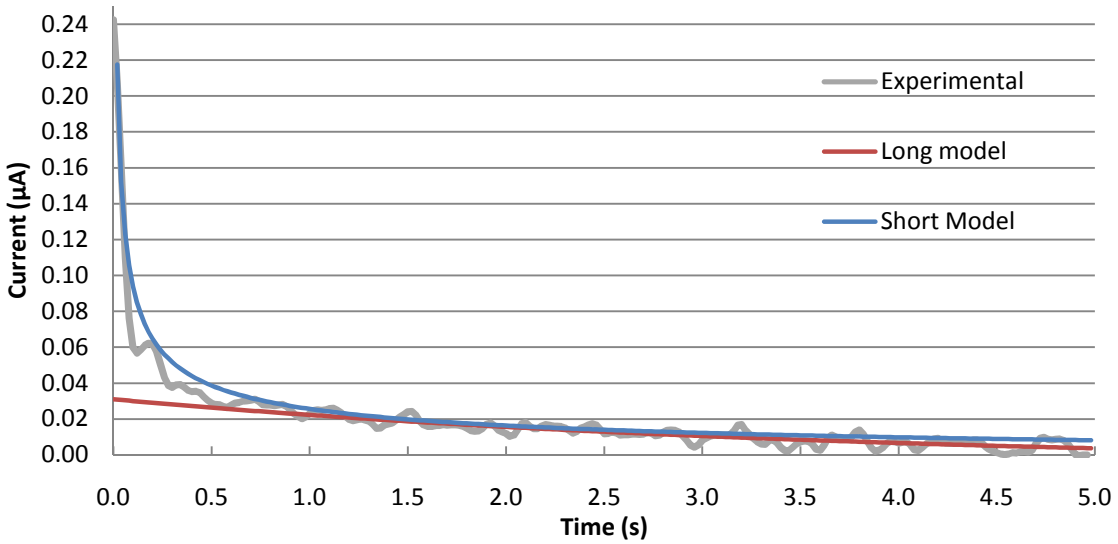

Figure 6.11. Anodic current from a 158 µm x 10 mm x 10 mm sample after a 3.0 % tensile strain was applied. Constants determined via regression using the long model were used to plot the short model.

6.1.3. Electrolyte Concentration

The HCl concentration did not have a large affect on the anodic current peak amplitudes in solutions greater than 0.01 M (Figure 6.12). Per Equation 3.12 for charge displacement, the total charge displaced should exhibit a linear dependence on steady-state concentration of anions in polyaniline. Because the observed charge displacement is nearly constant with decreasing electrolyte anion concentration, this test indicates that the anion concentration in the polyaniline is not directly dependent on the anion concentration in the surrounding electrolyte. At low HCl concentrations ($\leq$ 0.001 M), the conductivity of polyaniline began to decrease as it changed in oxidation state from emeraldine salt to emeraldine base or pernigraniline, which are more stable at higher pH's. Polyaniline is only conductive in its emeraldine salt state, so this transition increased the sample resistivity of the polyaniline. Increased sample resistance is

consistent with the reduced amplitude and slower discharge of current from the polyaniline observed when 0.001 M and 0.00001 M HCl concentrations were used.

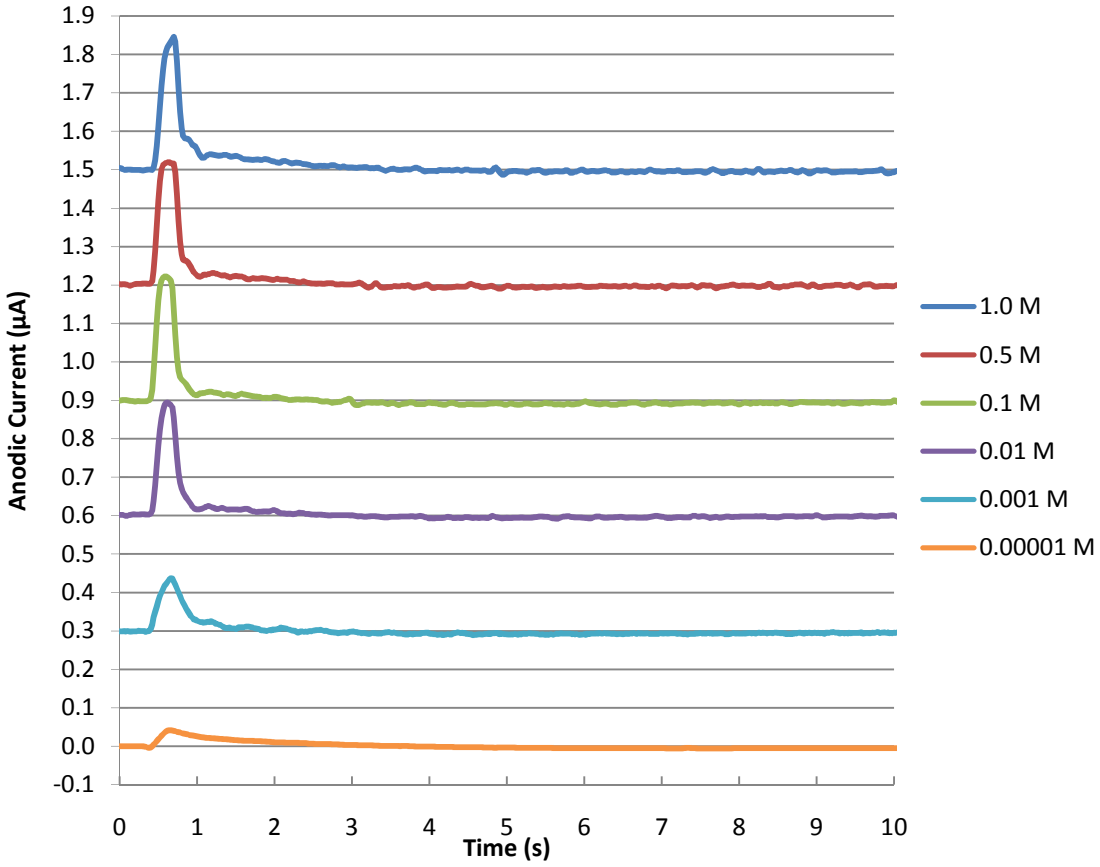

Figure 6.12. Typical anodic currents produced by 3.0 % strains to a 158 µm x 5 mm x 10 mm polyaniline film in HCl solutions of various concentrations. Each plot is artificially offset by 0.3 µA.

When HCl concentrations were decreased, the anodic current produced by a positive strain exhibited a small but consistent dip after the initial current peak. Figure 6.13 contrasts the current produced in a 0.1 M HCl solution, in which the current dip was observed, with the current produced in a 1.0 M HCl solution, in which the current dip was not observed. It is unlikely that mechanical factors such as relaxation are responsible for the current dip because it had a consistent dependence on concentration. It is more likely that the negative current occurs when H_3O^+ ions diffuse into the material. The

concentration dependence of this effect can be justified by a change in the average oxidation state with increasing pH (Figure 6.14). At low pH's, the amine groups will be saturated with hydrogen atoms, and positive charges at these sites will repel positively charged ions. These repulsions will cause the material to exhibit low cation solubility. At higher pH's, fewer amine groups will be positively charged, and cation solubility will increase. When an amine is not positively charged, the lone electron pair belonging to the nitrogen atom will interact strongly with small cations (Figure 6.15), leading to lower cation mobility within the polymer and a slower rate of cation absorption. This lone pair-cation interaction has been extensively studied with respect to the stabilization of metal ions in solutions using nitrogen containing "ligands" [8]. Specifically, the interaction of ligands with H_3O^+ cations has been demonstrated to reduce the diffusivity of H_3O^+ in aqueous solutions [9].

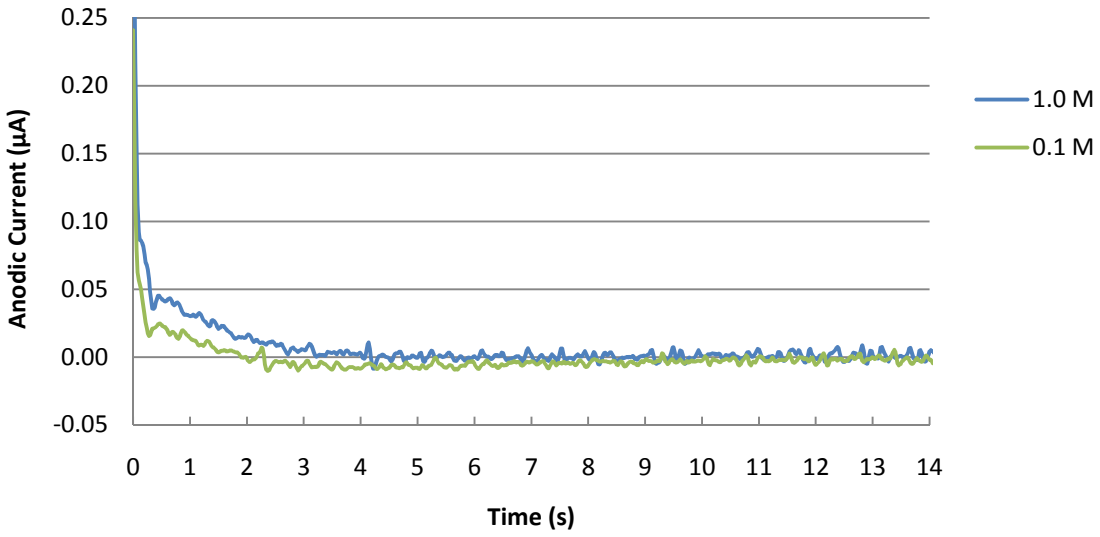

Figure 6.13. Anodic current produced by a 3.0 % strain to a 158 µm x 5 mm x 10 mm polyaniline film in 1.0 M and 0.1 M HCl solutions. The anodic current drops below zero when the lower HCl concentration is used.

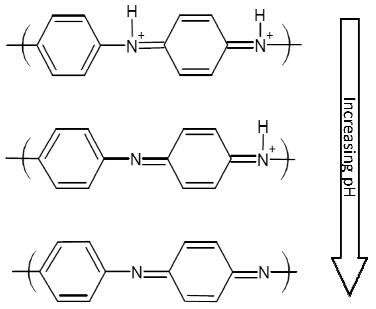

Figure 6.14. Deprononation of polyaniline in its pernigraniline state with increasing pH. Similar deprononation occurs in the emeraldine and leucoemeraldine states.

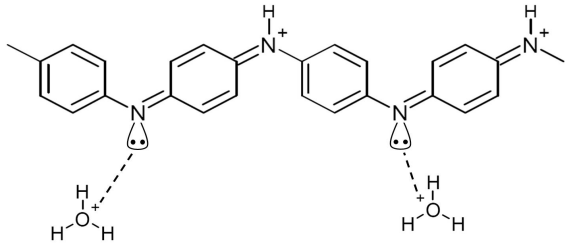

Figure 6.15. Interactions between lone pairs of unprotonated nitrogen atoms of polyaniline and hydronium cations.

Figure 6.16 shows that the positive and negative exponential decay functions of currents corresponding to anion absorption and slower cation absorption can be summed to yield the observed current profile.

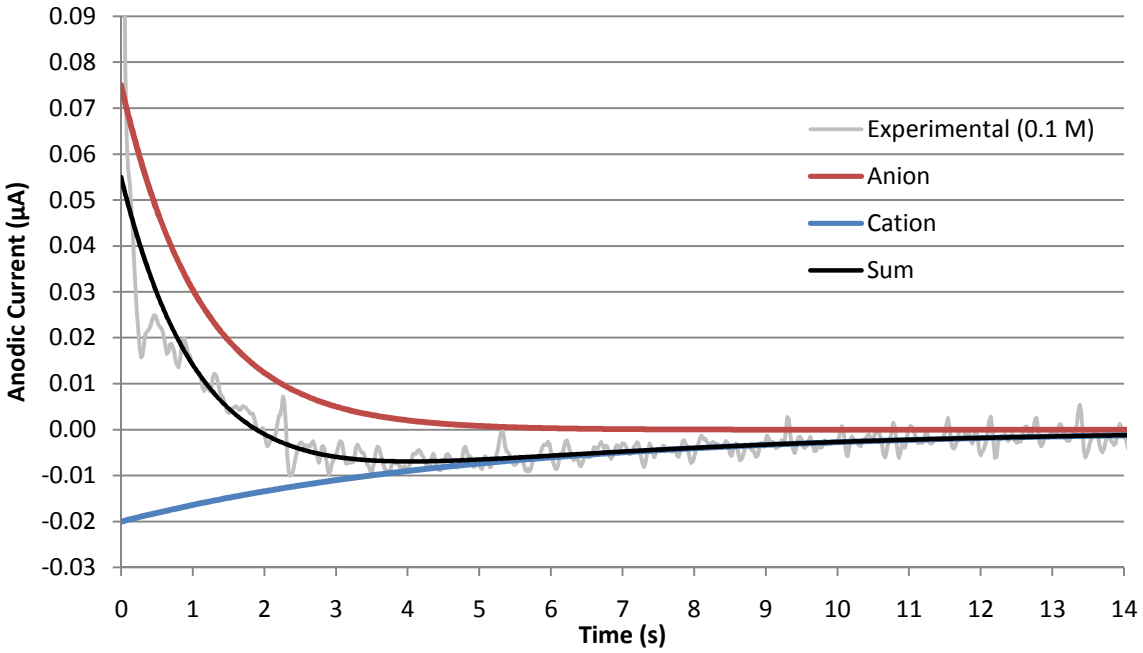

Figure 6.16. The anodic current from a 158 µm x 5 mm x 10 mm polyaniline film after a 3.0 % strain in 0.1 M HCl modeled as a sum of anion and cation transport processes.

Two important observations were made in assessing the effects of HCl concentration on the electrical properties of polyaniline sensors. First, the steady-state concentration of anions in polyaniline is primarily dependent on the chemical state of the polymer, not the anion concentration in the surrounding electrolyte. Second, polyaniline is not completely selective to negative ions, but will absorb positively charged ions in some cases.

6.1.4. Linearity

Linearity of the electrical output with strain exhibited dependence on the magnitude and history of applied strains. These dependences are observed as differences within and between instantaneous and stepwise strain tests.

6.1.4.1. Instantaneous Strain

The currents generated by strains of from 0.5 to 2.0 % applied to a 54.8 µm x 10 mm x 10 mm film in 1.0 M HCl are shown in Figure 6.17. As expected, the current amplitude increased with increasing strain. The oscillating strains in this method resulted in relaxation of the polyaniline over time (Figure 6.18). As the polymer relaxed, the true strain within the material decreased, decreasing the number of ions absorbed. This was observed as a 48 % decrease in the total charge displacement after 50+ cycles (Figure 6.19). Additionally, relaxation caused buckling of the film when the grips returned to their initial positions due to increase gauge length of the sample. This was observed as reduced charge displacement resulting in nonlinearity at low strains.

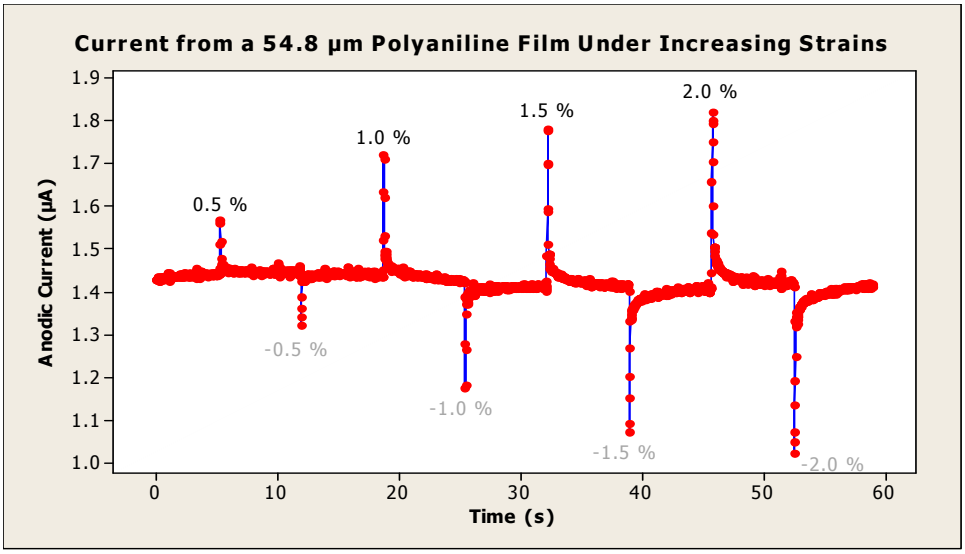

Figure 6.17. Peaks in anodic current resulting from strains between 0.5 % and 2.0 %. The negative peaks represent negative strain and desorption of ions as the film is returned to its initial position.

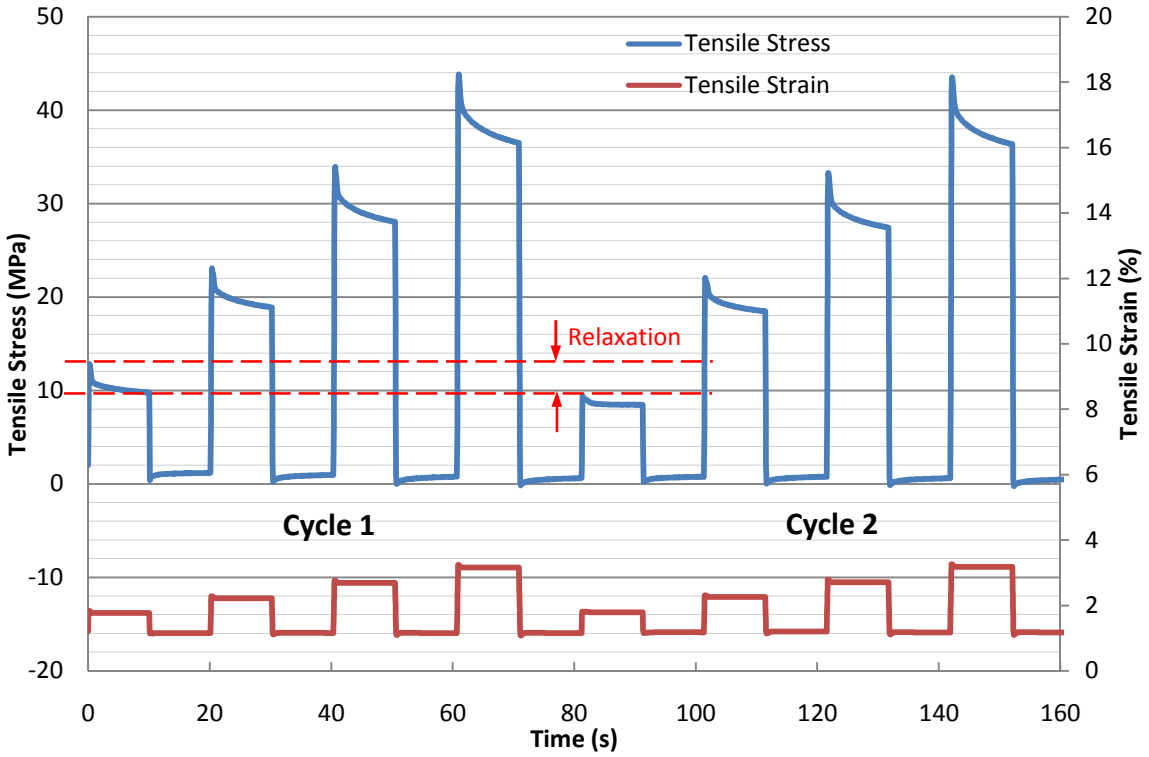

Figure 6.18. Tensile stress and strain profiles during the first two cycles of instantaneous strain linearity testing of a 54.8 µm x 10 mm x 10 mm polyaniline film.

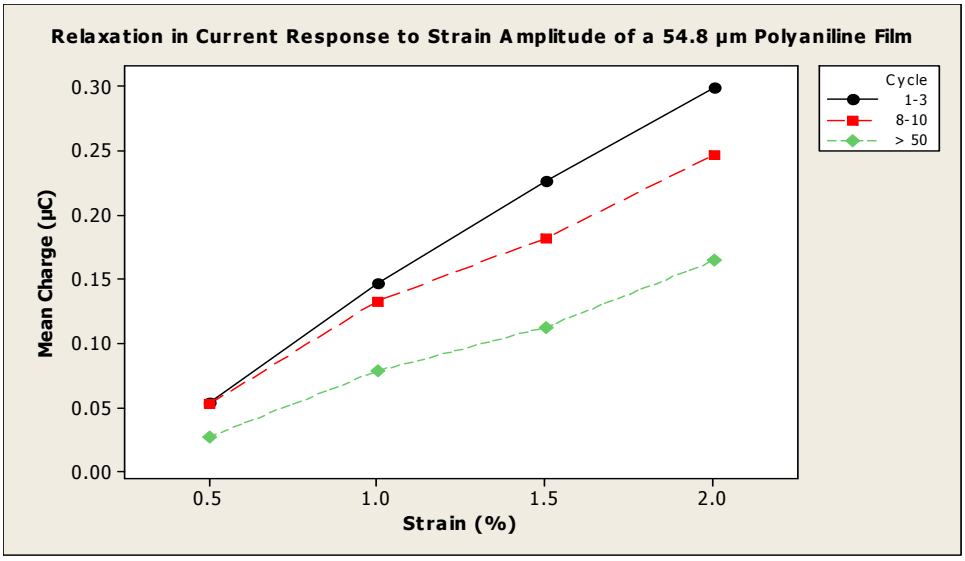

Figure 6.19. The mean charge displaced at strain amplitudes from 0.5 to 2.0 % observed at various periods in cyclic testing. The green line (cycles > 50) is representative of steady-state conditions.

Although the magnitude of the displaced charge was affected by relaxation of the polymer, the proportional charge displaced at incremental strains within a single cycle (i.e. linearity) was independent of the degree of relaxation. This was demonstrated by normalizing the four data points in each plot to the maximum charge displacement at 2.0 % strain. This method inherently resulted in zero deviation at 2.0 % strain, while the deviations at 0.5, 1.0 and 1.5 % strain were low (Figure 6.20). An unstacked one-way ANOVA test showed that the charge displaced per percent strain was significantly less at 0.5 % strain (CI = 0.95, p = 0.000), but was not significantly different among 1.0, 1.5, and 2.0 % strains (CI = 0.95, p = 0.785).

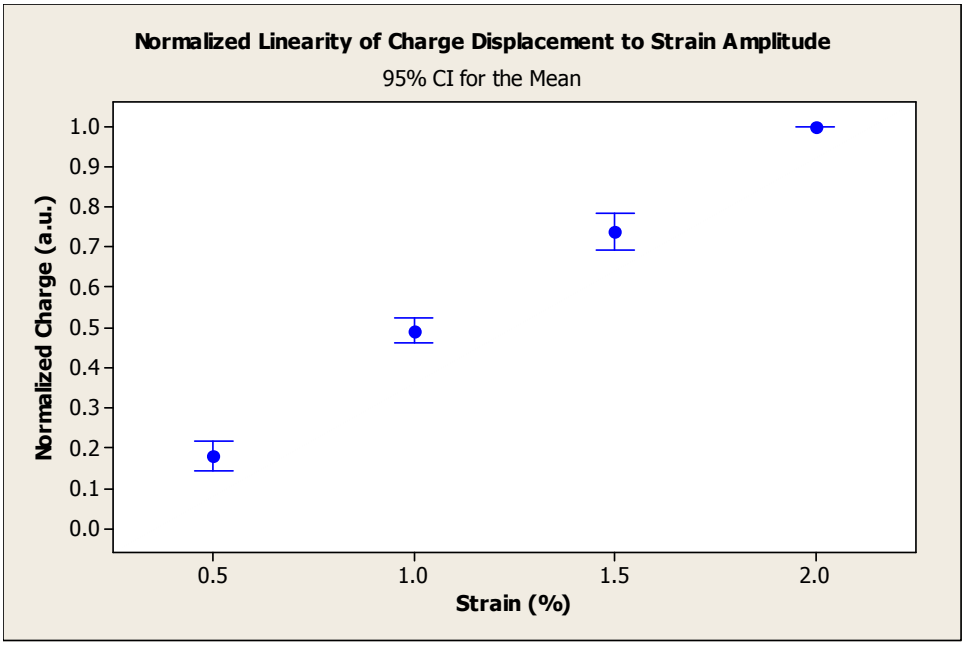

Figure 6.20. The charge displaced by instantaneous strains from 0.5 to 2.0 %, normalized by dividing each value in a single cycle by the charge displaced by 2.0 % strain.

6.1.4.2. Stepwise Strain

Relaxation during stepwise 0.5 % strains to 54.8 µm x 10 mm x 10 mm films are evident from the tensile stress profiles in Figure 6.21, however they appear to fully recover by the end of the cycle. The current generated by these strains is shown in Figure 6.22. The amplitude of each positive peak is similar, indicating that the electrical response is independent of the initial strain state. The area under each peak was found in order to determine the charge displaced by each step (Figure 6.23). An unstacked one-way ANOVA test showed that the mean charge displaced at each step was not significantly different (CI = 0.95, p = 0.453).

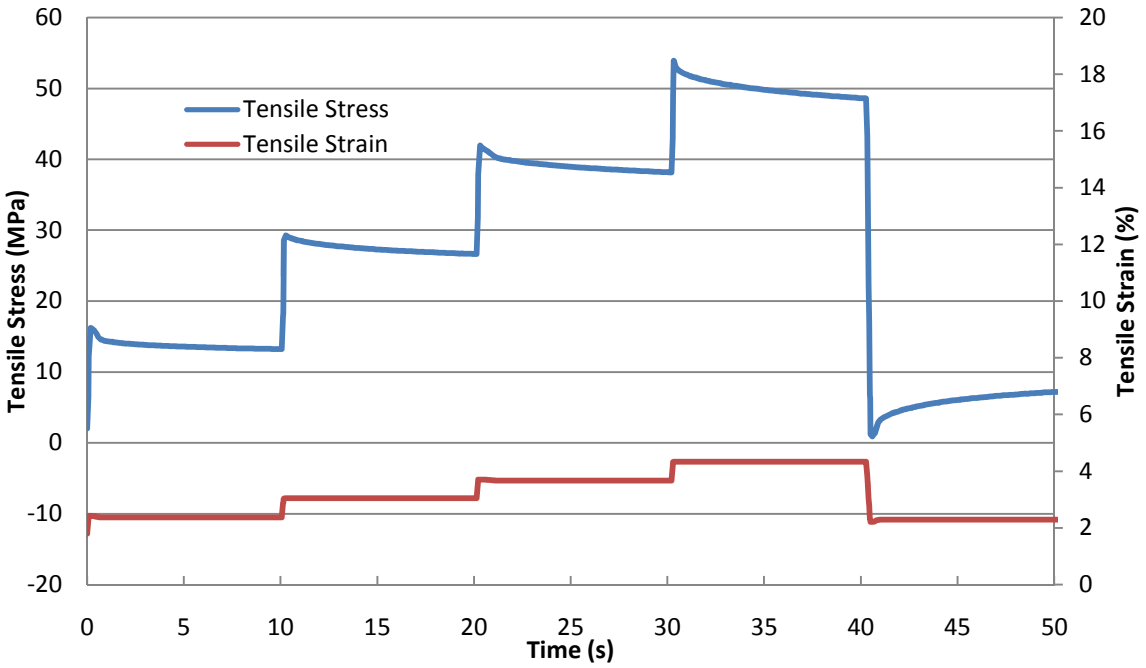

Figure 6.21. Tensile stress and strain profiles during one cycle of stepwise strain linearity testing of a 54.8 µm x 10 mm x 10 mm polyaniline film.

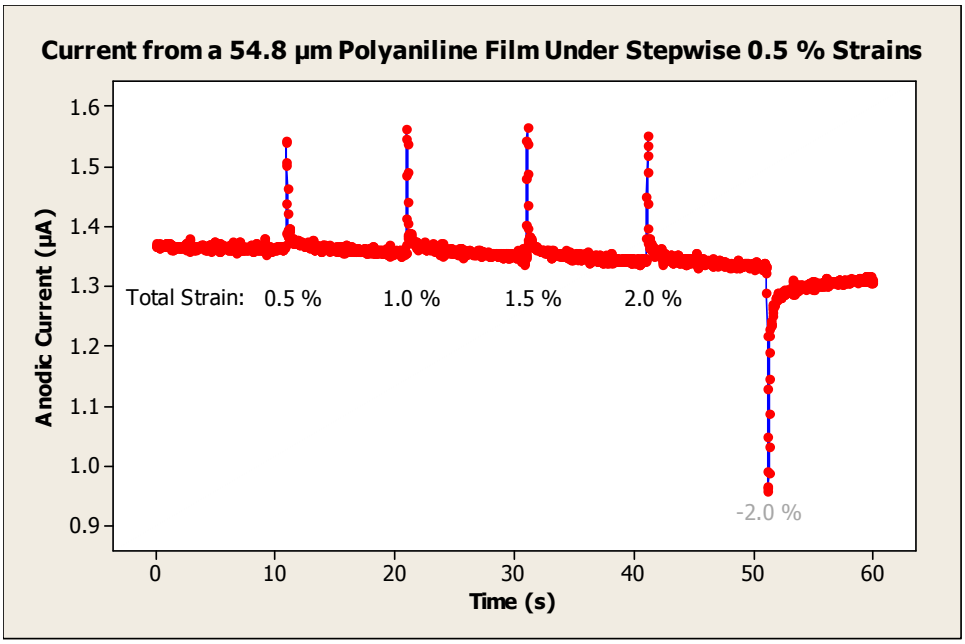

Figure 6.22. Current peaks resulting from four stepwise 0.5 % strains in a 54.8 µm thick polyaniline film. The large negative peak represents negative strain as the film is returned to its initial position.

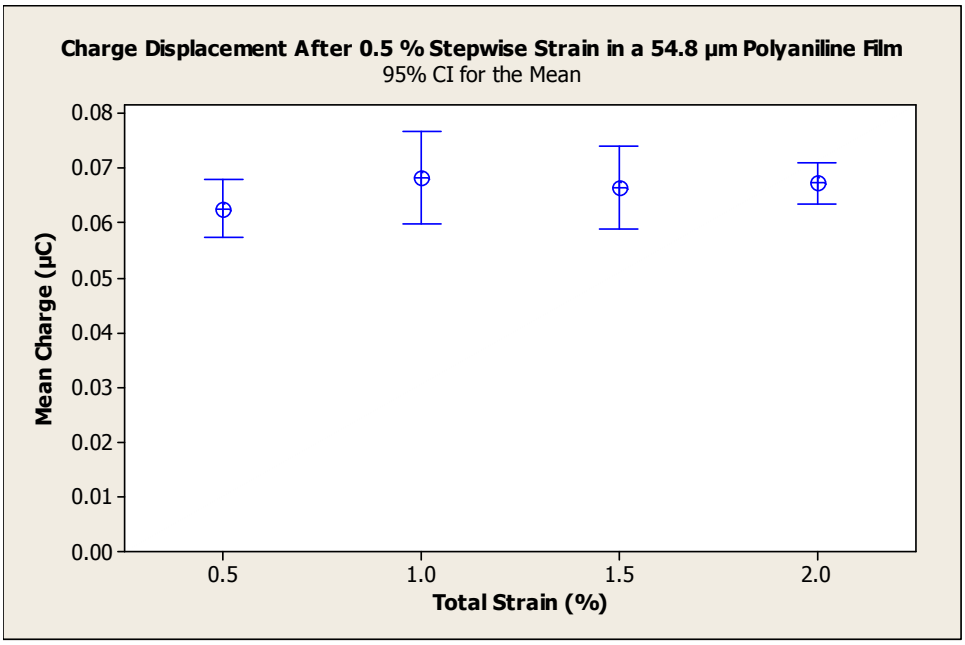

Figure 6.23. The charge displaced by a stepwise 0.5 % strains in a 54.8 µm x 10 mm x 10 mm thick polyaniline film showing dependence of charge displacement on the initial strain condition.

When the charges displaced by stepwise strain (Figure 6.23) were summed over increasing strains, they exhibited greater linearity than charges displaced with the

instantaneous strain method (Figure 6.24). These differences illustrate the strong dependence of linearity and efficiency on relaxation.

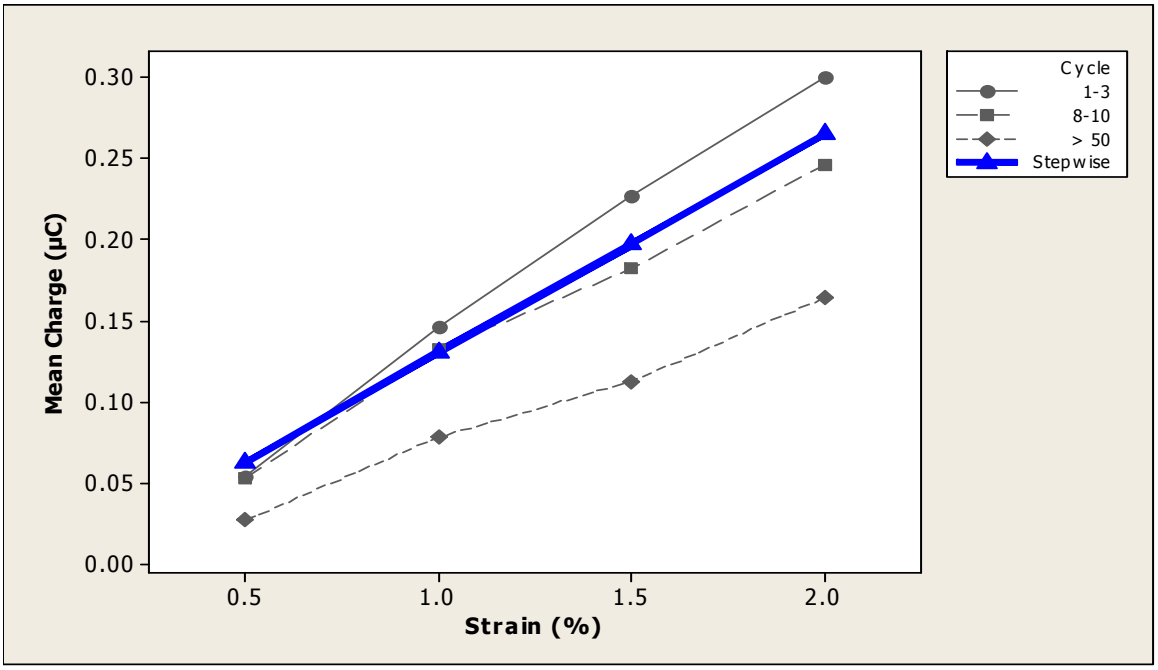

Figure 6.24. Comparison of charge displacements in instantaneous and stepwise strain methods.

6.1.5. Oxidation State

Figure 6.25 shows the oxidation of emeraldine salt (ES) to pernigraniline salt (PS) beginning at approximately +0.4 V (peak 1), and the reduction from ES to leucoemeraldine (LES) at approximately -0.4 V (peak 3). Peaks 2 and 4 correspond to the reduction from PS to ES, and oxidation from LES to ES, respectively, and are not immediately relevant because they do not correspond to the limits of the ES state. Current consumed through oxidation and reduction can be distinguished from that leakage current between the sample and counter electrodes because the current profiles when during increasing and decreasing and decreasing potentials do not overlap. The polyaniline structures corresponding to these oxidation states are shown in Figure 6.26.

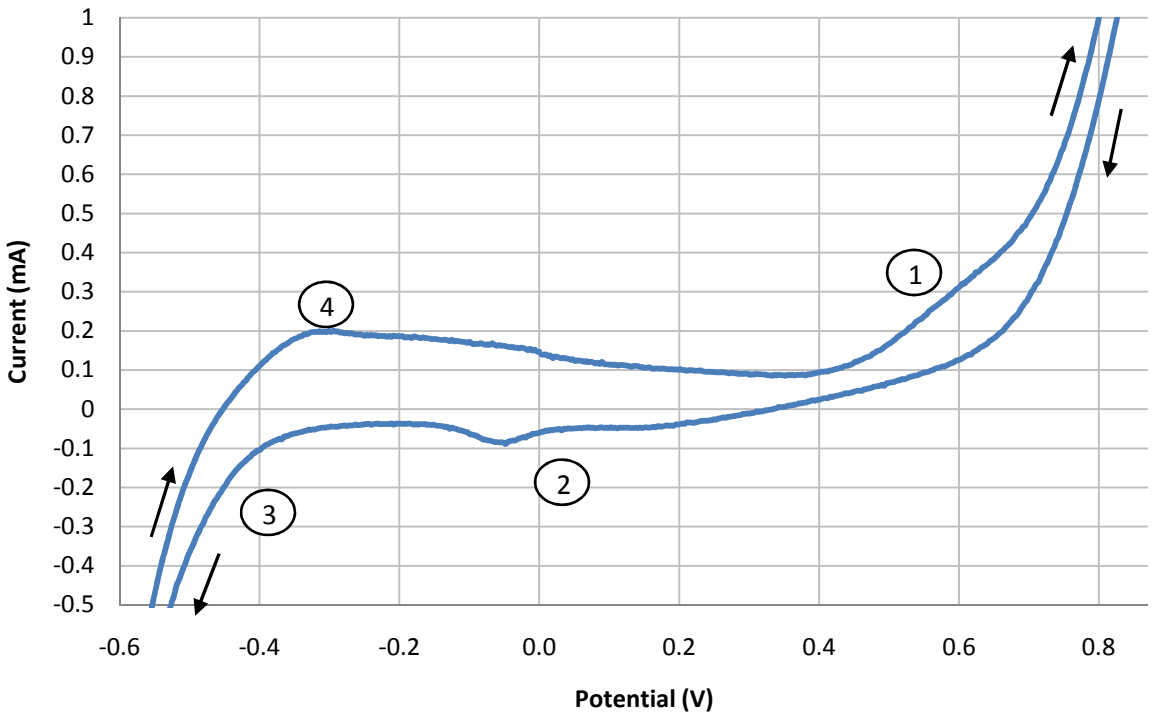

Figure 6.25. Cyclic voltammogram of a polyaniline film from -0.6 V to +1.0 V (vs. open circuit potential) in 1.0 M HCl indicating the ES→PES oxidation (1), PES→ES reduction (2), ES→LES reduction (3), and the LES→ES oxidation (4).

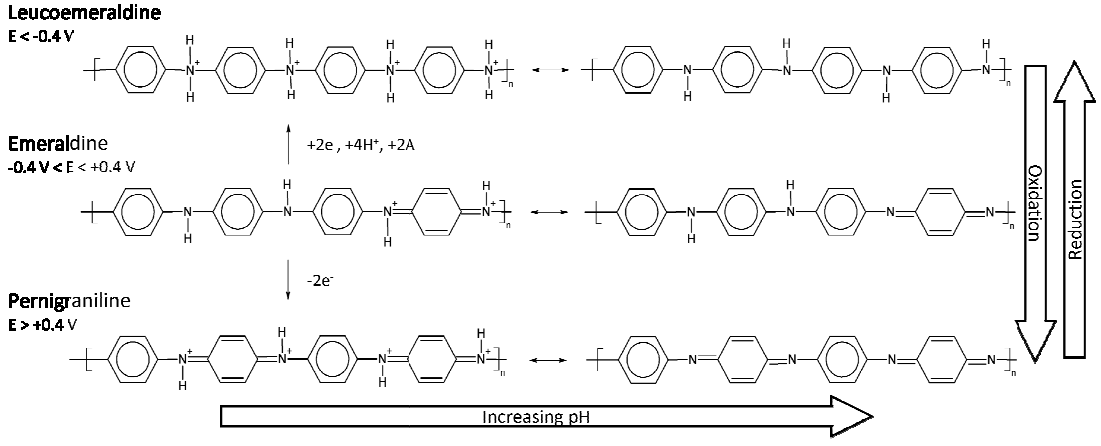

Figure 6.26. The relative dependence of the chemical structure of polyaniline on the pH of the supporting electrolyte and the oxidation potential.

Measuring the current output near the oxidation and reduction potentials was unsuccessful because high leakage currents amplified the effects of vibrations within the test bath, increasing noise and obscuring the current output from the sample. Reducing the solution concentration to 0.1 M did not sufficiently reduce the leakage current. It is possible to observe the effects of oxidation state in potential measurements rather than current measurements because the oxidation state of polyaniline will not immediately change when there is an open circuit between the sample and the counter electrode. This is an area for potential future study.

6.2. Open Circuit Potential

When the circuit between the polyaniline sample and the counter electrode was held open, the charge displacement described in the previous section resulted in a potential between the two electrodes. Linear charge displacement corresponded to a linear potential-strain relationship.

6.2.1. Bilayer Device

The postion sensor output at when actuate by hand at bending angles of ±45° is shown in Figure 6.27. Although the output is strictly qualitiative, it demonstrates the position sensitivity of the potential output as well as the ability to operate at frequencies of at least 6 Hz. The unamplified potential range of this device was approximately 0.17 V.

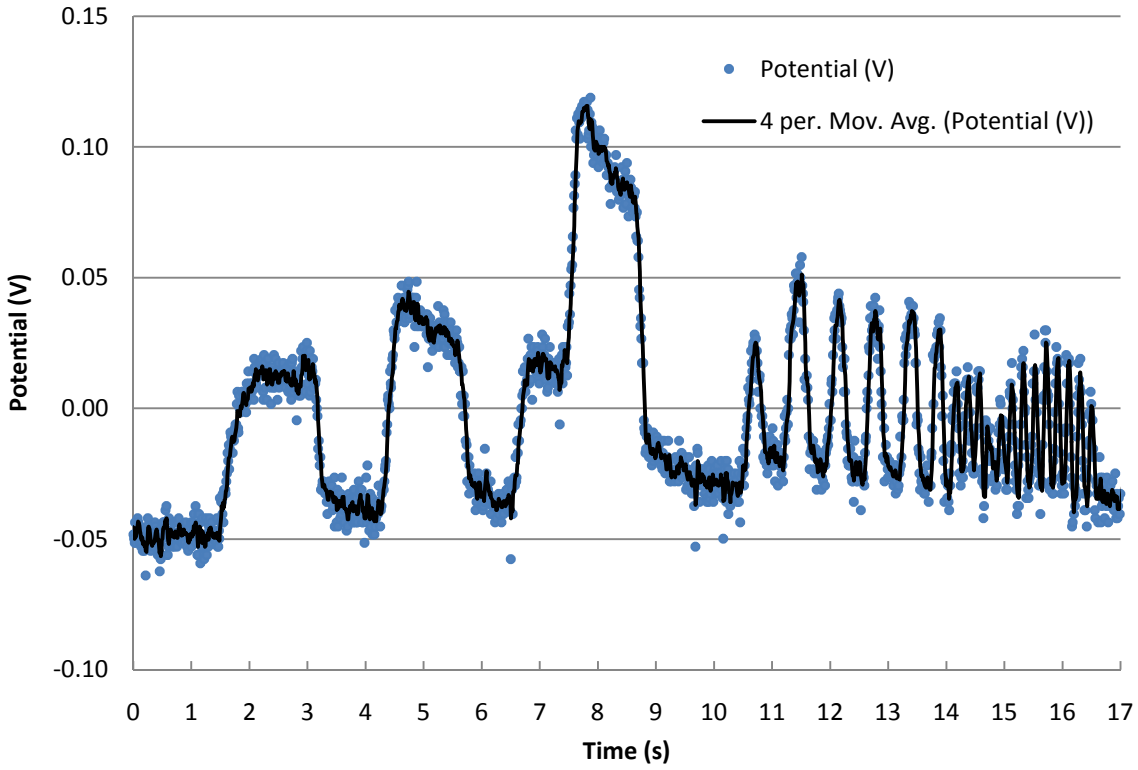

Figure 6.27. Open circuit potential across a hand-actuated polyaniline bilayer in a 1.0 M HCl solution.

6.2.2. Tensile Strain

A 54.8 µm x 10 mm x 10 mm polyaniline film was strained using the Instron MINI 55 to observe the potential response to strain more precisely. This method eliminated approximations and variation associated with the use of bending samples because the stresses and strains in the material could be directly measured and controlled. The potentials observed with this method were on the order of 0.1 mV, several orders of magnitude lower than the bilayer configuration, due to the greater capacitance of the experimental setup. Figure 6.28 shows the loads and potentials which correspond to a cycling stepwise strain. This plot illustrates the sensitivity of the output potential to applied strain, and the stability of the output potential over time. Figure 6.29 shows an oscillating strain cycling at the highest frequencies possible with the Instron. At 4 Hz, the

potential profile is distinct and closely matches the strain profile, indicating that higher strain frequencies could be used without significant output attenuation or distortion.

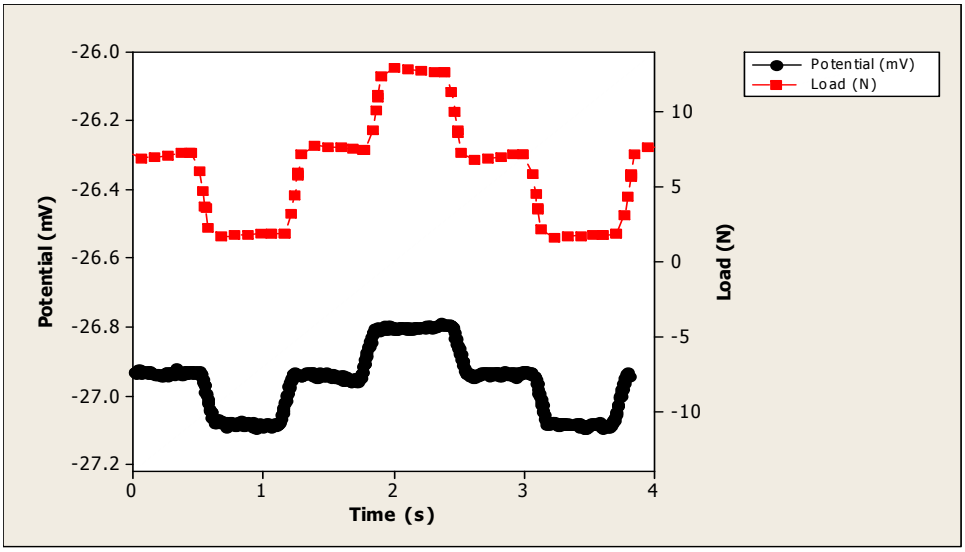

Figure 6.28. Potential produced by stepwise tensile strain applied to a 54.8 µm x 10 mm x 10 mm polyaniline film in 1.0 M HCl.

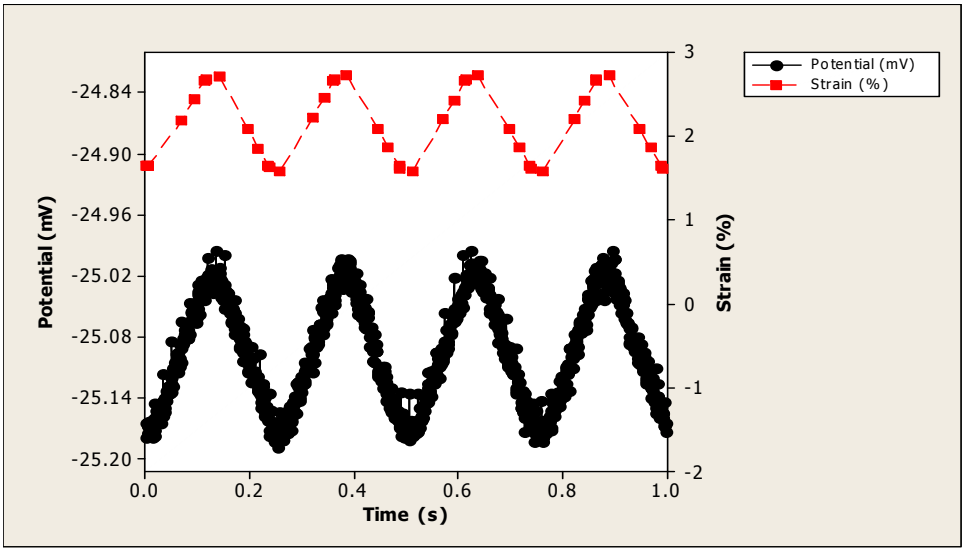

Figure 6.29. Potential produced by a 4 Hz oscillating tensile strain applied to a 54.8 µm x 10 mm x 10 mm polyaniline film in 1.0 M HCl.

6.3. References

[1] L. Wen, N. Kocherginsky. "Coupled HC/anion transport through polyaniline membranes." *Journal of Membrane Science*, vol. 167, pp. 135–146, 2000.

[2] H. Zhao, W. Price, C. Too, G. Wallace, D. Zhou. "Parameters influencing transport across conducting electroactive polymer membranes." *Journal of Membrane Science*, vol. 119, pp. 199-212, 1996.

[3] Z. Wang, E. Smela. "Understanding Ion Transport in Conjugated Polymers." Smart Structures and Materials 2005: Electroactive Polymer Actuators and Devices. SPIE, 2005.

[4] C. Deslouis, T. Moustafid, M. Musiani, M. Orazem, V. Provost, B. Tribollet. "Effect of cations on the diffusivity of the charge carriers in polyaniline membranes." *Electrochemica Acta*, vol. 44, pp. 2087-2093, 1999.

[5] I. Dzene, A. Putans. "Poisson's Ratio of Polyethylene in Creep Recovery." *Mekhanika Polimerov*, vol. 4, pp. 563-564, 1968.

[6] I. Dzene, A. Putans. “Poisson's Ratio of Polyethylene in One-Dimensional Creep." *Mekhanika Polimerov*, vol 3, pp. 947-949, 1967.

[7] I. Dzene. "Variation of Poisson's ratio in the course of a complete one-dimensional creep cycle." *Mekhanika Polimerov*, vol. 4, pp. 227–231, 1968.

[8] R. Hancock, A. Martell. "Ligand design for selective complexation of metal ions in aqueous solution." *Chemical Reviews*, vol. 89, pp. 1875–1914, 1989.

[9] M. Amini, M. Shamsipur. "Complex Formation of Hydronium Ion with Several Crown Ethers in 1,2-Dichloroethane, Acetonitrile, and Nitrobenzene Solutions." *Journal of Solution Chemistry*, vol. 21, pp. 1572-8927, 1992.

CHAPTER 7

CONCLUSIONS

7.1. Summary of Achievements

This section briefly outlines the final parameters which were used to fabricate and evaluate polyaniline films.

7.1.1. Sample Fabrication

Films employing electrochemically and chemically polymerized polyananiline were fabricated and evaluated for use as sensor materials. Electrochemically prepared polyaniline films produced via potentiostatic and galvanostatic methods exhibited poor mechanical properties, and could not be used. Processing difficulties of chemically polymerized polyaniline were overcome to produce homogeneous films with good mechanical properties from polyaniline solutions.

Chemically polymerized polyaniline with a weight average molecular weight of 65,000 was dissolved in a NMP solvent containing 1.1 mol of HPMI per 1.0 mol of aniline repeat units. After mixing in a Thinky ARE-100 mixer, homogeneous solutions with polyaniline concentrations of $\leq$ 10 wt% which would not immediately gel were obtained. From these solutions, polyaniline films of various thicknesses were cast on glass slide and annealed at 120°C for 2 hours. Polyaniline films were doped in 1.0 M HCl, which also caused them to delaminate from the glass slides.

7.1.2. Experimental Methods & Materials

Custom sample grips were fabricated, which applied tensile strain to rectangular sections of polyaniline film while submerging in HCl solutions and maintaining electrical contact with the samples. The grips interfaced with an Instron MINI 55 material tester which was controlled by Instron Bluehill Software. Electrical outputs to sample and counter electrodes were measured with a Prinston Applied Research PARSTAT 2273 electrostat.

Current output was the primary focus of study because the displaced charge can be directly calculated from this data, which can be used to predict the electrical response in a variety of conditions. Current was measured as the sample was held at a constant potential with respect to a counter electrode.

7.1.3. Analysis Methods

The diffusivity of chlorine ions in polyaniline was determined by fitting an equation designed to predict the diffusion of ions in a polymer to the observed exponential current decay. This method could also be used to determine the total charge displaced, however integration of experimental data was a more accurate method.

7.2. Material Characterization

The ultimate goal of testing polyaniline films was to determine property and performance benchmarks which could be used in further analyses of sensing characteristics of polyaniline, or to develop functional devices. There was some variance with film thickness, so the material characteristics of 54.8 μm thick films are presented as

they are appropriate intermediate values. Table 7.1 shows the specific material properties for polyaniline, and Table 7.2 shows the parameters of polyaniline based sensors.

Table 7.1. Material Properties Observed in 54.8 μm Polyaniline Films

Yield Stress	19.0 MPa
Young's Modulus	428 MPa
Conductivity (Emeraldine Salt)	5×10^{-2} S/cm
Diffusivity	4.15×10^{-7} cm^2/s
Charge Displacement[1]	3.12 mC/cm^3
Oxidation Potential	+ 0.5 V
Reduction Potential	- 0.5 V

[1]assumes Poisson's ratio of 0.35

Table 7.2. Sensing Parameters Observed in 54.8 μm x 1.0 cm^2 Free Standing Polyaniline Films

Input Range	Strain	< 8.5 %
Output Range	Charge	< 1.13 μC
	Peak Current	< 0.59 μA
	Voltage	< 1.5 mV
	Voltage (bilayer)	< 0.17 V
Noise	Current (stdev)	0.034 μA
Sensitivity	Charge	0.13 μC/%
	Voltage	0.18 mV/%
Operating Conditions	HCl Concentration	1.0 – 0.01 M
	Operating Potentials	- 0.5 V < E < + 0.5 V

The operating potentials were indicated by the oxidation and reduction peaks observed using cyclic voltammetry. Polyaniline sensors must be operated within this range of poltentials to ensure that the emeraldine salt state is maintained. A loss of conductivity will result from a change in oxidation state. Non-conductive polyaniline will not be effective in sensors, as the charge will not be able to escape the material or achieve a uniform distribution. In addition to electrical properties, reduction of the polyaniline into its pernigraniline state at potentials below -0.5 V embrittles the material. This embrittlement is a product of the shift from amine to imine nitrogen containing groups at reducing potentials. Unlike the σ-bonds of the amine, which may rotate 360˚ about the bond axis, the π-bonds which are formed in the imine configuration are stiffer and may

only be subject to limited rotation before breaking. The result of polyanilne with a high imine:amine ratio is a limited chain flexibility which cannot change its conformation to accomidate plastic deformation.

7.3. Future Work

The work performed in this thesis was intended to characterize the electrical response of polyaniline to mechanical strain at its most fundamental level. The following are areas of study which could build upon this knowledge.

7.3.1. Functional Sensors

The material characterization performed in this thesis should provide sufficient information to develop a complete strain sensor, which would display deflection as a function of current output. This work would incorporate materials, mechanical, electrical, and software disciplines, whereas the work to date has been primarily focused on chemistry and materials disciplines.

A functional strain sensor would provide an opportunity to couple sensing and actuation characteristics. An actuator/sensor could be developed from an existing sensor with little or no electrical or mechanical modifications because the physical format of these devices are identical, with software dictating the manner in which the device actively responds to mechanical strain.

7.3.2. Power Generation

The sensitivity of a sensor will dictate whether its output is sufficient to power an electrical device. A more detailed analysis of the maximum electrical energy produced by

a sensor should be conducted. This may be achieved by placing various resistive loads on the output circuit between the sample and counter electrode. The power output after mechanical strain is applied can calculated from the known value of the resistor and the instantaneous current from the sensor with the expression $P = i^2R$. Integrating the power output over time yields the electrical energy produced during one strain step. The electrical energy produced should reach a maximum over a range of resistive loads.

The efficiency of the sensor can be determined from the electrical energy produced relative to the mechanical work done on the sensor during one strain cycle. The energy required to elongate a sample is expressed as $E = ½ F\varepsilon$. The total mechanical work done on a sample is equal to the energy required to elongate the sample minus the elastic energy recovered when the sample was returned to its original position. The difference in applied and recovered strain energy is observed as hysteresis in the load-strain plot (Figure 7.1).

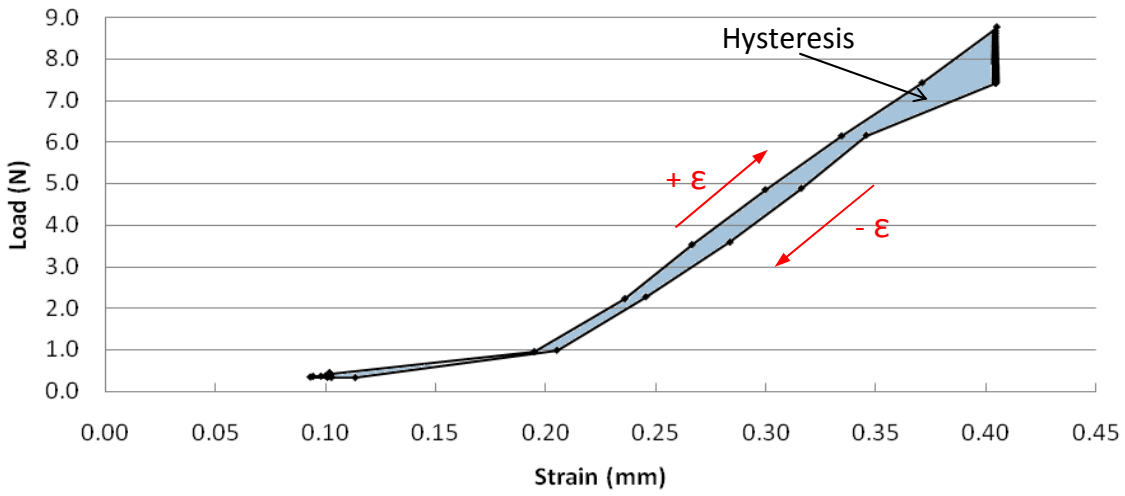

Figure 7.1. Hysteresis observed in a 54.8 µm x 10 mm x 10 mm polyaniline film during cyclic strain. The mechanical energy lost to hysteresis was 1.23 x 10^{-4} J.

7.3.3. Microsensing

Both electrochemical polymerization and casting methods can be readily integrated with existing microfabrication techniques. The very low diffusion path lengths of devices at this scale would reduce the signal decay time, allowing them to measure much higher frequencies with greater efficiency. Per Equation 3.17, which describes the number of ions which have diffused into polyaniline at a given time, the diffusion time increases as a function of path length squared. It took approximately 9 seconds to absorb 95% of the steady state number of ions into a 54.8 μm thick film, whereas a 1.0 μm thick film would require only about .0015 seconds to reach the same condition. In addition to reducing the invasiveness of an implantable sensor, microfabricated sensors could be used to monitor movement of organisms on a cellular level.

7.3.4. Electrolyte Species

Although the electrical response of polyaniline in the simple hydrogen chloride electrolyte was useful in evaluating sensing properties and processes, an understanding of sensing characteristics in a variety of electrolytes is necessary before polyaniline can be utilized in biological application. Most biological environments cannot sustain the low pH's needed to operate polyaniline sensors in the manner presented in this thesis, so the development of dopant/electrolyte systems which will operate at neutral pH's are most critical. As discussed in section 2.3.1., large dopant ions such as dodecylbenzene sulfonate has been used to produce actuators which are functional in neutral media. This technique could likely be applied to polyaniline sensors as well. No published studies have specifically evaluated the differences in performance between polyaniline actuators

which function in acidic and neutral media. It would be valuable to assess whether the concepts and performance characteristics developed in this thesis remain valid when large dopant ions are used.

The goal of developing polyaniline sensors which function in neutral electrolytes is their application to biological environments. Therefore, the performance of these devices should be optimized with electrolyte species and concentrations similar to those in the body. Commercially available solutions such as Hanks' balanced salt solution or saline which mimic electrolytes in the body could be valuable in this respect.

APPENDIX A: Dimensioned Test Fixture Drawings

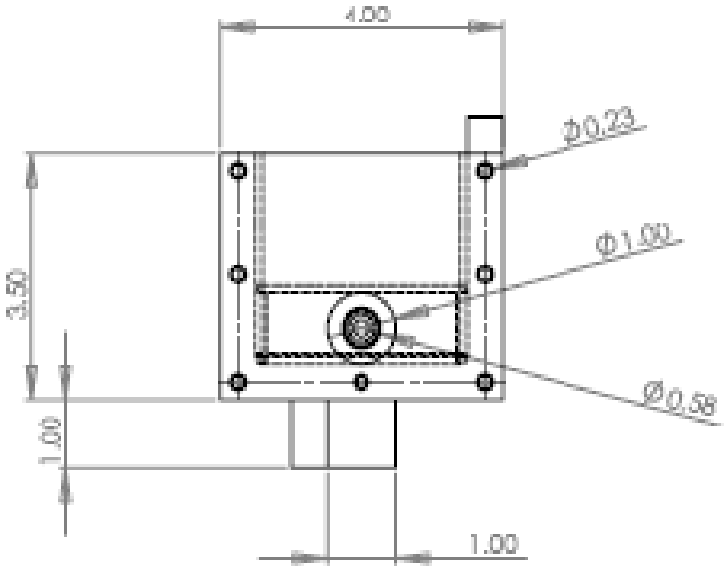

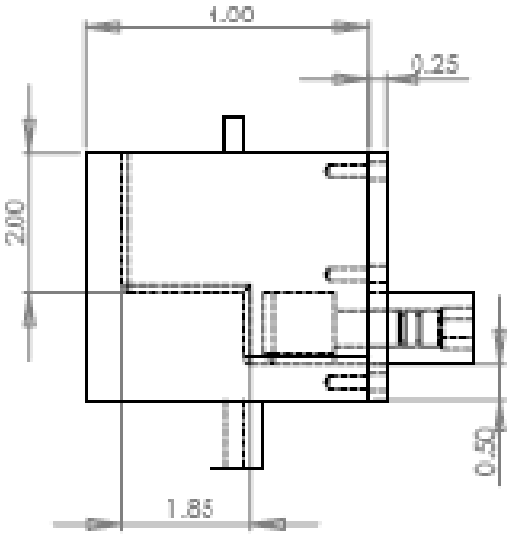

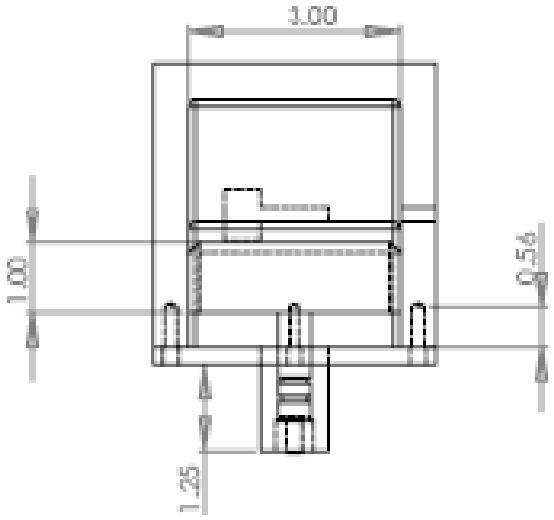

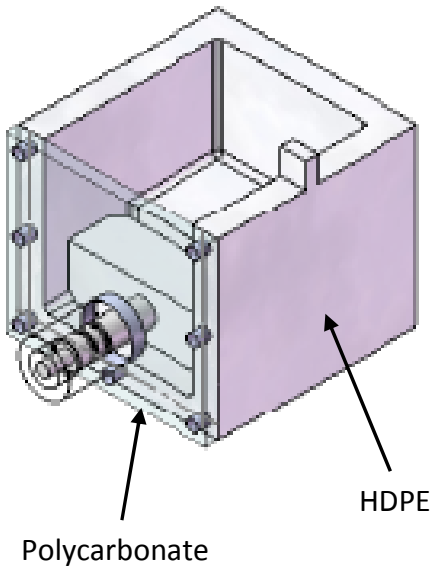

All units are displayed in inches

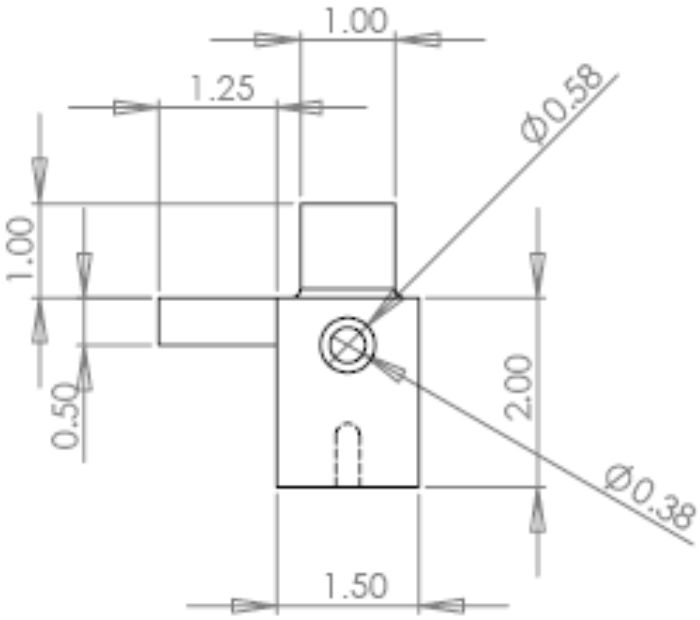

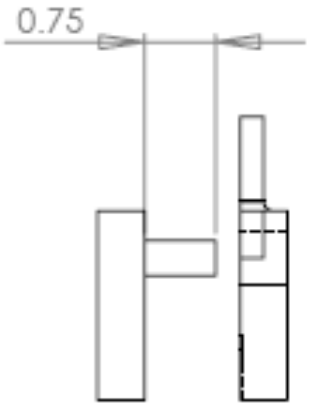

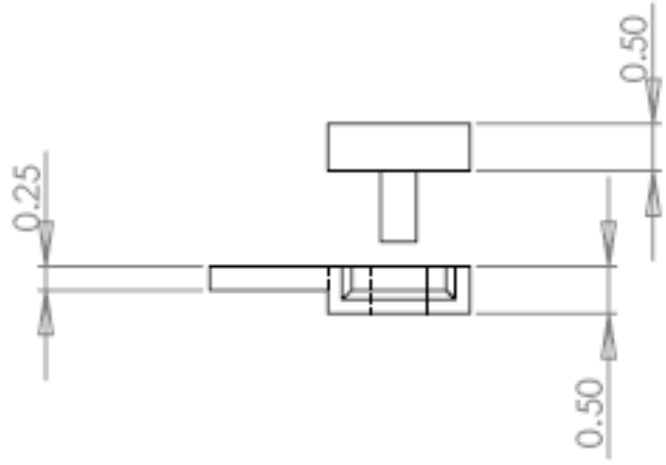

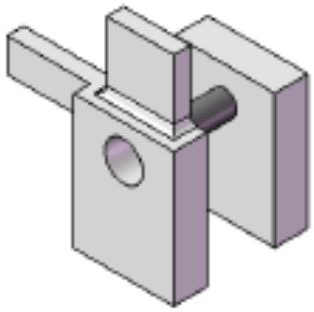

All units are displayed in inches

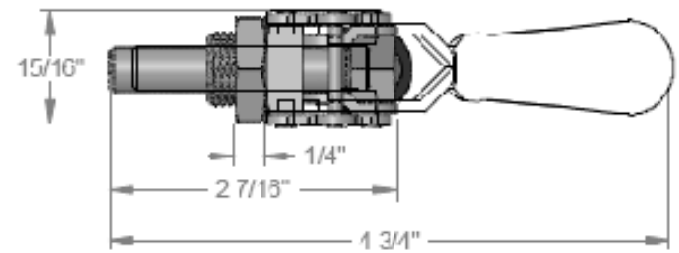

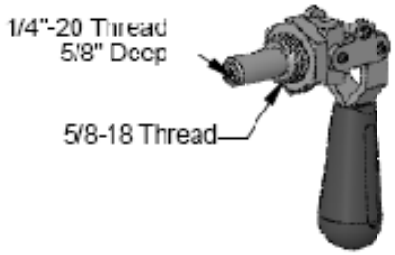

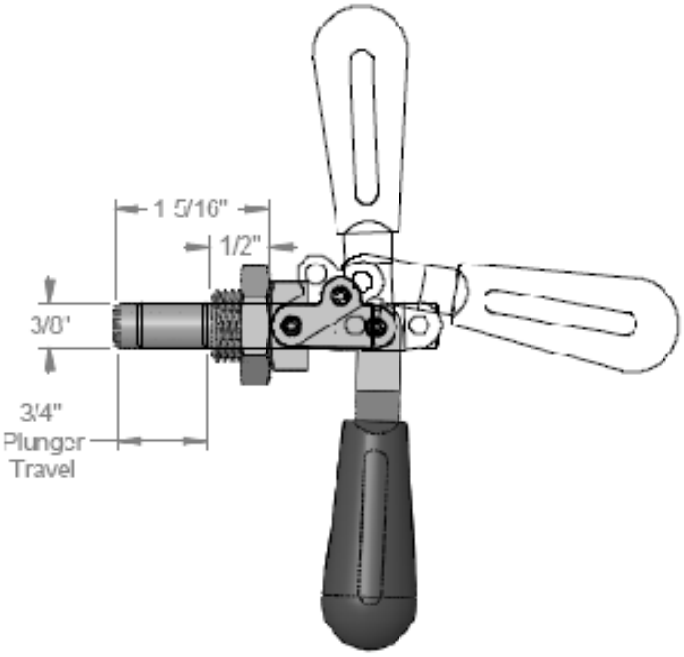

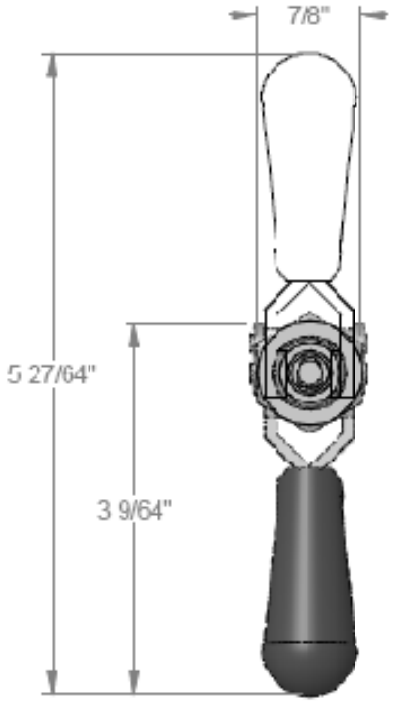

McMASTER-CARR CAD

PART NUMBER 5093A56

http://www.mcmaster.com

Steel Push/Pull-Action Toggle Clamp

Unless otherwise specified, dimensions are in inches. Information in this drawing is provided for reference only.